AN ABSTRACT OF THE THESIS OF

Margaret Leinen for the degree of Master of Science
(Name) (Degree)

in Oceanography presented on September 18, 1975
(Major) (Date)

Title: BIOGENIC SILICA SEDIMENTATION IN THE CENTRAL EQUATORIAL PACIFIC DURING THE CENOZOIC

Abstract approved: Redacted for privacy

Tjeerd H. van Andel

A new technique for determining the amount of opal in deep-sea sediments of any age is described. Using a normative calculation, a portion of the analytical silica concentration of sediments is subtracted as non-biogenic in proportion to the concentration of aluminum in the sample. The ratio of SiO_2:Al_2O_3 used to characterize the non-biogenic sediment fraction was determined by X-ray diffraction analysis of opal-free sediments. The procedure was tested against the X-ray diffraction method for determining opal in deep-sea sediments.

The biogenic silica content of Cenozoic sediments from 20 Deep Sea Drilling Project sites in the central equatorial Pacific was determined using the normative calculation technique for opal determination. The equatorial Pacific lies beneath the equatorial current system where upwelling of nutrient-rich waters results in high plankton productivity. Accumulation rates of biogenically produced

silica were calculated from the opal contents. Maps of these accumulation rates for time intervals during the Cenozoic show that opal accumulation was highest near the equator or paleoequator during the last 50 m.y. Superimposed on this pattern are fluctuations in the rate of opal accumulation in the entire area with time. Regional maxima in opal accumulation in the entire area with time. Regional maxima in opal accumulation occurred during the middle Eocene (42 - 45 m.y. ago) and the late Miocene (7 - 10 m.y. ago). The accumulation rates during these maxima are an order of magnitude higher than those during times of minimum accumulation: the late Oligocene (25 m.y. ago) and the present. The percent of biogenic silica in the sediments varies synchronously with the accumulation rates, but is low to the east due to dilution by non-biogenic sediment from terrigenous and volcanic sources.

Surface productivity controls the accumulation of opal in the equatorial Pacific and opaline sediments are not subject to differential solution with depth. The opal productivity indicated by opal accumulation rates is not related to changes in sea surface or bottom water temperatures and is therefore not directly governed by climate. The association of equatorial productivity and upwelling suggests that changes in circulation which cause upwelling were the principal factors controlling productivity and accumulation of biogenic silica in the past.

Biogenic Silica Sedimentation in the Central Equatorial Pacific During the Cenozoic

by

Margaret Leinen

A THESIS

submitted to

Oregon State University

in partial fulfillment of
the requirements for the
degree of

Master of Science

June 1976

APPROVED:

Redacted for privacy

Professor of Oceanography
in charge of major

Redacted for privacy

Dean of School of Oceanography

Redacted for privacy

Dean of Graduate School

Date thesis presented September 18, 1975

Typed by Margie Wolski for Margaret Leinen

ACKNOWLEDGEMENTS

I would like to take this opportunity to acknowledge three years of advice and encouragement from Dr. Tjeerd H. van Andel, who, as my major professor, bore the brunt of my frustrations over this work. Dr. G. Ross Heath has contributed above and beyond the call of duty as a committee member with patient answers and advice. My especial thanks go to these two members of my committee for their guidance and personal concern. I also wish to acknowledge the other members of my committee, Drs. E. J. Dasch and P. Klingeman, for their comments and suggestions.

I am grateful to the faculty and technicians who guided me from broken pipettes and blank diffractograms to real data: Dr. J. Dymond, J. P. Dauphin, R. Stillinger, C. Muratli, and P. Price. Mrs. C. Rathbun and Mrs. E. Asbury performed the carbonate analyses. Samples were provided by the Deep Sea Drilling Project.

As usual, my fellow students have been some of my best critics and several have been especially helpful in straightening out my more circuitous thoughts: A. Molina-Cruz, D. Stakes, M. Lyle and J. Clark. Some deserve special mention for warm encouragement on cold days: S. Hee, D. Rea, L. Dowding, C. Sancetta, C. Wenkam and R. Graham.

I would also like to thank M. Dibble for her assistance in drafting and Mrs. M. Wolski for her patience in typing a thesis from 3000 miles distance.

Finally, I want to thank Roger and Dan, who have given and have given up the most so that I might finish. They have made it worth the effort.

The financial assistance of the National Science Foundation (Grant No. GA-31478) and a fellowship from Amoco Production Corporation are gratefully acknowledged.

TABLE OF CONTENTS

Table of Contents, continued:

LIST OF FIGURES

List of Figures, continued:

LIST OF TABLES

BIOGENIC SILICA SEDIMENTATION IN THE CENTRAL EQUATORIAL PACIFIC DURING THE CENOZOIC

PART I: A NORMATIVE CALCULATION TECHNIQUE FOR DETERMINING BIOGENIC SILICA IN DEEP SEA SEDIMENTS

The opaline skeletal remains of marine plankton such as diatoms, radiolarians and silicoflagellates are important constituents of marine sediments. Quantitative estimates of the amount of this biogenic silica are necessary to characterize sediments for geologic and paleoceanographic studies. Methods for determining the amount of opal in modern sediments are complicated, however, and have proven unreliable for sediments older than about one million years.

The techniques commonly used to determine opal are X-ray diffraction, infrared spectroscopy and chemical dissolution. An X-ray diffraction technique for measuring the opal content of deep-sea sediments was developed by Goldberg (1958) and Calvert (1966) and modified by Ellis (1972). The technique relies on the conversion of amorphous opaline silica to cristobalite upon heating and has been used routinely for Pleistocene sediments by many investigators. While the method gives reproducible results for modern sediments, attempts to use it on sediments older than one million years have been unsuccessful because aged opal does not seem to convert completely to cristobalite. The thermal-inversion relationship is probably affected by bond changes in the opal molecules as they age (Heath, 1975). Opal which has been converted to quartz or which has been dissolved and redeposited as a siliceous coating on other sediment fractions is also undetected by this method.

Chester and Elderfield (1968) used infrared spectroscopy to determine opal. In this method the absorbance of carbonate-free samples is matched to a standard curve obtained from discs containing pure opal in KBr. This technique compared well with results from X-ray diffraction. However, the presence of more than 5% quartz in the sediment interferes with the opal absorption band. In this case, which is common in marine sediments, a modified technique must be used. A "balancing disc" containing an estimated amount of quartz is placed in the reference beam of the spectrophotometer and the original carbonate-free sample is run against it. The amount of quartz in the "balancing disc" must be changed until it is within ± 0.5% of that in the sample, whereupon the quartz band is eliminated. Opal may then be measured from the standard absorbance curve. If the opal:quartz ratio is less than three it is not possible to estimate the opal content. A further complication arises because the technique measures Si - OH stretch frequencies with which some marine constituents like palagonite interfere.

A dissolution method for removing amorphous silica from clays which has been used to measure the opal content of sediments was described by Hashimoto and Jackson (1960). The technique involves repeated leaching of samples with 0.5N NaOH. The concentration of silica in the supernatant is measured after each dissolution. The authors indicate that poorly cyrstallized clay minerals are also attacked by this treatment. In a test of the procedure on biogenous opal, Ellis (1972) found the method to be very inefficient for opal-rich samples since appreciable quantity of opal was left undissolved after four leaches. In addition, a variable number of dissolutions, ranging up to seven, was required to remove all of the opal from duplicate standards.

A second differential dissolution method using sodium carbonate has been used by Russian investigators (Bezrukov, 1955; Lisitzin, 1971a) but their results are not compared to other techniques. Hurd (1972) also dissolved samples in 5% Na_2CO_3. He measured the silica content of the supernatant by colorimetry (Strickland and Parsons, 1968) and related its net absorbance to a standard curve obtained from various percentages of opal mixed with an artificial sediment. Silicate minerals were also dissolved by this treatment, especially palagonite and montmorillonite. Therefore, variability and/or poor crystallinity in the non-biogenic sediment fraction introduce errors in the opal content estimated by this technique. A comparison of opal in surface sediments from the southern South Atlantic determined by sodium carbonate dissolution (Lisitzin, 1972) with those determined by X-ray diffraction (Ellis and Moore, 1973) reveals discrepancies which indicate that this dissolution also yields low values for samples with high opal contents. Both dissolution techniques become questionable when applied to older sediments because the solubility of opal also changes with geologic age due to bond changes in the opal molecules (Heath, 1975).

Bostrom and Fisher (1971) reasoned that the SiO_2:Al_2O_3 ratio of oceanic and continental crust is about 4:1 (Boström and others, 1971, chose 3:1, a ratio representing the continental crust), and that chemical data could, therefore, be corrected for "excess" or opaline silica to yield non-biogenic sediment compositions. They used the relation:

$$SiO_2 \text{ "excess"} = SiO_2 \text{ measured} - 4\ Al_2O_3 \text{ measured}$$

(where 4 Al_2O_3 is the estimate for non-biogenic silica). This technique is a potential method for determining the amount of opal in sediments of any age by making a normative calculation in which some of the analytical silica concentration is subtracted as non-biogenic in proportion to the amount of other chemical constituents in the sample. The non-biogenic fraction of marine sediments is made up of clay mineral assemblages with various admixtures of volcanic ash, authigenic minerals, manganese nodules and hydrated ferromanganese oxides. Since the proportion of each component varies widely from one area to another, the non-biogenic fraction, taken as a whole, cannot be assumed to have an $SiO_2:Al_2O_3$ ratio equal to that of average continental crust. In clays, generally the major non-biogenic component, the ratio ranges from 2:1 to almost 7:1 (Weaver and Pollard, 1973) and varies with structure and the amount of cation substitution. In order to determine whether the method of subtracting non-biogenic silica is feasible and capable of giving reliable opal concentrations, a study was made of surface and subsurface sediments from Deep Sea Drilling Project cores in the central equatorial Pacific Ocean.

METHODS

To establish a $SiO_2:Al_2O_3$ ratio appropriate for the central equatorial Pacific, 42 samples which had little or no recognizable skeletal opal in smear slides were chosen from Deep Sea Drilling Project cores spanning the entire area and time range of interest. After calcium carbonate was removed with acetic acid buffered to pH=5, ferromanganese hydroxyoxides were removed by the dithionite-citrate-bicarbonate technique of Mehra and Jackson (1960). The samples were Mg^{++} saturated and the $< 2\mu m$ fraction was mounted as oriented aggregates and X-rayed in duplicate. Relative proportions of the smectite, illite, kaolinite and chlorite groups were estimated from peak-areas using the weighting factors of Biscaye (1965). This technique assumes that these clays account for all the sediment finer than 2μm.

In addition, quartz and opal were determined (Till and Spears, 1969; Ellis, 1972) on 2 - 20μm carbonate-free aliquots of the same samples, as well as on thirteen composite samples made up from DSDP samples spanning the last one million years at each site.

Finally, a portion of each sample was dissolved with aqua regia and hydrofluoric acid in Teflon-lined bombs, neutralized with boric acid after dissolution (Bernas, 1968), and analyzed for Si, Al, Mg, Mn and Fe by atomic absorption spectrophotometry (AAS). In this way the $SiO_2:Al_2O_3$ values estimated from ideal mineral compositions could be compared directly with the actual values for each sample.

RESULTS

Clay Mineralogy

Smectite is the dominant clay phase in all but one of the 42 samples which were analyzed for clay mineralogy (see Table 1). Eight percent of the samples contained at least 60% smectite and over half contained more than 80% smectite. These results are in general agreement with those of Heath (1969b) who found that only the most recent of his cores in the equatorial Pacific ocean contained less than 60% smectite. The smectite concentration in the samples from the

TABLE 1. Semi-quantitative clay mineral abundances, theoretical SiO_2:Al_2O_3 ratios and quartz content of opal-free sediments. (Sample number indicates DSDP Site. Age interval is in parentheses. Samples are listed in order of distance from East Pacific Rise at time of deposition.)

Sample	Smectite	Illite	Kaolinite	Chlorite	SiO_2:Al_2O_3 (calculated)	% Quartz
80(21-22)	91.5± 5.5	7.3± 8.9	0.5± 0.1	1.2± 1.3	3.886	1.3
81(16-17)	99.6± 0.8	0	0	0.4± 0.8	4.000	2.0
83(10-11)	96.9± 1.4	0	0	2.7± 2.3	4.000	2.0
77(37-38)	85.2± 4.6	10.5± 3.8	1.7± 0	2.6± 1.0	3.808	1.8
75(31-32)*	14.5	63.2	0	22.3	3.052	4.8
74(44-45)	85.1± 3.4	12.3± 1.8	0	2.6± 5.2	3.816	4.0
162(49-50)	92.6± 2.4	5.5± 3.0	1.9± 0.6	0	3.880	1.5
159(23-24)	81.5± 3.2	13.2± 3.0	1.5± 3.0	3.7± 1.8	3.768	1.9
159(22-23)	91.3± 0.2	7.2± 1.3	0.6± 1.2	0.8± 0.1	3.876	1.0
79(20-21)	95.1± 1.1	2.8± 1.4	0	2.1± 2.6	3.958	0.0
74(36-37)*	88.4	0	5.0	6.5	3.896	2.0
79(19-20)	93.1	0	2.1± 4.2	4.8± 4.3	3.958	2.0
79(18-19)	100.0	0	0	0	4.000	2.0
80(20-21)	94.5± 1.8	0	0	5.5± 1.8	4.000	2.0
77(28-29)	51.3± 15.5	28.7± 6.7	7.8± 15.5	12.2± 0.4	3.416	5.0
159(19-20)	93.7± 6.5	3.4± 6.8	2.2± 1.1	0.7± 1.4	3.905	2.3
74(33-34)*	75.8	18.9	2.1	3.2	3.675	3.7
79(18-19)	100.0	0	0	0	4.000	2.0
163(69-70)	71.9± 3.0	26.0± 0.9	1.4± 0.7	0.7± 1.5	3.386	0.0
72(27-28)*	45.0	39.9	8.1	7.1	3.244	3.1
77(20-21)	85.4± 1.7	10.5± 1.0	1.8± 1.0	2.4± 2.8	3.807	1.1
71(28-29)	83.0± 0.8	13.4± 0.2	1.2± 2.4	2.4± 1.8	3.775	2.3
75(21-22)*	52.5	27.9	12.3	7.3	3.336	1.8
73(20-21)*	43.8	38.6	10.1	7.5	3.219	5.2
75(16-18)	89.6± 0.6	8.9± 0.1	0.4± 0.7	1.2± 1.2	3.863	3.9
159(13-14)	57.9± 0	16.2± 1.4	15.3± 1.5	10.6± 0.7	3.615	0.0
160(1-2)	73.0± 1.9	13.8± 2.2	4.1± 0.9	9.1± 0.6	3.711	5.3
75(1-2)*	59.5	23.0	9.0	8.5	3.475	4.0
40(	68.5± 8.5	21.3± 10.8	4.8± 1.4	5.5± 3.7	3.589	3.2
41(0-1)	49.5± 2.9	30.5± 0.4	9.8± 1.5	10.2± 1.0	3.347	3.9

* Insufficient sample to run duplicate

study area decreases roughly with distance from the East Pacific Rise at the time of deposition from 90 - 100% smectite in samples deposited at or near the rise crest to approximately 50% in samples furthest from the rise crest. Illite was next in abundance and made up 0 - 40% of the clay fraction. It is negatively correlated with the smectite content. Kaolinite and chlorite exceed 10% only in samples with low smectite concentrations. The negative correlation between smectite and the remaining components results from forcing the data to sum to 100% when one component is dominant (Chayes, 1960).

An $SiO_2:Al_2O_3$ ratio was estimated for the clay phase of assigning each clay group an average ratio based on compiled analyses of clay minerals (Weaver and Pollard, 1973). The ratios chosen were: smectite - 4:1; illite - 2.5:1; kaolinite - 2:1; and chlorite - 4:1. Using these values, ratios were calculated for the clay fraction which ranged from about 4.0:1 for samples deposited near the East Pacific Rise to about 3:1 for samples deposited furthest from the rise crest. Samples representing the last one million years of sedimentation had ratios of about 3:1. The average for the entire group was 3.68:1, but it is biased toward samples with high smectite contents.

Quartz and Opal

Quartz made up approximately 1 - 5% of the 2 - 20μm fraction of all samples except those from the last 5 million years, which had

2 - 20 μm fraction quartz contents of 10 - 11%. Rex and Goldberg (1958) found that most detrital quartz in their Pacific sediment samples was in the 2 - 20 μm size range. This fraction made up about half of the carbonate-free sediment, by weight, in samples from this study. Therefore, 5% of the carbonate-free silica content of the 0-1 million year samples was attributed to quartz. Based on the quartz contents of older samples determined in this study and in a study of equatorial Pacific sediments by Heath (1969) a similar quartz correction can be made for samples older than one million years. Assuming the 2 - 20 μm size fraction to account for about half of the carbonate-free sediment, 2.5% of the carbonate-free silica of samples between one and 40 million years old is detrital quartz and 1% of the carbonate-free silica of samples older than 40 million years is detrital quartz.

The opal content of the thirteen 0 - 1 million year samples as determined by the X-ray technique and the normative calculation (using a SiO_2:Al_2O_3 of 3:1) is shown in Table 2. The values are calculated on a salt-free (bulk sediment) and on a carbonate-free and salt-free basis. All values are corrected for quartz contents. The agreement between the two methods for the salt-free calculation is very good (r = .942, see Figure 1). On a carbonate-free basis the agreement is not as close (r = .883) because the differences are multiplied by carbonate correction factors.

TABLE 2. Bulk and Carbonate-Free Biogenic Silica Content of 0 - 1 Million Year Sediment Samples from DSDP Sites in the Central Equatorial Pacific Ocean

Site	Bulk Biogenic Silica Percent				Carbonate-Free Biogenic Silica				$CaCO_3$ %*
	X-Ray# (calculated)		AAS#		X-Ray#		AAS# (calculated)		
70	20.35	1.4	20.39	1.4	20.42	1.4	20.65	1.4	1.16
71	7.27	0.3	7.09	0.1	37.19	1.3	36.26	0.31	80.45
72	13.81	0.4	13.45	0.5	76.74	2.0	74.72	2.80	82.00
73	14.93	0.7	7.07	0.6	99.61	4.6	47.16	4.0	85.01
74	42.07	2.0	40.48	1.2	41.57	2.1	40.95	1.2	1.17
75	0.00	0.5	1.85	0.1	0.00	0.5	1.87	0.1	0.87
77	15.43	0.1	12.77	0.6**	73.48	0.5	60.08	2.9**	79.00
79	11.86	0.6	12.09	0.8**	74.46	4.0	75.89	4.8**	84.07
81	9.47	0.2	6.13	0.1	85.38	3.1	55.27	0.1	88.91
82	18.35	1.1	17.23	0.8**	76.55	12.5	71.88	3.5**	76.03
83	15.42	0.1	15.03	0.1**	35.61	0.2	34.70	0.3**	56.69
159	3.26	1.6	1.33	2.3**	3.27	1.6	1.34	2.3**	0.26
160	18.90	1.5	8.34	1.6	19.54	1.5	8.62	1.8	3.27

* Values below 80% from LECO-714 analyzer, values above 80% from AAS

\# Samples run in duplicate

\## Samples run in triplicate

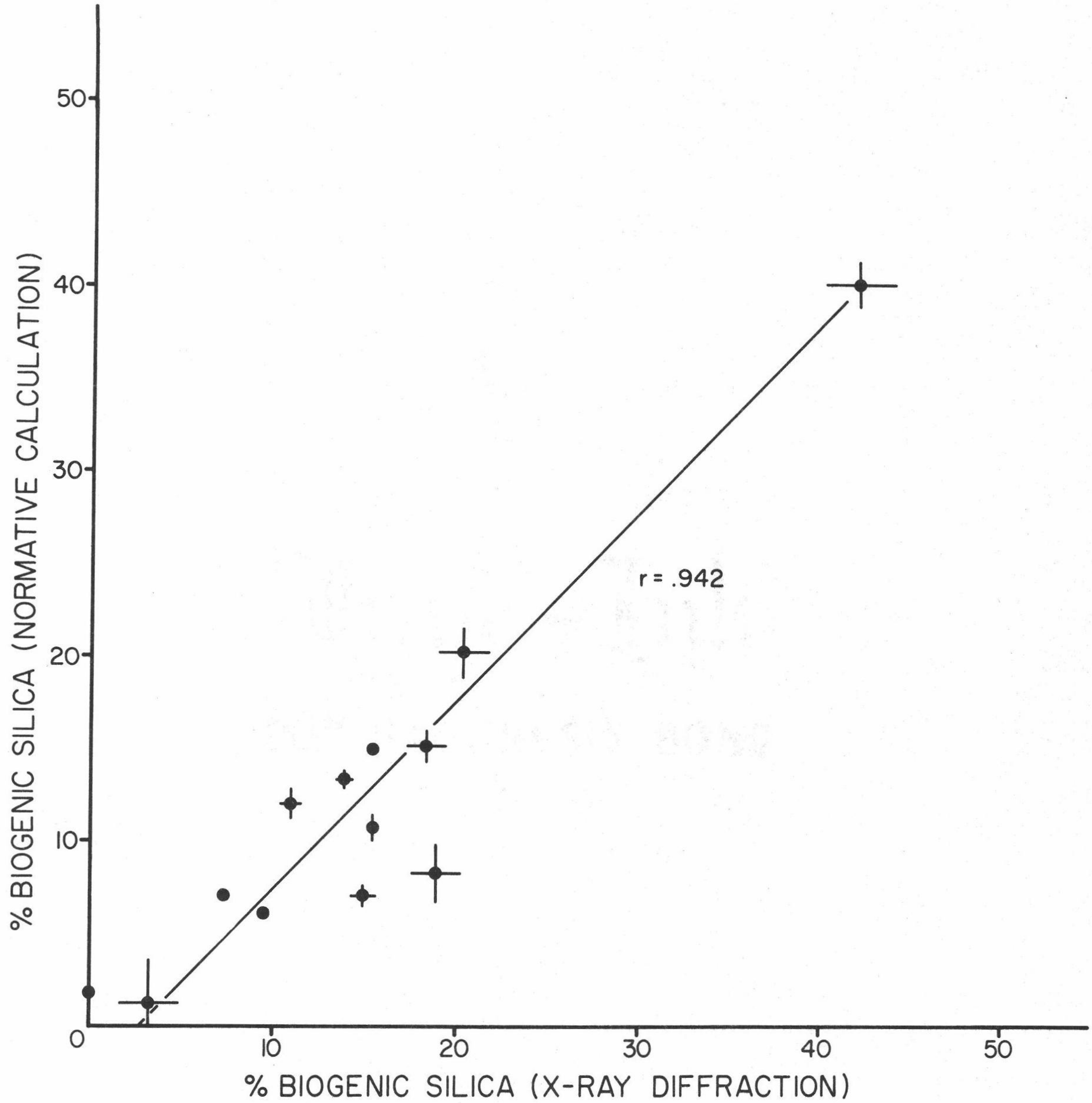

Figure 1. Percent biogenic silica in bulk sediment calculated from X-ray diffraction data vs. Percent biogenic silica in bulk sediment determined by normative calculation technique. Bars on sample points indicate error.

DISCUSSION

The X-ray technique has an accuracy of ± 5% for samples having less than 60% opal, but may be less accurate for those with greater opal contents (Ellis, 1972). The precision of the atomic absorption analyses varies from about 1 to 2% for Si and Al in samples low in calcium carbonate to about 2 to 5% for those high in carbonate. Comparison with USGS standard rocks and pure opal standard indicated no systematic error. Determinations of Al in standard rocks were accurate to ± 1 weight percent and Si determinations were accurate to ± 1.5 weight percent. The maximum error for the opal determinations using a SiO_2:Al_2O_3 ratio of 3:1 is, therefore, about ± 5% for low carbonate samples and ± 6% for high carbonate samples.

A known and consistent SiO_2:Al_2O_3 ratio for the area studied is a prerequisite for accurate biogenic silica estimates. The effect or ratio variability is greatest at low opal concentrations. At 0% opal, the error is 12% for each integral departure from the actual SiO_2:Al_2O_3 ratio (see Figure 2). The error decreases linearly so that at 100% opal all ratios correctly determine the opal content because there is no alumina in the sample. This makes the normative calculation more accurate for samples with high opal content where X-ray diffraction and differential solution techniques are particularly unreliable. Estimates of the chemical composition of the non-biogenic

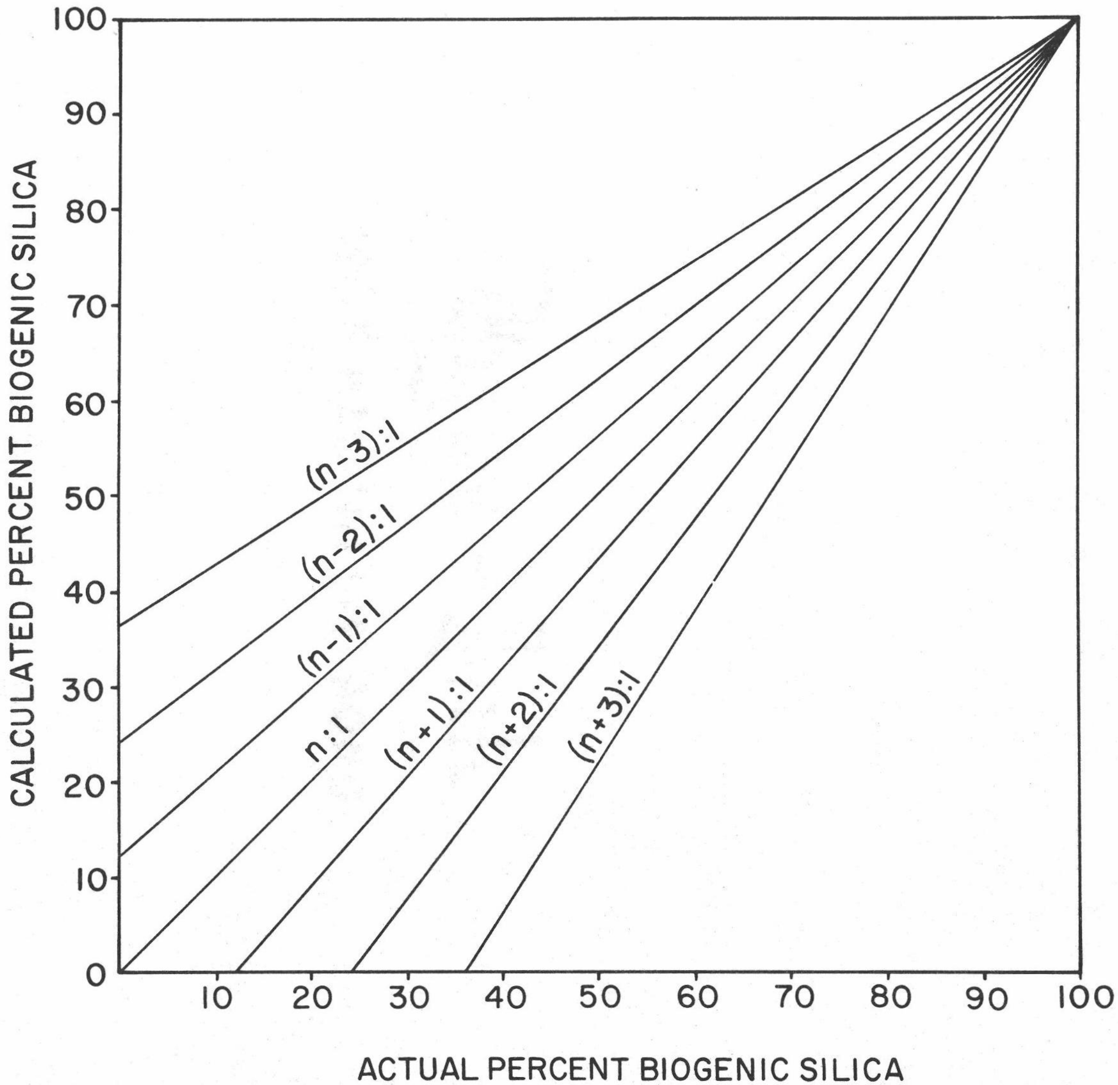

Figure 2. Effect of error in SiO_2:Al_2O_3 ratio chosen for normative calculation. Curves represent integral departures from an actual ratio of n : 1.

fraction based on clay mineralogy provide reasonable SiO_2:Al_2O_3 values for the calculation since clays are usually the major non-biogenic component that contains silica. Where clay mineral data are not available, it is probably more accurate to use an average ratio based on pelagic clays than the continental ratio of 3:1. El Wakeel and Riley (1961) list chemical analyses of 11 pelagic clays. If these are corrected for their biogenic silica contents, the average SiO_2: Al_2O_3 is 4.3:1. Analyses of nine pelagic red clays from the Pacific described by Revelle (1944) have an average SiO_2:Al_2O_3 of 3.9:1. These values are appropriate for samples with little terrigenous influence. The value originally used by Bostrom and Fisher (1971) of 4:1 is therefore a good estimate of the ratio for deep-sea sediments.

An important source of error for determining opal on a carbonate-free basis lies in the calcium carbonate values themselves. The effect of errors in carbonate content is particularly great for samples having more than 85% carbonate. For example, a bulk sample biogenic silica content of 3% represents 43% of the carbonate-free sediments if the carbonate content is 93%, but represents 60% of the carbonate-free sediment if the carbonate content is 95%. Carbonate determinations for this study were initially calculated from measurements by a LECO-714 carbon analyzer. These values seemed to be systematically low compared to measurements made on the same core intervals by the Deep Sea Drilling Project. Ca was then measured by atomic absorption and calcium carbonate was calculated using the relation:

$$\text{CARBONATE \%} = 100 \left(\frac{\text{Ca\%} - (0.0041 \text{ SALT \%}) - 0.73}{39.31} \right)$$

which corrects for calcium in the salt and non-carbonate fractions. The error introduced by assuming a constant Ca content of the non-biogenic fraction (0.73%) is less than 1% for samples with more than 90% calcium carbonate and less than 3% for samples with more than 80% calcium carbonate (Dymond and others, in press). The error increases exponentially with decreasing carbonate content. Therefore, the atomic absorption value for Ca was used to calculate calcium carbonate contents above 80% and the LECO value was used for those below 80%. The carbonate contents estimated by atomic absorption differed by as much as 10% from the carbonate percentages determined by LECO and markedly improved agreement between the X-ray estimate and the calculated normative estimate of carbonate-free opal concentrations. Biogenic silica values for bulk samples are unaffected by carbonate values so that accumulation rate calculations can be made regardless of the quality of the carbonate data for the sediments.

The normative calculation method described above gives results which are compatable with those of the standard X-ray technique for sediments younger than one million years, but the X-ray technique may still be preferable for such samples since it measures opal and quartz directly. Both methods involve a moderately extensive laboratory preparation. There are two applications for which the normative calculation has a distinct advantage. One is the case where samples are to be analyzed for chemical composition so that the normative calculation requires no additional laboratory work. The second is for pre-Pleistocene sediments for which X-ray and dissolution techniques are unreliable.

PART II. BIOGENIC SILICA SEDIMENTATION IN THE CENTRAL EQUATORIAL PACIFIC DURING THE CENOZOIC

In the span of a few years the central equatorial Pacific Ocean has become one of the most intensively studied pelagic geologic provinces in the world ocean. This area lies beneath the biologically productive equatorial current system, which has existed through the Cenozoic. The plankton of the equatorial current have supplied abundant skeletal material which, together with terrigenous and authigenic sediment, has produced an unusually thick and complete marine record. Because the high productivity of the region is a direct consequence of the large nutrient concentrations associated with upwelling at the equator, this sedimentary section is a record of the paleoceanography and history of productivity of the equatorial Pacific.

Since Arrhenius (1952) described the first long piston cores from the east Pacific, various aspects of equatorial Pacific sedimentation have been studied (e. g. Burckle, 1967; Heath, 1969a, b; Hays and others, 1969; Winterer, 1973), three Deep Sea Drilling Project legs have focused on the area and its history (Tracey and others, 1971; Hays and others, 1972; van Andel and Heath, 1973) and two summary studies of the sedimentation history have been made (Berger, 1973; van Andel and others, 1975). In spite of this wealth of published information, only the history of carbonate sedimentation in the central equatorial Pacific is well known. The DSDP summaries and the study by Berger (1973) have dealt primarily with sedimentary facies and furnish general descriptions of the types of sediment present and of the sedimentation history. The DSDP summaries and the study by Berger (1973) have dealt primarily with sedimentary facies and furnish general descriptions of the types of sediment present and of the sedimentation history. The work of van Andel and others (1975) modeled the depositional history primarily on the basis of carbonate sediments and interpreted the paleoceanography in terms of the calcite compensation depth and carbonate sedimentation.

Carbonate sedimentation, however, is not well suited for reconstructing the paleoceanography of surface waters. Ocean waters are undersaturated in carbonate beneath the upper few hundred meters, leading to dissolution of calcareous sediments in the water column and after deposition. The dissolution rate increases rapidly below the lysocline (Heath and Culberson, 1970) until the rate of solution equals the rate of supply of calcium carbonate at the calcite compensation depth (CCD; Bramlette, 1961; Berger, 1970) below which no calcareous sediment is preserved. The distribution and concentration of calcareous sediments are, therefore, determined by the balance between the supply of calcium carbonate from the surface and the dissolution of calcite at depth. Since the depth of the lysocline and of the calcite compensation depth fluctuate with time it is impossible to estimate the original supply of sediment without knowing the level of the lysocline and the gradient of dissolution.

Seawater is also undersaturated with respect to opaline silica (Krauskopf, 1956; Jones and Pytkowicz, 1973). The opaline tests of radiolarians, diatoms and silicoflagellates dissolve in the water column and in surface sediments, but the rate of solution is almost indpendent of depth (Heath, 1974; Edmond, 1974). For siliceous sediments below 2000 m Johnson (1974) found that the only preservation - depth correlation for the eastern tropical Pacific was a result of hydraulic sorting: deeper depositional sites receive a statistically higher amount of opaline tests than do shallow sites. Because preservation is largely independent of depth, opaline sediments are a less distorted indicator of surface productivity than are carbonate sediments. Studies of Holocene and Quaternary opal distributions in the equatorial Pacific (Heath and others, in prep.) reflect the patterns of primary productivity in the area (Ryther, 1963; Koblentz-Mishke and others, 1970; Lisitzin, 1972).

All previous studies of the Cenozoic sedimentation history of the equatorial Pacific have, of necessity, dealt qualitatively with siliceous biogenic sediments because there has been no analytical technique for determining the opal content of sediments older than one million years. The development of a new technique for determining the opal content of marine sediment of any age (see Part I) permits a quantitative evaluation of the Cenozoic budget of opaline silica. This procedure has been used in this study to determine the opal content of selected samples from DSDP sites in the central equatorial Pacific. With this information to estimate the rate of accumulation of biogenic silica can be estimated which, together with the history of carbonate accumulation, can be used to reconstruct changes in the equatorial current system and in its associated biologic productivity during the past 50 million years.

Biostratigraphic and Tectonic Models

This study supplements van Andel and others' (1975) larger synthesis of central equatorial Pacific sedimentation. Their synthesis provides the tectonic framework and a detailed analysis of carbonate sedimentation with which the analysis of biogenic silica sedimentation can be coupled. To facilitate comparison, the biostratigraphic and tectonic models used in the previous study have been adopted unchanged. In addition, the samples were chosen to complement those of the first study as much as possible.

Samples were chosen from 22 drill sites from Legs 5, 8, 9 and 16 of the Deep Sea Drilling Project (Figure 3; Appendix I); which are the same ones used by van Andel and others (1975). The biostratigraphic zonation for each site is presented in that study. This zonation is based on the biostratigraphic zonations presented in the Initial

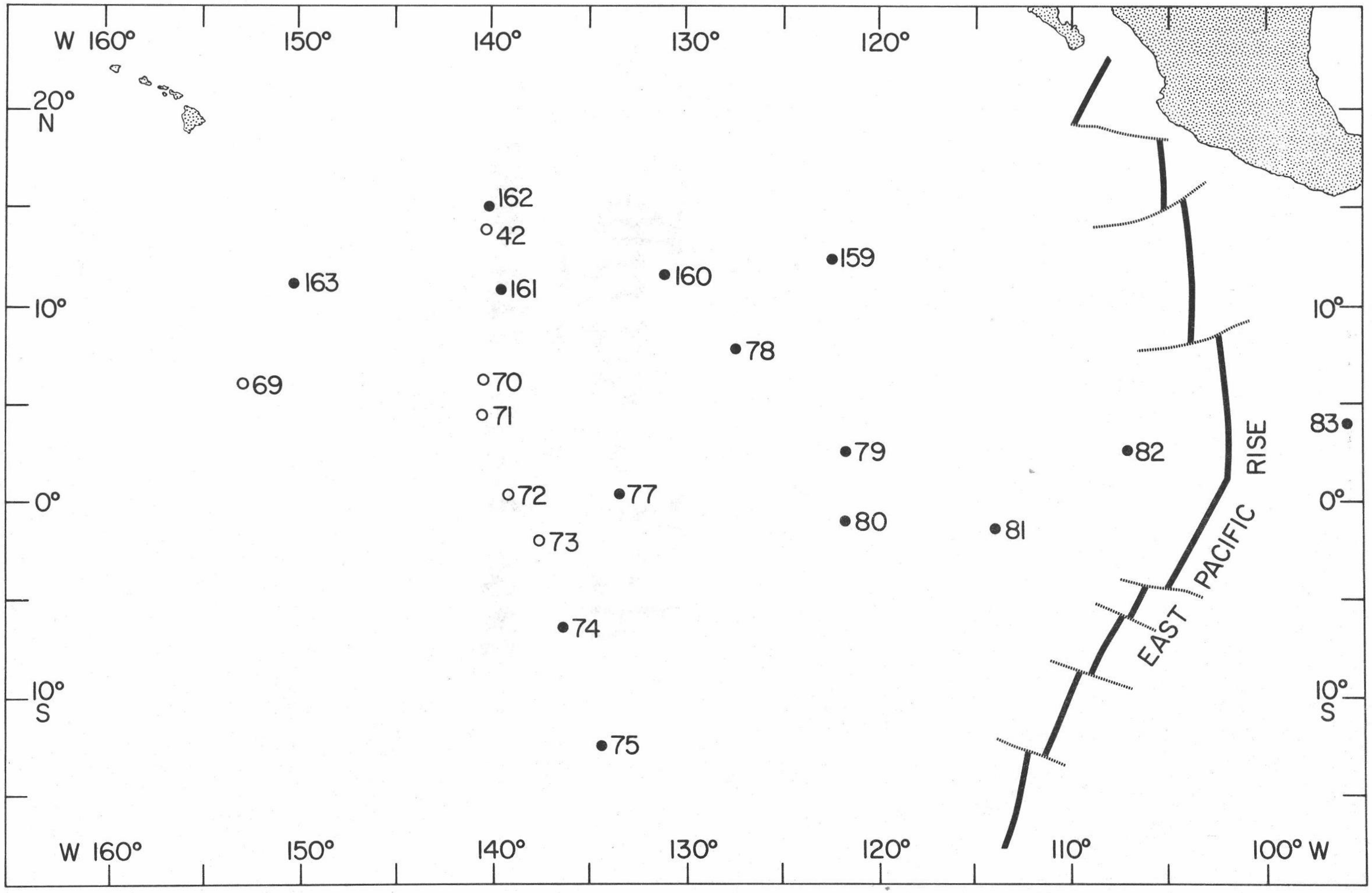

Figure 3. Location of Deep Sea Drilling Project sites in the central equatorial Pacific. Dots represent sites which ended in basalt interpreted as basement. Open circles are sites which did not reach basement.

Reports for each of the DSDP legs with revisions by D. Bukry. The absolute chronology is based on Berggren (1972). Ages of sediment-basement contacts and ages of the oldest cored sediment in holes which did not reach basement were taken from van Andel and Bukry (1973). One-million-year absolute age boundaries were determined for the entire length of cored sediment at each site by plotting the absolute ages of all available biostratigraphic zone boundaries against ages of all available biostratigraphic zone boundaries against depth in the hole. A curve, fitted by hand to all points, was then used to determine the depth of all one million year age boundaries at each site. The uncertainty in the absolute ages of zone boundaries used to determine one million year age boundaries does not exceed 1 m.y. for intervals less than 10 million years old, 2 m.y. for those 10 to 27 million years old and 3 m.y. for intervals 27 to 50 million years old. An extensive discussion of the assumptions and uncertainties associated with the biostratigraphic zonation, absolute ages and one million year age boundaries is given in van Andel and others (1975).

All sites used in the study except one, site 83 on the Cocos Plate, are on the Pacific plate which has moved northwestward with respect to the present equator throughout the Cenozoic (Francheteau and others, 1970). This movement has produced a progressive northward displacement of equatorial deposits with increasing age (van Andel and Heath, 1973; van Andel and others, 1975; Winterer, 1973).

Consequently, it is essential to know the exact migration path of each site with time for paleoceanographic reconstructions. This location of the Pacific pole of rotation and the motion of the Pacific plate around this pole of rotation during the Cenozoic have not yet been determined unambiguously. Several pole positions and rates of rotation have been suggested (Morgan, 1972; Clague and Jarrard, 1973; Minster and others, 1974). The time of shift from the Cretaceous and early Cenozoic Emperor pole of rotation to the present Hawaiian pole is also uncertain. Van Andel (1974) and van Andel and others (1975) determined axes of maximum equatorial sedimentation for several time intervals during the Cenozoic. These axes were migrated according to several rotation schemes and a model was finally chosen which kept the axis parallel and well-centered on the present equator. The rotation system used in that study and in this one is:

INTERVAL	POLE	ROTATION
Pacific Plate:		
0 - 25 m.y.	67°N, 59°W	0.83°/m.y.
25 - 50 m.y.	67°N, 59°W	0.25°/m.y.
> 50 m.y.	11°N, 84°W	0.80°/m.y.
Cocos Plate:		
0 - 15 m.y.	23°N, 119°W	1.47°/m.y.

The migration paths of the sites used in this study are shown in

Figure 4. A detailed discussion of alternative Pacific plate poles and rotation rates and of the basis for choosing the rotation scheme above is included in van Andel and others (1975).

Finally, ocean crust formed at rise crests gradually subsides as it ages. This subsidence can be described by a quantitative relationship between crustal age and basement depth (Sclater and others, 1972; Berger, 1973). The depth of each site during its northwestward migration has been computed on the basis of a subsidence curve constructed from the age and present depth of basement at the DSDP sites (van Andel and others, 1975). This curve parallels the one determined by Sclater and others (1972).

METHODS

Composite samples were made up of several 1 cm DSDP sediment samples which were chosen from cores spanning a series of one million year time intervals at each site. Where possible, samples from time intervals used by van Andel and others (1975) to map sedimentation, accumulation and carbonate accumulation rates were used so that the opal data could be compared directly with those maps. A complete list of the composite samples and the DSDP samples used to make them is compiled in Appendix 2. Using the procedures outlined above, each of the 122 composite samples has been assigned to a one million year age interval and its paleolatitude, paleolongitude

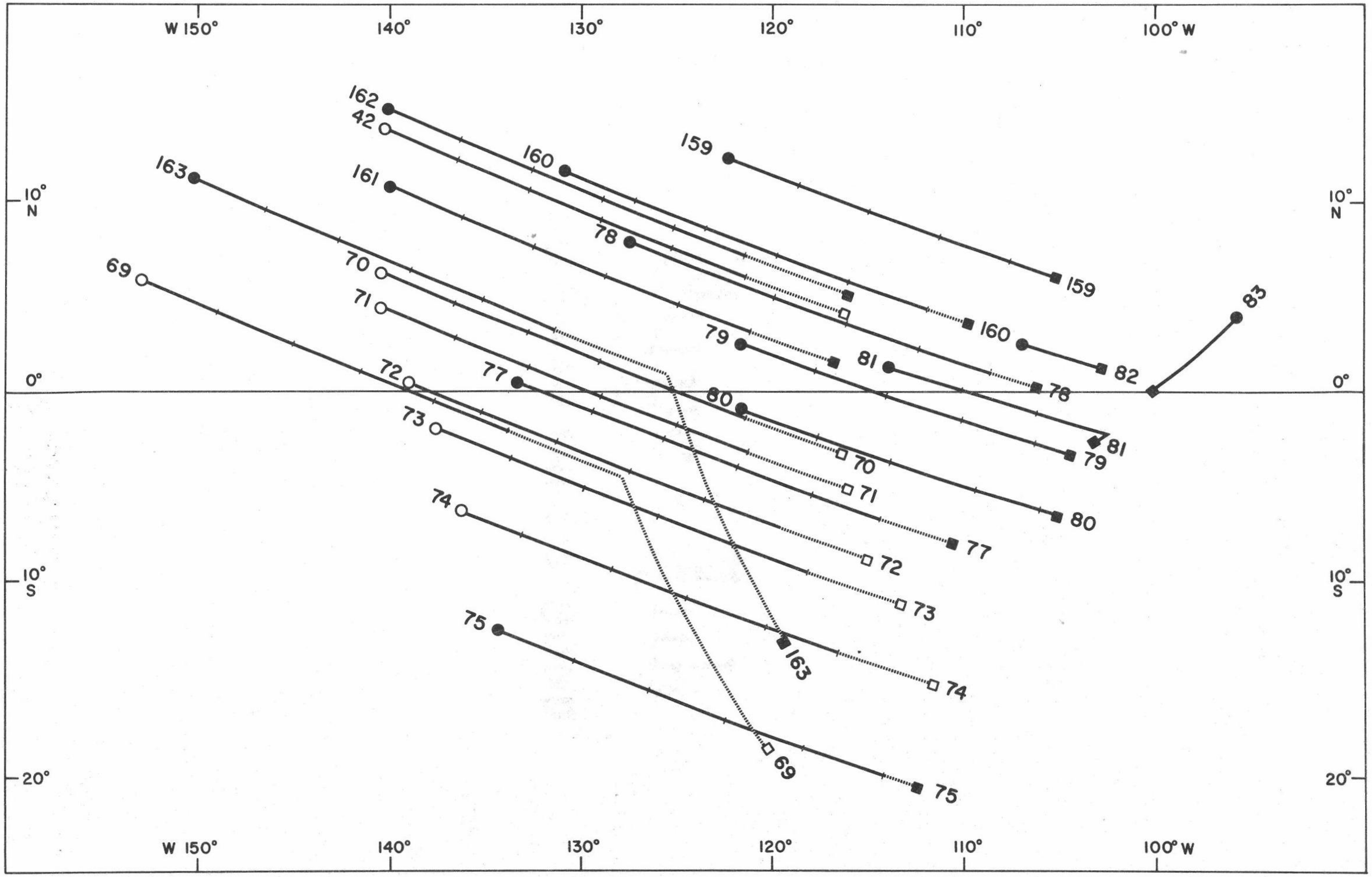

Figure 4. Migration paths of DSDP sites used in this study. Circles are present locations of sites and squares are positions of sites at time of origin. Solic characters represent drill sites ending in basement, open characters are those ending in sediment. Paths are marked at 5 m. y. intervals for the past 25 m. y. Rotation model is given in text. Dashed portion of migration path of Hawaiian pole rotations indicates change in rotation rate.

and paleodepth have been determined. In choosing samples, portions of the core in which mixing across one million year boundaries was obvious from core photographs and/or biostratigraphy were rejected, as were anomalous samples which were not typical of the time interval.

The DSDP samples were freeze-dried and combined in equal weight to form the composite samples. The composites were then ground briefly, split and recombined ten times to homogenize the sediment. The calcium carbonate and organic carbon content of each sample were determined from measurements by a LECO-714 carbon analyzer. Duplicates which did not agree to within 1 weight percent total carbon were rerun. Samples of 100 to 300 mg, depending on carbonate content, were used for chemical analysis. They were dried overnight, reweighed, and then dissolved with aqua regia and hydrofluoric acid in Teflon-lined bombs. The samples were neutralized with boric acid after dissolution (Bernas, 1969) and analyzed for Si, Al, Mg, Mn and Fe by atomic absorption spectrometry using standard solutions made from pure metals. The standard solutions and experimental accuracy were tested against USGS standard rocks, AGV-1 and GSP-1.

Since most of the DSDP samples arrived partially dried, the usual correction for water loss and salt content based on weight loss after drying could not be made. Instead, the water loss was calculated from the porosities and bulk densities of the sediments using the following relationships:

$$\text{WATER LOSS (\%)} = \left(\frac{\text{true porosity}}{1.012 \times \text{bulk density}} \right) \times 100$$

$$\text{SALT (\%)} = \left(\frac{\text{Water loss (\%)} \times .035}{100 - \text{Water loss (\%)}} \right) \times 100$$

Porosities and bulk densities are routinely measured on DSDP cores onboard by the Gamma Ray Attenuation Porosity Evaluator (GRAPE). The error in GRAPE porosity is about ± 5% and that for bulk density is ± .05 g/cm^3 (Bennett and Keller, 1973). Plots of the original GRAPE data were used since those in the Initial Reports are on a small scale and are frequently matched to the core sections improperly. From these plots, the porosity and bulk density of the individual samples were read directly. Improper alignment of the GRAPE data with depth in core could introduce an additional error, but this error is minimal since the ends of sections are easily picked out on the plots. Errors due to core distortion are also minimal since samples from badly disturbed sections were not used. Maximum reading errors are about 1% for porosity and about 0.02 g/cm^3 for bulk density, so that errors in the water loss and salt corrections should not exceed 6%.

The biogenic silica content of the composite samples was determined by a normative calculation method in which a fraction of the analytical silica concentration proportional to the concentration of other elements in the sample is subtracted as non-biogenic. For composite samples from the 0 - 1 m.y. time interval, the opal content was also determined by X-ray diffraction using the method developed by Goldberg (1958) and Calvert (1966), as modified by Ellis (1972). These determinations served as a cross-check on the validity of the results from the normative calculation. A complete discussion of the normative calculation technique and a comparison with the X-ray diffraction technique is given in Part I.

Detrital quartz is a common constituent of marine sediments in the central equatorial Pacific. Heath (1969) has shown that the percentage of quartz in the 2 - 20 μm carbonate-free sediment fraction of equatorial Pacific sediments depends on age. A correction was made for the detrital quartz content of the composite samples based on his data. Five percent of the SiO_2 content of samples 0 - 1 m.y. in age were subtracted from the carbonate-free silica concentration before determining opal content with the normative calculation. For samples 1 - 40 m.y. old, 2.5% SiO_2 were subtracted and for samples older than 40 m.y. 1% was subtracted from the carbonate-free SiO_2 concentration before correcting for non-biogenic silica.

Three different $SiO_2:Al_2O_3$ ratios were used to correct the bulk silica content for non-biogenic silica depending on the age of the sample. These ratios were determined by a study of the analytical and theoretical $SiO_2:Al_2O_3$ ratio in the principal non-biogenic sediment fraction, the clay minerals. A $SiO_2:Al_2O_3$ ratio of 3:1 was used to represent the non-biogenic silica fraction of sediments 0 - 5 m.y. old. Thus, three times the analytical concentration of Al_2O_3 were subtracted from the SiO_2 concentration; the remainder is biogenic silica. A ratio of 3.5:1 was used for subsequent samples except for those within 300 km of the point at which the site originated on the East Pacific Rise. (It took 5 to 8 m.y. for sites to migrate 300 km from their point of origin depending on the rotation rate of the Pacific plate during the interval.) For these samples a ratio of 4:1 was used.

The precision of the atomic absorption analyses varies from about 1 to 2% for Si and Al in samples low in calcium carbonate to about 2 to 5% for those high in carbonate. Comparison with USGS standard rocks and pure opal standard indicated no systematic error. Determinations of Al in standard rocks were accurate to ± 1 weight percent and Si determinations were accurate to ± 2 weight percent. The maximum error for the opal determinations using a $SiO_2:Al_2O_3$ ratio of 3:1 is, therefore, about ± 5% for low carbonate and ± 6% for high carbonate samples. For an $SiO_2:Al_2O_3$ ratio of 4:1 the errors are ± 6% and ± 7%, respectively. An additional source of error arises from using an $SiO_2:Al_2O_3$ ratio that is too high or too low. The effect of ratio variability is greatest at low opal concentrations and increases from zero at 100% opal to 12% when there is no opal in the sample for each integral departure from the correct ratio.

The X-ray technique for opal determination is thought to be accurate to ± 5% opal (Ellis, 1972). Only two of the thirteen samples run by both techniques differed by more than 5% opal when calculated on a salt-free basis. On a carbonate-free and salt-free basis the agreement was not as good, but it is likely that much of the error is due to inaccurate carbonate determinations.

RESULTS

The biogenic silica content of the composite samples was calculated on a bulk sediment basis and on a carbonate-free basis. All values were corrected for salt content. Using the bulk biogenic silica percentages, a biogenic silica accumulation rate was calculated using van Andel and others (1975) bulk accumulation rates in $g/cm^2/my$. These rates are independent of factors such as differential compaction of sediments and the dilution or masking effects of calcareous and non-biogenic sediments.

Carbonate accumulation rates were also calculated from the measured calcium carbonate contents. The percent biogenic silica, percent carbonate, and accumulation rates for each composite sample are listed in Appendix 3. The original chemical data used for the calculations are given in Appendix 4 (corrected for salt only) and Appendix 5 (corrected for salt and carbonate).

The first-order feature in the pattern of biogenic silica deposition in the central equatorial Pacific through the Cenozoic is a zone of maximum accumulation along the equator. Eight sites were sampled at intervals which included the time during which they crossed the equator (1 °N to 1 °S). The remainder either did not cross the equator, had a hiatus at the time of crossing, or were not cored over the equator-crossing interval. Of the eight sites sampled, five have distinct maxima associated with the crossing, one has a minimum, and two were not sampled at close enough intervals to define an equator-crossing peak, but do have accumulation rates charactertistic of the equatorial zone during that time interval (Figure 5).

The best evidence for the influence of the equatorial zone of high productivity on biogenic silica accumulation appears in a set of maps covering 9 discrete time intervals during the last 50 m.y. (Figure 6). The 9 intervals chosen correspond roughly to those of van Andel and others (1975) so that carbonate and biogenic silica accumulation can be compared. They chose 11 time intervals which were keyed to maxima and minima which they observed in the sedimentation rate (m/m.y.), accumulation rate ($g/cm^2/1000$ yr) and carbonate accumulation rate data. The time intervals used to map biogenic silica accumulation rates have been made somewhat longer in order to include enough data for reliable contouring. Where

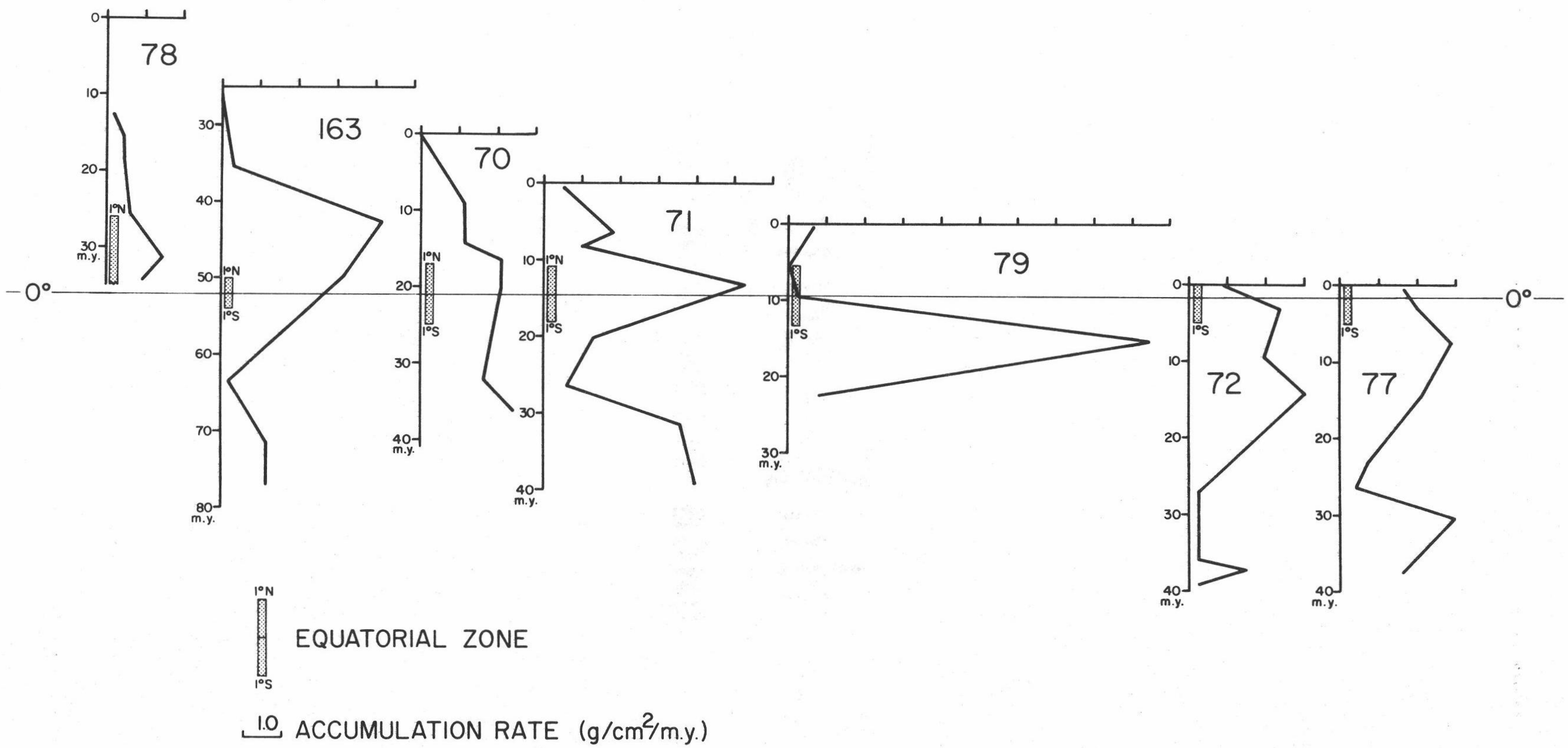

Figure 5. Biogenic silica accumulation rates in 8 sites which crossed the equatorial zone (1 °N to 1 °S) during the last 50 m. y.

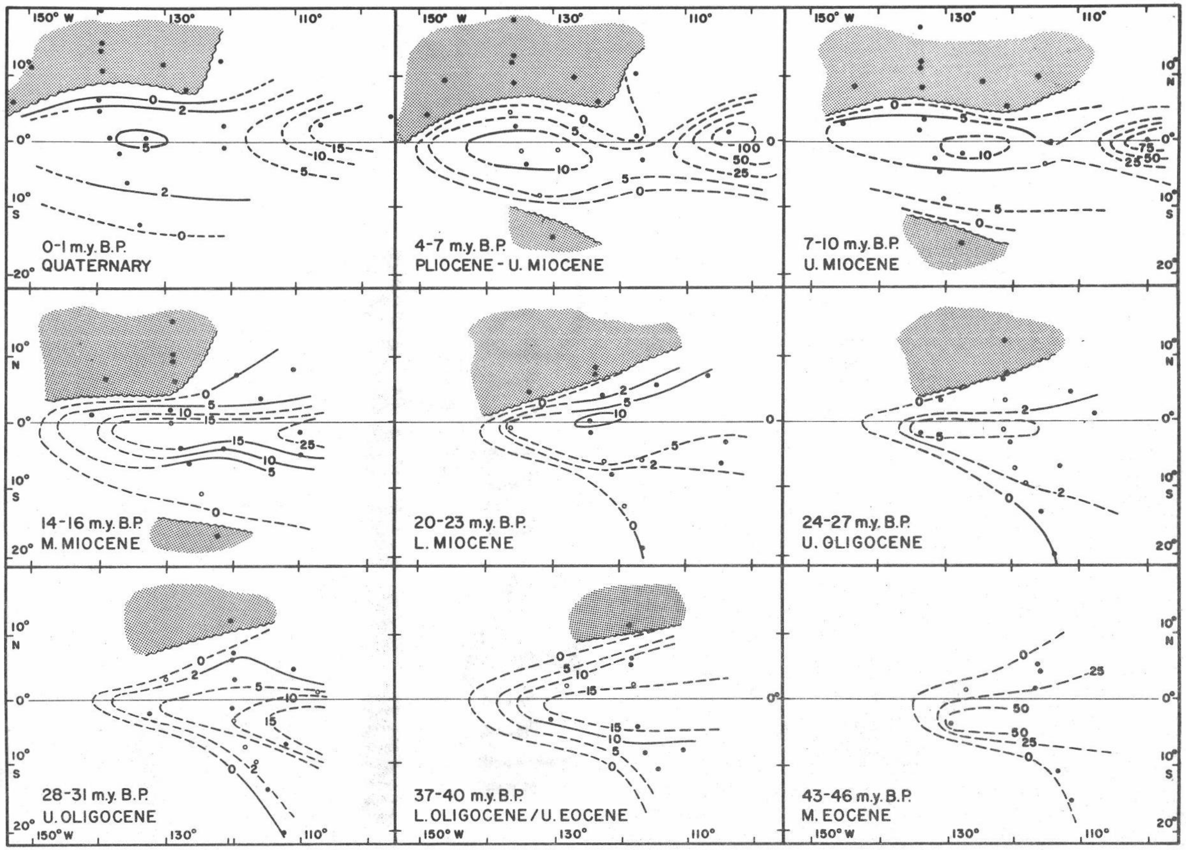

BIOGENIC SILICA ACCUMULATION RATE

(contours in g/cm²/1000 yr x 100)

Figure 6. Isopleth maps of biogenic silica accumulation for various intervals of the Cenozoic. Stippled pattern represents areas which have been eroded. Sites sampled during the interval are shown as dots. Open circles represent data extrapolated from within 1 m.y. of the mapped time interval.

justified, extrapolated data from either side of the interval for the remaining sites were used as a guide in contouring. Although the maps are based on widely spaced points, the excellent match between the 0 - 1 m.y. map and similar maps from the central equatorial Pacific based on many more points (Heath and others, in prep.) suggests that the shape of the equatorial zone and the range of accumulation rates defined by the data points are correct. Each time interval is characterized by an axis of maximum biogenic silica accumulation centered on or near the equator. For intervals prior to 25 m.y. the axes seem to be consistently offset to the south. At present, both the axis of maximum primary productivity and the axis of maximum opal content of recent central equatorial Pacific sediments are associated with meridional divergence located about 2° south of the geographic equator (Pak and Zaneveld, 1974; Heath and others, in prep.). It is unclear whether the southerly offset of the maximum accumulation axes for the four oldest intervals reflects this productivity pattern, or whether it results from an error in the Pacific plate rotation parameters used for 25 - 50 m.y. Van Andel and others (1975) also noted a southward offset of their oldest carbonate accumulation axes which they attributed to either imprecision in the positioning of the axes or to slight errors in the rotation parameters.

Biogenic Silica Accumulation Rates

The rate of accumulation of biogenic silica on the ocean floor is virtually indpendent of depth or of hydrographic features. Thus, it is a valuable tool for interpreting past rates of production of biological detritus in surface waters. Figure 7 shows the accumulation rate of biogenic silica at all sites during the last 50 m.y. The curves lack detail because the average sample spacing is 4 m.y. Nevertheless, three intervals of intensified opal accumulation can be recognized. During the Middle Eocene from about 42 - 45 m.y. ago, five of the seven sites show clear maxima. The remaining two, at 10° to 15°S, were well outside the equatorial high productivity zone. Deposition declined gradually from this time until about 25 m.y. ago. A second maximum is centered at 15 to 16 m.y., when all except one of the equatorial Pacific sites show an increase in opal accumulation rate. Two sites have major peaks and none of the sites have a minimum at this time. Finally, there is some suggestion of greater biogenic silica accumulation during the Upper Miocene to Pliocene (about 5 - 7 m.y. ago), although this maximum is not well defined. A distinct minimum occurred 25 - 27 m.y. ago when biogenic silica accumulation rates were lowest for the entire Tertiary and every site had a minimum or a declining accumulation rate. Except for sites near the East Pacific Rise, beneath the zone of highest Holocene primary

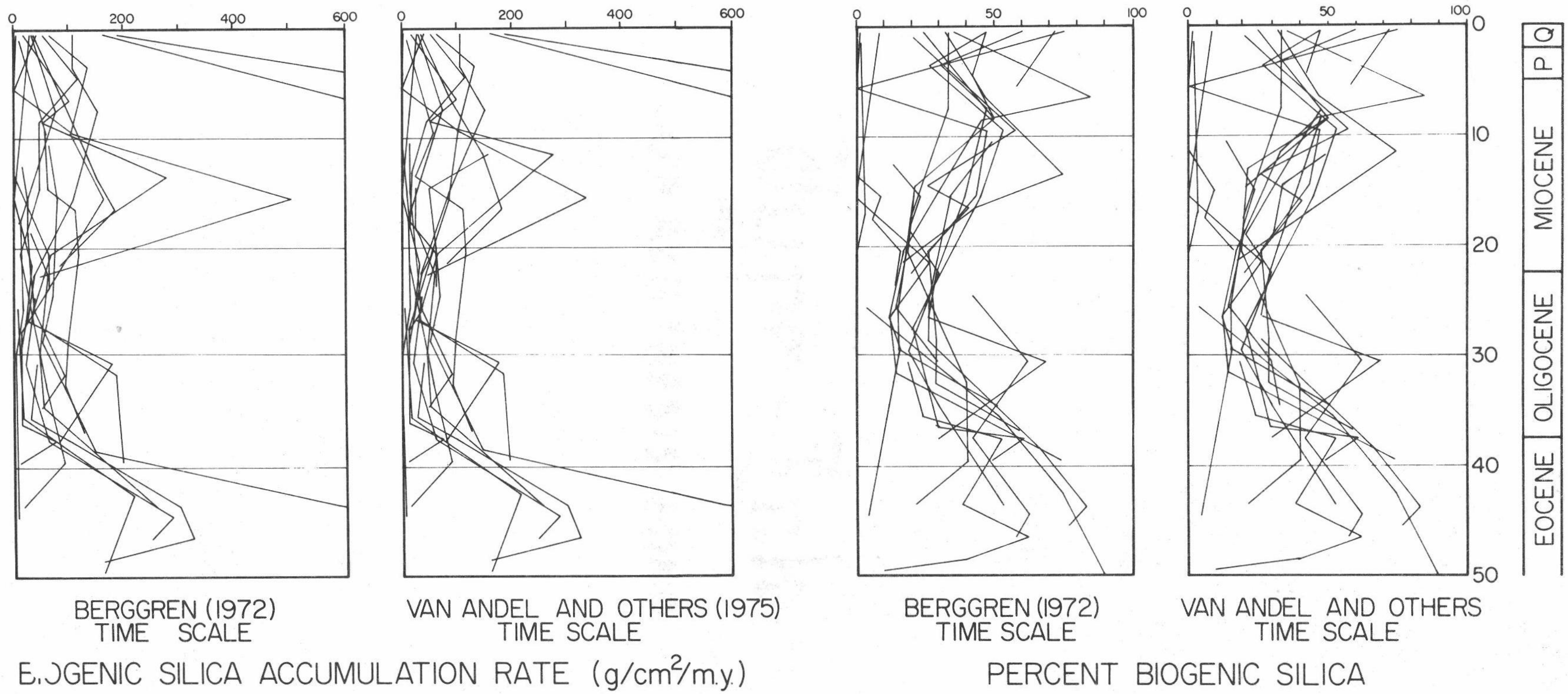

Figure 7. Biogenic silica accumulation rates and percent biogenic silica curves for each site plotted on the Berggren (1972) and van Andel and others (1975) time scales.

productivity, the interval from 0 - 1 m.y. is also characterized by very low opal accumulation rates.

Maps of the changes in opal accumulation through time (Figure 6) define the geographic limits of accumulation and of high productivity areas. The alternating periods of high and low productivity during the Cenozoic are especially striking in these maps. During the Oligocene biogenic silica accumulation rates in the equatorial Pacific decreased from their highest Tertiary values (250 - 500 $g/cm^2/m.y.$ during the Middle Eocene) to a mid-Tertiary low when accumulation rates averaged 30 $g/cm^2/m.y.$ Opal deposition then increased to a second maximum during the Middle Miocene. Although opal accumulation rates during this maximum are clearly larger than those of the rest of the Miocene, they are only about half those of the Middle Eocene. Several sites having low Middle Miocene accumulation rates were well outside the equatorial belt of high productivity (Figure 6). Since the Middle Miocene the deposition of biogenous silica has changed little, although there is some evidence for a small increase during the Pliocene. Further work is needed to determine whether this increase is real or due to a slight error in absolute age assignments.

Since the Middle Eocene, the biogenic silica accumulation has been highest along the equator (or just south of it). Since the Late Miocene a pattern of very high opal accumulation at the eastern end of the equatorial zone has been superimposed on the axial maximum.

It is difficult to set limits on the extent of the equatorial zone of biogenous deposition from the maps since the zero contour is poorly defined. Before the Early Miocene, southern sites indicate that the zero contour extended to at least 20°S in the east. Van Andel and others (1975) attribute a similar feature in carbonate accumulation rate maps to a broad shoal which enabled more carbonate to escape dissolution. However, since the dissolution of opal is not depth dependent, the similar pattern of opal accumulation suggests that this feature is related to surface productivity rather than bottom topography. There are no data for the Neogene to determine whether the feature persisted into upper Tertiary time. Similarly, a lack of data for the southwestern part of the central equatorial Pacific prior to 24 - 27 m.y. makes it impossible to determine whether the feature was a southward extension of the eastern high productivity zone or whether the entire zone was much wider during the early Tertiary and the contours should be more parallel to lines of latitude.

Biogenic Silica Content of Carbonate-Free Sediments

Additional insight into opal deposition patterns can be found in the percentage of biogenic silica in the carbonate-free sediment fraction (Figure 7). The carbonate-free opal percent is not modified by differential dissolution effects of depth, but it is sensitive to changes in the amount of non-biogenic sediment being deposited. Temporal variations in the percent biogenic silica parallel those of the biogenic silica accumulation rate. After the middle Eocene when opal made up more than 50% of the carbonate-free sediment fraction, the percentage decreased in all sites until 38 m. y. ago and in all but two sites until 27 m. y. ago. Upper Oligocene samples contain less than 25% biogenic silica in the carbonate-free fraction (Figure 7). After this minimum in opal content, which coincides exactly with that of the biogenic silica accumulation rate, the percent opal in equatorial Pacific sediments increased to a maximum centered at 8 m. y. Biogenic silica makes up about 40 - 50% of the carbonate-free fraction of those sediments.

Since then, the biogenic silica content first decreased to a low about 3 m. y. ago and then increased to present levels. Maps of silica content (Figure 8) show the equator-centered pattern seen in the accumulation rates, but the pattern is modified by the influx of non-biogenic sediment from the east which decreases the opal percentage. The dilution effect is seen most clearly in the Paleogene when opal content decreased to the east and west from a maximum centered along the equator, and is also apparent again in Quaternary sediments.

Non-Biogenic Sediment Accumulation Rates

The final element in any budget of central equatorial Pacific deposition is the non-biogenic sediment. This fraction is composed

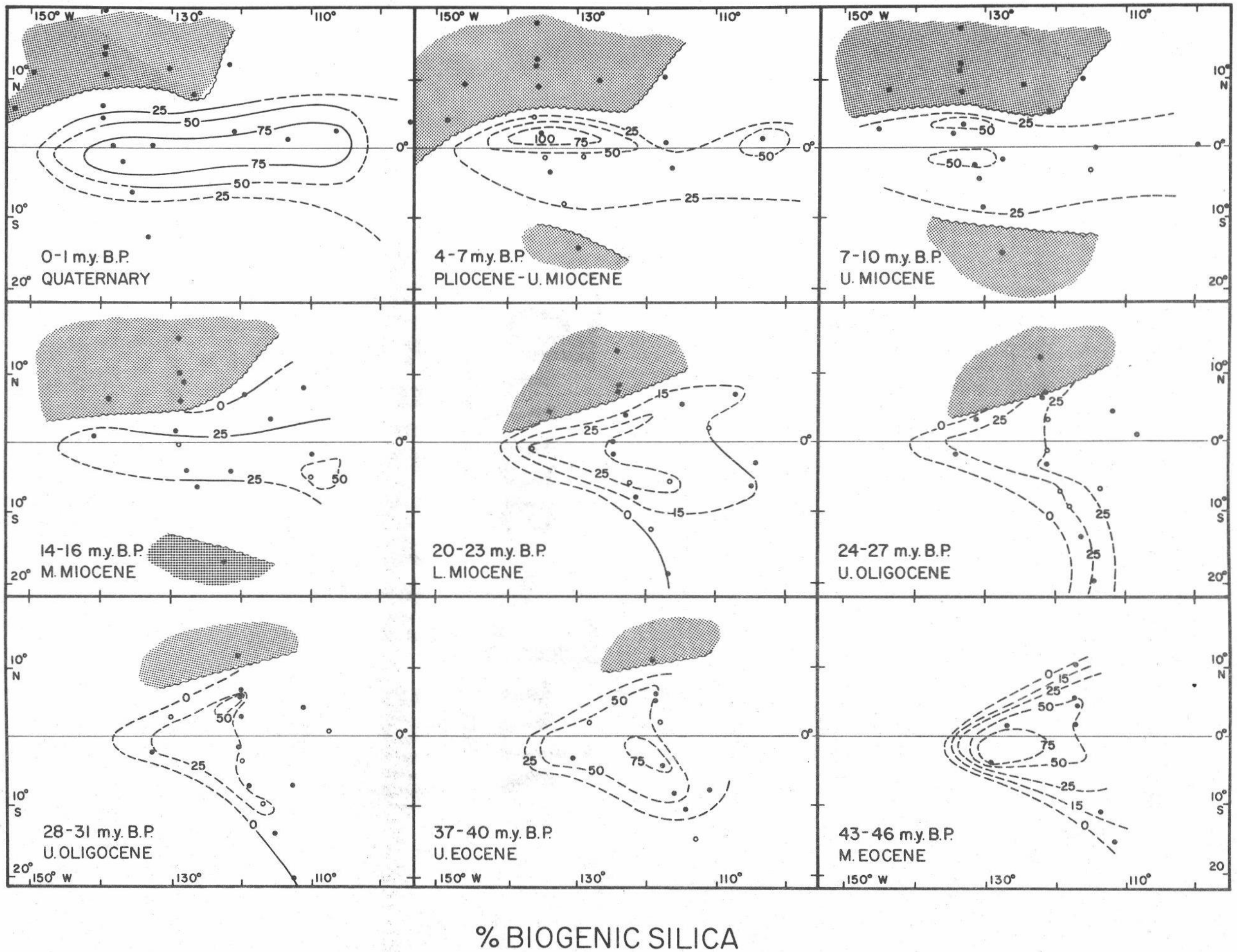

Figure 8. Maps of percent biogenic silica in sediments for various intervals of the Cenozoic. Stippled pattern represents areas which have been eroded. Open circles represent data extrapolated from within 1 m.y. of the mapped time interval.

of terrigenous material brought to the area from the east, volcanic ash and altered volcanic debris, and authigenic and hydrothermal material. The rate of accumulation of this component through time is dependent on a great many facts, but, with the exception of six points, all sampled intervals had accumulation rates below 400 $g/cm^2/m.y.$ and the rates did not vary systematically through time (Figure 9). This argues against serious distortion of the time scale and implies that long-term changes in opal content (Figure 7) did not result from dilution by non-biogenic sediment. Five of the accumulation rates above 400 $g/cm^2/m.y.$ reflect deposition close to the East Pacific Rise, a source of non-biogenic sediment: a lobate zone of accumulation extending west from the East Pacific Rise along the equator, and a zone of enhanced accumulation along the East Pacific Rise. The lobate forms of the isopleths of Figure 10 resemble the patterns for the biogenic sediments (Figure 6), but are not well-centered on the equator. There are two possible explanations. The normative silica correction may be too large and a portion of the biogenic silica may be included in the non-biogenic component. If this were true, however, the non-biogenic accumulation rates should display a periodicity like that of the biogenic silica accumulation rates. Furthermore, since the SiO_2:Al_2O_3 ratio used is largest in the early Tertiary samples, these should have the largest amount of excess non-biogenic sediment. This is clearly not the case; the lobate

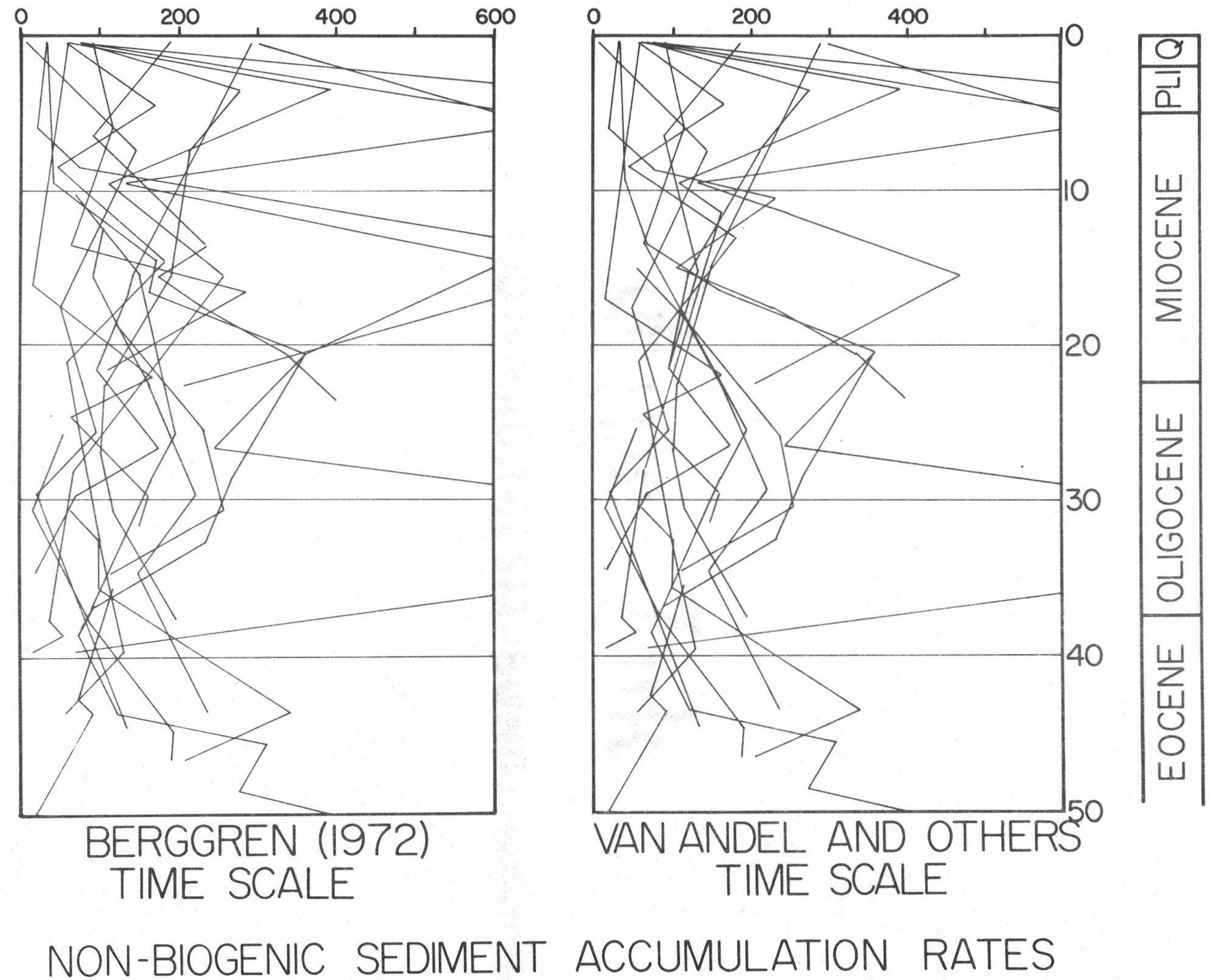

Figure 9. Non-biogenic sediment accumulation rates for each site plotted on the Berggren (1972) and van Andel and others (1975) time scales.

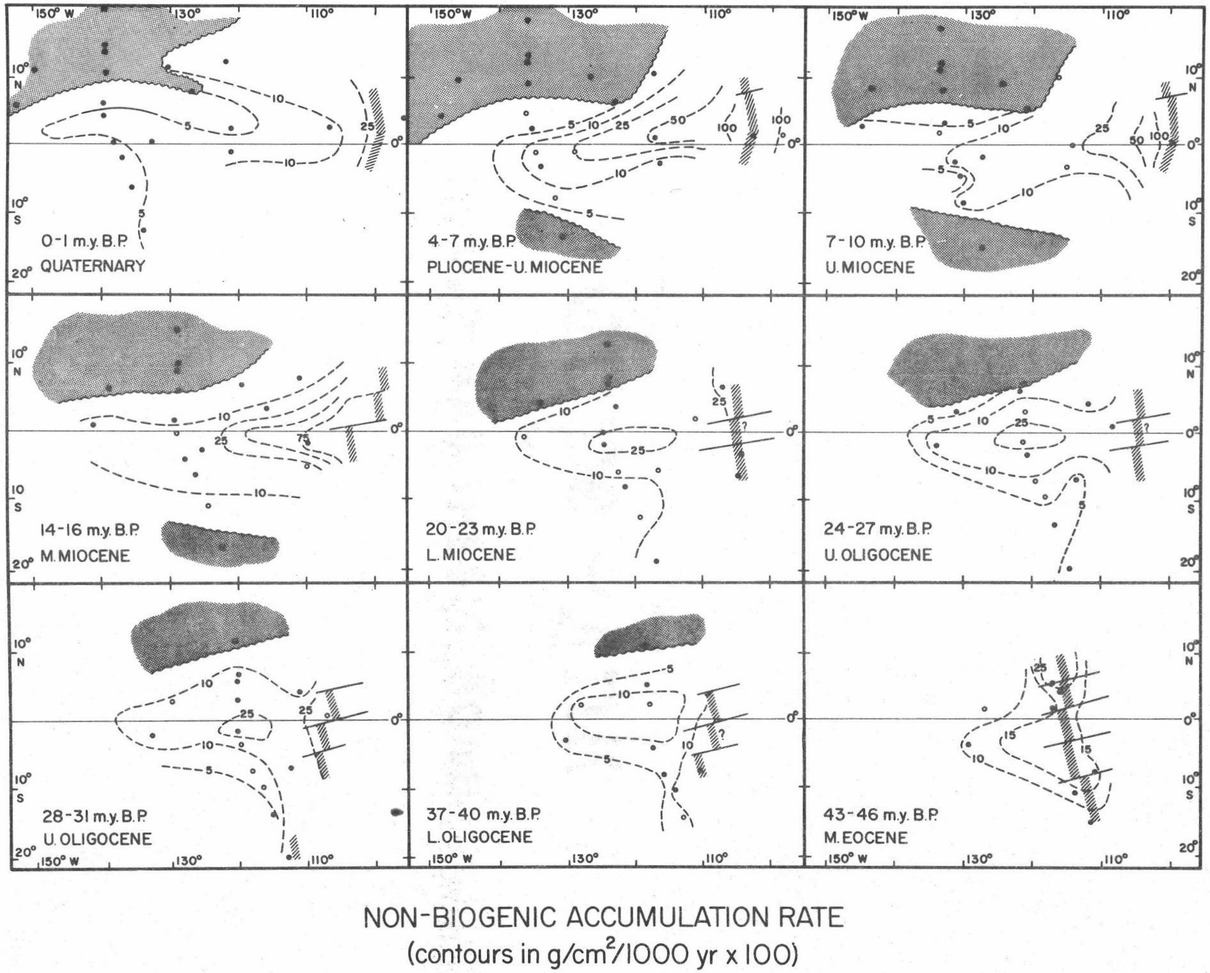

Figure 10. Isopleth maps of non-biogenic sediment accumulation for various intervals of the Cenozoic. Stippled pattern represents areas which have been eroded. Open circles represent data extrapolated from within 1 m.y. of the mapped time interval.

distribution pattern is least well developed during the early Tertiary. Although the accumulation rate along the East Pacific Rise crest varies a great deal through the Tertiary, the area enclosed by the lower value isopleths (the 10 $g/cm^2/1000 \times 100$ isopleth, for example) stays about the same until the Quaternary.

Secondly, the dispersal of non-biogenic sediment may be influenced by some factor or factors which also affect the distribution of plankton, for example, transport by the north and south equatorial currents. The South Equatorial Current, in which the upwelling responsible for high biological productivity occurs, may carry volcanic ash and terrigenous material westward. The northeast and southeast trade winds may complement the currents by depositing eolian dust in a belt along the equator.

DISCUSSION

Effects of Errors in the Time Scale

Van Andel and others (1975) found several maxima and minima in the rate of carbonate accumulation in the central equatorial Pacific. These authors considered the possibility that these maxima were due to internal distortion in the Berggren (1972) time scale, especially during the Miocene. They treated the problem in two ways: first by generating a time scale based on a constant sedimentation rate at each site (with the exception of equator crossings), and second, by constructing an alternative time scale for the Miocene based on radiometric ages from marine sections. They concluded that the constant sedimentation rate model as applied to five drill sites does not provide a reasonable time scale. The alternative Miocene time scale reduced a 14 - 15 m.y. sedimentation rate maximum and moved it to 14 - 16 m.y., but did not eliminate it. A new maximum was introduced at 10 - 11 m.y. Van Andel and others (1975) concluded that the rate maxima did not result from time scale errors and adopted the alternate time scale. Of the maxima in carbonate accumulation only those at 6 - 7, 14 - 15 and 42 - 46 m.y. are also evident in the biogenic silica accumulation rate. This is itself strong evidence against major distortion of the time scale. If the carbonate maxima were caused by errors in the time scale, apparent opal maxima would also occur and would match the carbonate maxima in relative magnitude and age.

Opal accumulation rates which were recalculated using the alternate Miocene time scale are compared with the earlier values based on Berggren's (1972) time scale in Figure 7. On the basis of the recalculated rates, only two sites have clear maxima at 14 - 16 m.y. and one of these represents an equator crossing. The accumulation rate increases in all sites from the 25 m.y. minimum to a maximum at 6 - 7 m.y. A comparison of accumulation rate maps for the Miocene time intervals using the Berggren (1972) time scale and the alternate time scale (Figure 11) confirms the change in biogenic silica accumulation. The new maps suggest that the Late Miocene was the time of most active silica sedimentation in the late Cenozoic.

The accumulation patterns for both time scales are plausible; neither has unreasonable maxima or minima. Thus, a choice between the two must be based on other information. Berggren and van Couvering (1974) proposed a scale similar to that of van Andel and others (1975) based on biostratigraphy and radiometric dating. There are also indications from within the data set that the alternate time scale proposed in van Andel and others (1975) is more reasonable than the Berggren (1972) time scale for the Middle Miocene. For example, with the exception of the Middle to Late Miocene, changes in the carbonate-free opal percent mirror changes in accumulation rates (calculated from the Berggren, 1972, scale). But there is no maximum in opal content to match the 14 - 16 m.y. opal accumulation rate maximum. The percent biogenic silica gradually increases from about 27 m.y. until about 7 - 10 m.y. ago. The alternate time scale changes the positions of the curves of percent biogenic silica vs. time (Figure 7) but does not change the silica percents themselves since they are experimentally determined values independent of the time scale. The maximum in opal content at about 7 m.y. ago become more pronounced using the alternate time scale. Thus, the accumulation rate and opal content data match more closely when the alternate

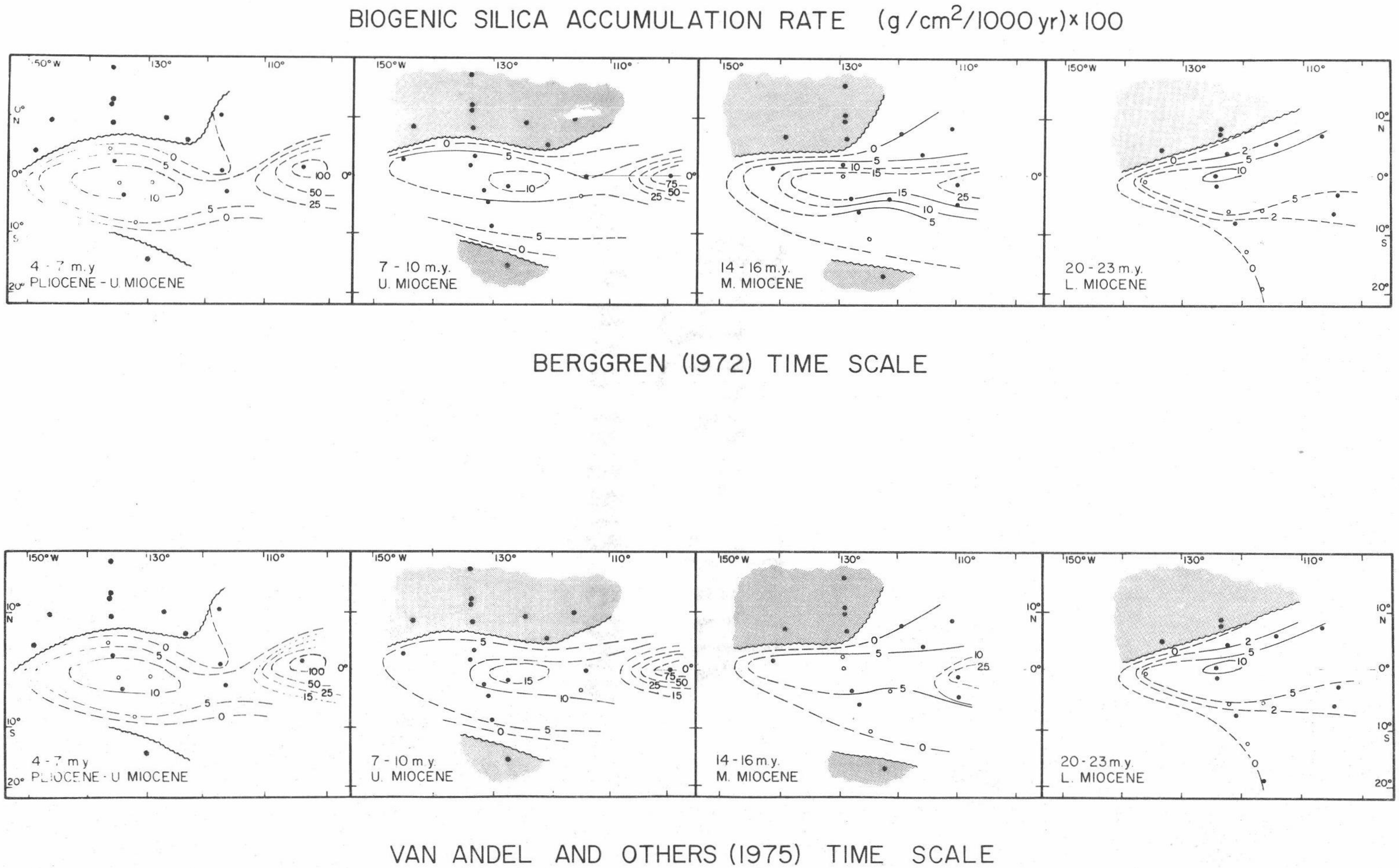

Figure 11. Comparison of isopleth maps of biogenic silica accumulation calculated with the Berggren (1972) and van Andel and others (1975) time scales. Stippled pattern represents areas which have been eroded. Open circles represent data extrapolated from within 1 m.y. of the mapped time interval.

time scale is used. The alternate scale will be used in all further discussion.

Surface Productivity

Because ocean waters are so highly undersaturated with respect to amorphous silica, most opal secreted as skeletal material dissolves in the water column during settling and in the bioturbated sediment layer. Hurd (1973) found that only 0.05 to 0.15% of the opal produced at the surface was preserved in his samples from the equatorial Pacific. However, his estimate was based on the amorphous silica productivity for equatorial regions given by Lisitzin (1972) which was calculated assuming that all opal productivity is a function of the primary productivity of organic carbon by diatoms. In the equatorial Pacific, radiolarians which are zooplankton of the second trophic level (grazers), make up a significant portion of the siliceous plankton. This increased the calculated production of opal which implies that Hurd's estimate of the amount of opal preserved is too low. Calvert (1968) suggested that about 2% of the opal produced through time has been incorporated into sedimentary rocks. This value is consistent with those proposed for marine sediments by Lisitzin (1971) and Heath (1974) and seems to be a reasonable estimate of the amount of opal finally incorporated into the geologic record. This figure has been used to estimate the siliceous surface productivity of the central equatorial Pacific during the last 50 m.y. (Figure 12). Two opal supply curves are shown. The first, "regional supply," is the supply of biogenic silica to the area averaged over all sites in each time interval. The second, "equatorial supply," is a curve for sites within 3° of the equator or paleoequator. The values are rough estimates and the supply is assumed to be a linear function of accumulation rate (supply x 0.02 = accumulation). The large supply indicated for 4 - 7 m.y. is strongly influenced by one value from the eastern end of the high productivity zone. This site was on the East Pacific Rise at the time the accumulation rates for all components are almost an order of magnitude higher than those for the rest of the equatorial Pacific, the high biogenic silica accumulation rates may represent addition of hydrothermal silica or downslope transport of material to a sediment pond on the East Pacific Rise. The dashed curve represents the regional supply rate recalculated without the anomalous point. In addition, Figure 12 shows an estimate of the carbonate supply rate. This estimate is van Andel and others' (1975) "extrapolated surface supply in the equatorial area" (3°N to 3°S) which assumes a constant dissolution rate to the surface. In fact, of course, some of the variation in "extrapolated supply" is undoubtedly due to changes in the depth of the lysocline.

If one assumes that calcareous and siliceous productivity generally co-vary, the biogenic silica supply can be used to interpret the

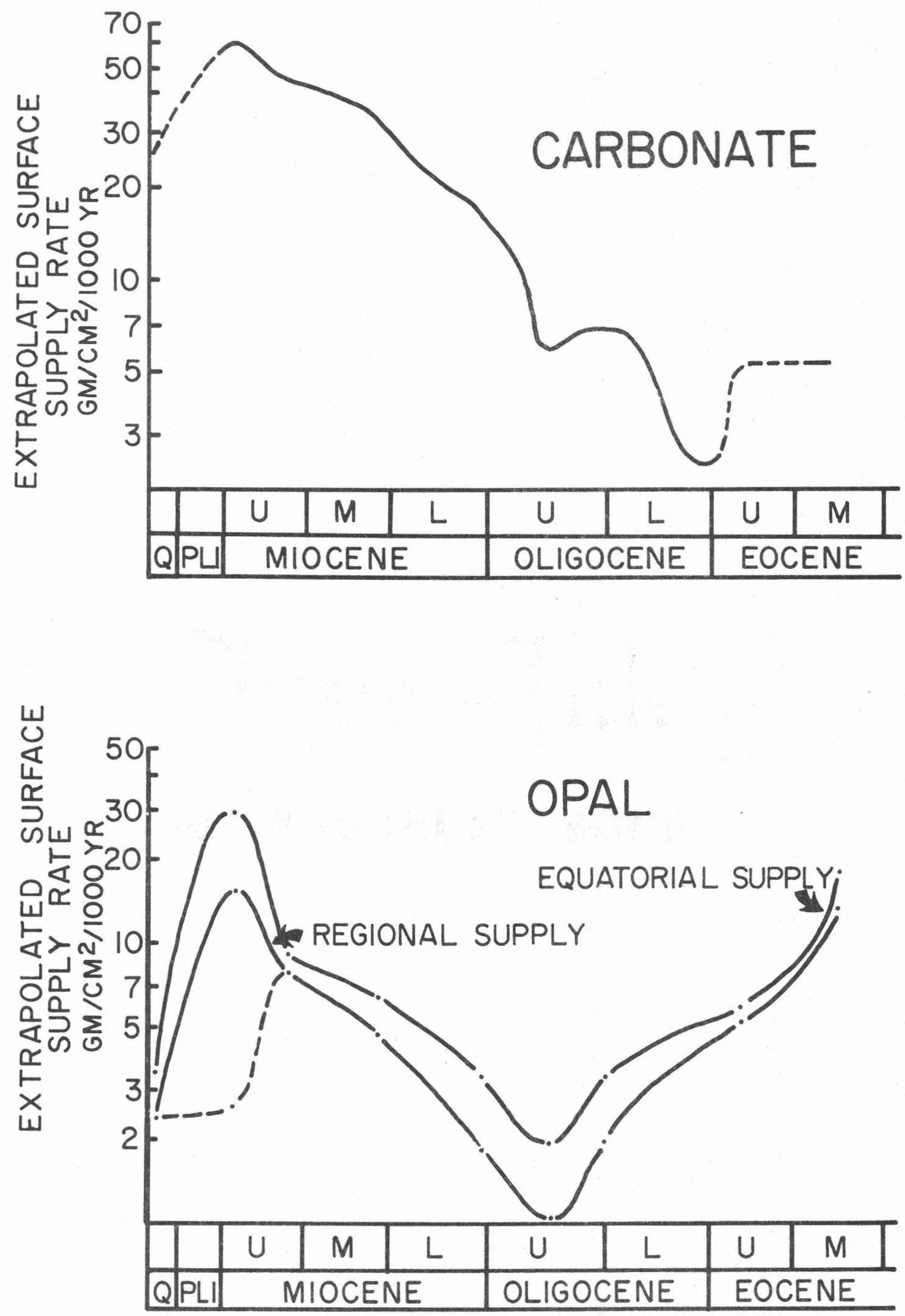

Figure 12. Extrapolated rates of supply of biogenic components for the last 50 m. y. Carbonate supply diagram from van Andel and others (1975). Opal supply represented by "equatorial" curve includes only sites within 3° of the paleoequator. "Regional" supply includes all sites. Dotted curve is regional supply recalculated to exclude anomalous accumulation rates along the East Pacific Rise.

carbonate supply curve. This may not be a good assumption for intervals prior to the Late Eocene, when there are indication that the carbonate supply was very low (van Andel and others, 1975; van Andel, 1975) at a time of high siliceous productivity. Since that time, however, the equatorial current system seems to have been stable and to have supplied nutrients to support a plankton population whose distribution is much like that of the present.

Comparison of Carbonate and Biogenic Silica Accumulation and Supply

Van Andel and others (1975) found carbonate accumulation rate maxima at 2, 6 - 7, 10 - 11, 21 - 22, and 28 - 30 m.y. ago. Two maxima in siliceous productivity are indicated by this study: one at 42 - 46 m.y. ago and one at about 10 - 12 m.y. The middle Eocene maximum is missing in the carbonate accumulation rate curves. At that time the CCD for the entire Pacific (CCD_{pac}) and for the equatorial zone (CCD_{eq}, 3°N to 3°S) were far above their present levels (see Figure 13 after van Andel and others, 1975), so that calcite was deposited only at sites on the East Pacific Rise. At the end of the Eocene the CCD dropped precipitously and carbonate accumulation increased gradually to the maximum between 28 and 30 m.y. ago. Van Andel and others (1975) suggests that in addition to enhanced preservation of calcareous skeletal material following the deepening of

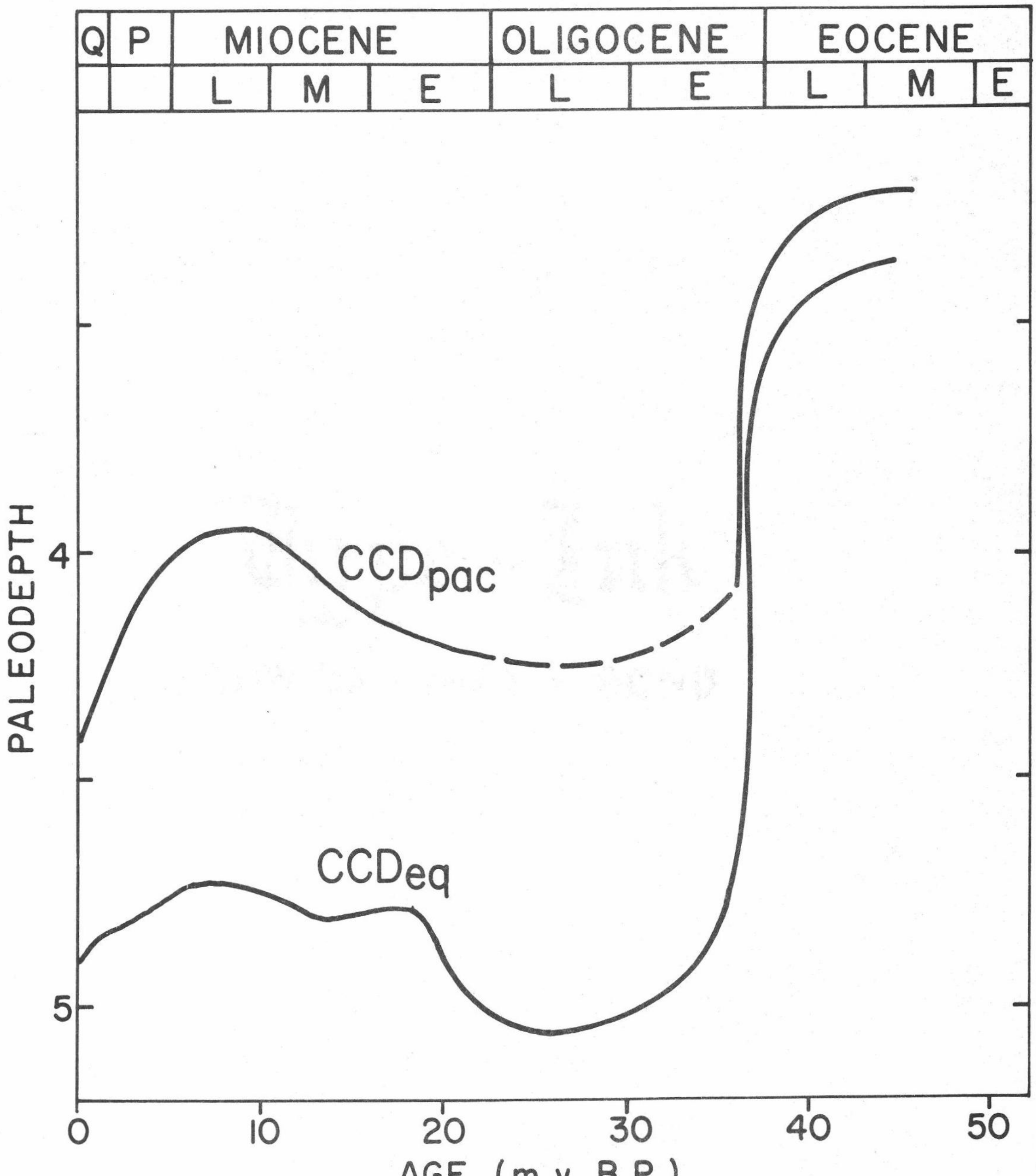

Figure 13. Variation in depth of calcium carbonate compensation depth with time (from van Andel and others, 1975).

the CCD, the supply of carbonate increased during this time. They also suggest that an increase in the non-carbonate accumulation rate at the same time reflects increased biogenic silica supply. When the non-biogenic component is subtracted from the non-carbonate fraction, however, this increase in biogenic silica is not apparent. The accumulation rate over the entire area was actually less than the early Oligocene rate. Both the "equatorial zone" and "regional" supply of opal were declining during this interval (Figure 12). Thus, the increased "extrapolated supply" of carbonate reported by van Andel and others (1975) probably represents a deepening of the lysocline rather than an increase in supply.

Both carbonate and biogenic silica curves have accumulation rate minima at 25 m.y., suggesting that the middle of the Late Oligocene was a period of very low plankton productivity in the equatorial Pacific. The appreciable carbonate accumulation at that time must have been due only to reduced dissolution of calcite.

The early Miocene maximum (21 - 22 m.y.) in carbonate accumulation was not as large as the 38 - 40 m.y. peak. There is no corresponding peak in opal accumulation rates which were still extremely low compared to other Tertiary times although about twice the 25 m.y. minimum values. The smaller size of the carbonate high may show the effect of the generally low productivity when coupled with enhanced dissolution and/or a shoaling lysocline.

The next major peak in carbonate accumulation is at 10 - 11 m.y. (alternate time scale). Two composite silica samples in the interval from 10 - 12 m.y. show opal maxima, but they do not, by them themselves, define a peak in the opal accumulation. If carbonate accumulation rates are plotted for only those time intervals in which biogenic silica accumulation rates are available, the 10 - 11 m.y. peak is not evident. Only a peak at 7 m.y. is apparent. A Late Miocene silica productivity maximum at 7 m.y. corresponds to a small peak in carbonate accumulation. Since the CCD_{eq} and CCD_{pac} were shallower than at any other time during the Neogene at 7 - 8 m.y. and were above the paleodepth of several sites at that time, a significant increase in carbonate supply may be masked by enhanced dissolution. Holocene and Quaternary carbonate accumulation rates have remained low even though the CCD_{eq} and CCD_{pac} have returned to deep levels. The surface productivity is indicated by opal accumulation rates has decreased since the Late Miocene. The present situation seems analogous to the 25 - 27 m.y. period when the CCD was deep but little carbonate accumulated because of low surface productivity.

Paleoceanography

Opal accumulation in the equatorial Pacific is directly related to the productivity of surface waters (Pisias, 1974). The high plankton productivity is, in turn, dependent on high nutrient concentrations in waters upwelled from below the thermocline (Ryther, 1963). Therefore, changes in opal accumulation in the central equatorial Pacific through time can be used to place constraints on the strength of upwelling at the equator in the past.

Upwelling along the central and eastern Pacific equator is related to two features of the circulation:

1) Most upwelling is due to meridional divergence of waters in the South Equatorial Current under the influence of the southeast trade winds. Since the deflecting Coriolis force disappears at the equator, the Eckman transport changes from southwest to northeast across the equator causing deeper waters to rise to the surface (Cromwell, 1953; Pak and Zaneveld, 1974).

2) Since the discovery of the Equatorial Undercurrent or Cromwell Current, it has been postulated that this current brings regenerated nutrients in the upper part of the thermocline to the surface by vertical mixing and by forcing waters above it to diverge (Knauss, 1966; Jones, 1973). Surfacing of the Undercurrent has been observed to cause upwelling southwest of the Galapagos (Pak and Zaneveld, 1974).

It can, therefore, be inferred that changes in the intensity of equatorial upwelling with time are due to changes in the strength or position of the South Equatorial Current or to changes in the strength, position or amount of vertical mixing in the Equatorial Undercurrent. There are two ways in which these changes may have taken place:

1) Climatically controlled changes in the position of the southeast trade winds may have led to variation in the strength of the South Equatorial Current and Equatorial Undercurrent. This would cause variation in the total amount of upwelling and/or in the proportion of upwelling due to meridional divergence compared with that due to surfacing of the Equatorial Undercurrent.

2) Tectonic changes in the boundaries of the Pacific Ocean may have caused reorganization of equatorial circulation and have changed the strength and position of equatorial upwelling.

Wyrtki (1974b) has related fluctuations in the position and strength of the equatorial currents to the trade winds and has shown that the equatorial currents are influenced more by the position of the trade winds than by their strength. Fluctuations in the Equatorial Undercurrent fluctuations are synchronous with those in the South Equatorial Current while those of the Equatorial Countercurrent are synchronous with the North Equatorial Current (Wyrtki, 1974a). The two sets of currents are out of phase. During the Northern Hemisphere summer the southeast trade winds extend furthest to the North. The South Equatorial Current and the Equatorial Undercurrent are weakest at this time (Wyrtki, 1974b).

Climatically controlled variation in circulation have certainly influenced productivity of the equatorial Pacific during the Quaternary (Luz, 1973; Dinkelman, 1974; Pisias, 1974; Molina-Cruz, 1975). In a study of Quaternary sediments from the southeastern subtropical Pacific Molina-Cruz (1975) found that the strength of the South Equatorial Current was related to the position of the southeast trade winds during the late Quaternary as indicated by the concentration of detrital quartz carried to the ocean by these winds. The strength of the South Equatorial Current also determined the amount of upwelling associated with the Equatorial Undercurrent: when the South Equatorial Current was weak the Undercurrent was able to surface causing upwelling and intensified productivity of its associated fauna. Molina-Cruz (1975) also found that the faunal component associated with the Equatorial Undercurrent was highly correlated with opal production and that opal accumulation rates were highest where the Equatorial Undercurrent broke the surface, both at present and in the past. Opal accumulation rates in the Panama Basin determined by Dinkelman (1974) were also highly correlated to a faunal assemblage associated with the Equatorial Undercurrent.

The high productivity associated with equatorial upwelling is reflected in maps of biogenic silica accumulation for the last 50 m.y. (Figures 6 and 11). Holocene primary productivity is also highest at the eastern end of the central equatorial Pacific where there is intensified upwelling associated with the Equatorial Undercurrent west of the

Galapagos. Without additional evidence it is difficult to determine whether similar upwelling took place in the Cenozoic, but map intervals since the middle Miocene (Figure 6) do show enhanced opal accumulation rates to the east.

Quaternary climate changes have taken place over a few thousand years so that it is difficult to draw analogies between them and the long term trends in global climate of the last 50 m. y. Nevertheless, one important characteristic should be common to any global change in climate: cooler climates appear to be accompanied by greater equator-to-pole temperature gradients, which cause the major wind belts to shift toward the equator and to become stronger (Lamb and Woodroffe, 1970; Newell, 1974). A northward shift and intensification of the southeast trade winds would cause enhanced upwelling in the South Equatorial Current. An extreme southward shift would cause the South Equatorial Current to weaken but might allow the Equatorial Undercurrent to surface.

Cenozoic paleotemperatures for surface and bottom waters based on oxygen isotope determinations in the central north Pacific (Douglas and Savin, 1973) and in the high latitudes of the south Pacific (Shackleton and Kennett, 1975) indicate that the overall climate trend for the entire Cenozoic has been on of global cooling. The temperature of the Pacific has gradually declined through the Cenozoic with a major phase of cooling at the boundary between the Eocene and the

Oligocene and some warming during the early to middle Miocene. If a major drop in surface water temperature like the one at the Eocene-Oligocene boundary (about 5° of cooling, Shackleton and Kennett, 1975) affected equatorial circulation in the same manner as cooling associated with Quaternary glacial ages, it should have caused an overall intensification of the southeast trade winds, strengthening of the South Equatorial Current, and an increase in upwelling related productivity. There is, however, no increase in opal accumulation during the early Oligocene (Figure 6) and no increase in extrapolated surface supply of opal (Figure 12). In fact, the late Eocene and early Oligocene are times of decreasing opal supply and accumulation in the equatorial Pacific. Not until the early Miocene (20 - 23 m.y. ago) did opal supply rates begin to increase again and they did not reach the late Eocene values until the middle to late Miocene. Thus, global cooling does not lead inevitably to increased equatorial productivity.

The middle Miocene to early late Miocene (10 - 13 m.y. ago) was also a time of major development of the ice cap on East Antarctica and of the first recorded ice rafting in northern Antarctic waters (Kennett and others, 1975). Thus, the increasing opal supply may be related to circulation changes accompanying ice cap development rather than to those associated with non-glacial global cooling. Newell (1974) has suggested that ice ages are caused by changes in the poleward energy flux in the atmosphere and ocean. Geological evidence for reduced oceanic energy transport during glacial ages (McIntyre and others, 1972), increased temperature of upwelling water before ice caps begin to melt (Imbrie and others, 1973) and a lag time between changes in bottom water temperature and changes in surface circulation (Pisias and others, 1975) supports Newell's model. Polar ice cover and low latitude upwelling are important constraints on temperature fluctuations and atmospheric circulation in this model suggesting that they may be closely related.

From the preceding discussion, it is apparent that only the increase in opal supply during the middle Miocene to late Miocene can be explained in terms of climatic controls on the circulation of the equatorial Pacific. The decline in opal supply from the middle Eocene to early Miocene, on the other hand, cannot be related to the global cooling that took place during that time. In addition, the decrease in opal supply in the Equatorial Pacific since the Pliocene, while glaciation has been extended to the Northern Hemisphere and sea surface temperatures have decreased slightly (Shackleton and Kennett, 1975) indicates that even the Pliocene change should not be attributed to global climatic fluctuations.

The circulation pattern in the equatorial Pacific is influenced not only by the wind patterns, but by the shape of the Pacific Ocean basin. The South Equatorial Current is fed by eastern boundary currents moving north along the coast of South America and by the

Equatorial Undercurrent which is deflected to the south in the eastern Pacific (Figure 14). The western Pacific is blocked by land masses so that the trade winds pile up water and create a pressure gradient which drives subsurface water back to the east as the Equatorial Undercurrent (Veronis, 1960).

During the last 50 m.y. three major tectonic events have changed the geography and the circulation patterns of the equatorial Pacific:

1) The northward migration of Australia has closed a passage from the western Pacific to the Indian Ocean and to the low latitude inter-ocean seaway, Tethys.
2) The separation of Australia from Antarctica has allowed the development of the high latitude Antarctic Circumpolar Current.
3) The elevation of Central America and closing of the Isthmus of Panama has interrupted low latitude circulation between the Pacific and Atlantic Oceans.

The closing of the western Pacific was probably the first of these events to occur. Separation of Australia from Antarctica started about 55 m.y. ago (Weissel and Hayes, 1972). A deep equatorial passage existed north of Australia and south of Asia until the middle Eocene (Kennett and others, 1972), but as the Australian landmass moved north the exchange of Indian and Pacific waters was gradually restricted. India was also moving north at this time

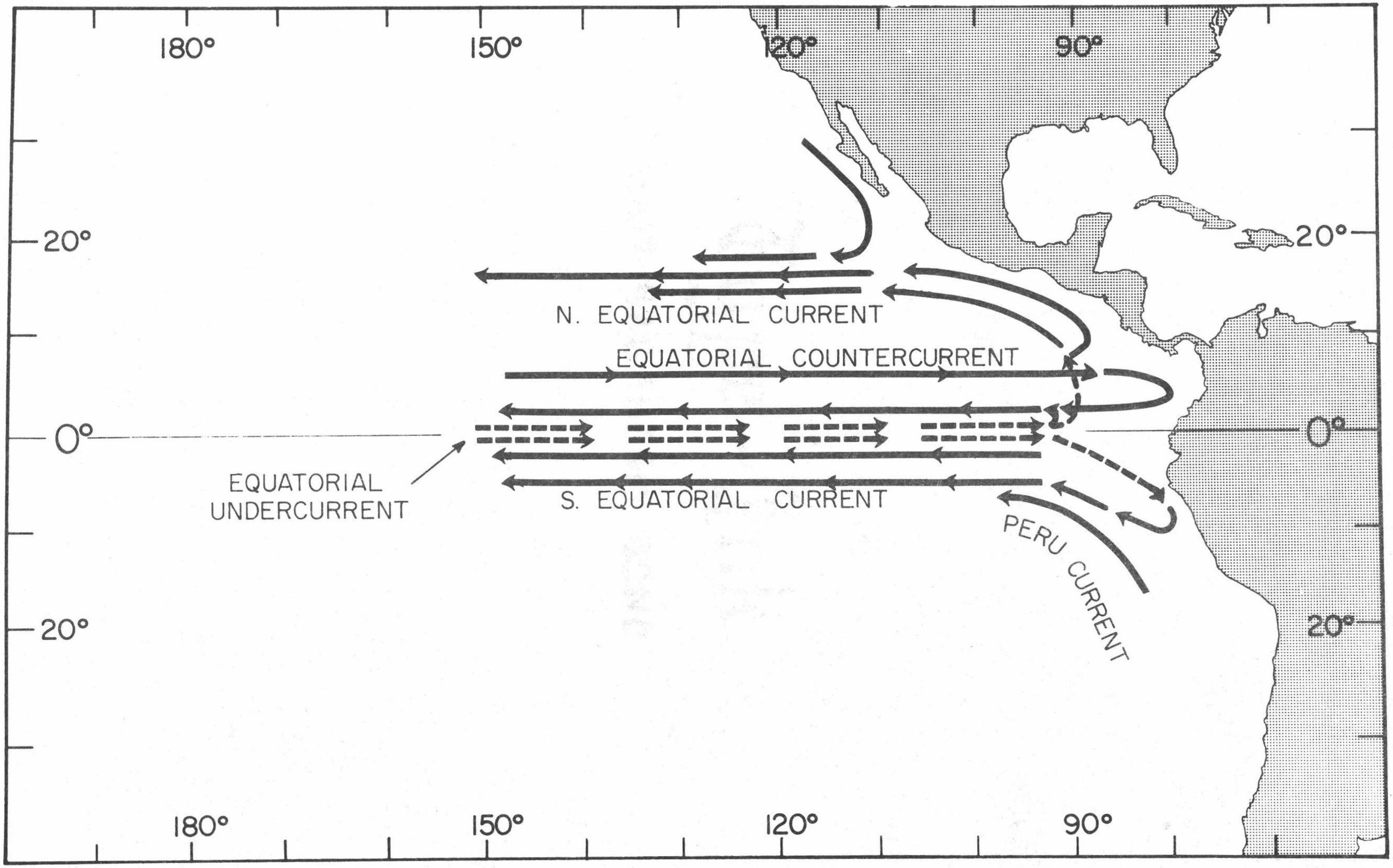

Figure 14. Present circulation of the equatorial Pacific Ocean (from Wyrtki, 1967).

(McKenzie and Sclater, 1971) further inhibiting Pacific to Indian flow. This passage was closed in the late Eocene to early Oligocene (Moberly, 1972) by tectonism in southeast Asia (Katili, 1971), in the Philippines (Gervasio, 1964) and in northern Australia (Veevers, 1969). Before this closure a "Tethys" current is presumed to have circulated from east to west through the passage between North America and South America, across the north Pacific and into the Indian Ocean. There is also evidence of a strong current from the Indian Ocean to the Pacific north of Australia at this time (Kennett and others, 1972).

The Eocene and Oligocene were times of declining siliceous productivity in the equatorial Pacific. The Equatorial Undercurrent could not have developed before the early Oligocene when the western Pacific was blocked off. This implies that unless there was another mechanism for bringing nutrient-rich waters to the surface, the decline in fertility of equatorial Pacific waters was due to a decrease in the upwelling associated with meridional divergence. Luyendyk and others (1972) have postulated that closure of the western Pacific led to sluggish circulation in the equatorial Pacific because the Tethys current could no longer flow around the globe and because the strong Indian to Pacific current north of Australia was cut off. The gradually declining opal productivity during the Eocene and Oligocene is consistent with such a model.

The development of the Antarctic Circumpolar Current after the separation of Australia from Antarctica was the second major event in the development of modern Pacific circulation. It was not until the middle to late Oligocene that the separation was complete and that the Antarctic Circumpolar Current was free to circulate through the passage between the two continents (Kennett and others, 1975). The effect of this even on the equatorial Pacific productivity was indirect. The development of the circumpolar current increased the residence time of waters in high latitudes and probably contributed to the global cooling that has taken place through the Neogene even though there was no abrupt change in surface temperatures associated with the initiation of the current.

The initiation of the Antarctic Circumpolar Current has had a major effect on the vertical structure of the Pacific Ocean, however, through its influence on the production of bottom waters near the Antarctic continent (Kennett and others, 1975). These bottom waters have largely controlled the record of carbonate accumulation in the central equatorial Pacific through solution effects (van Andel and others, 1975), but have not directly influenced rates of opal supply or accumulation. Minor upwelling associated with mixing in the Antarctic convergence zone is first evident in early Miocene sediments deposited about 22 m.y. ago (Kennett and others, 1975). The intensity of upwelling remained low until the late Miocene to early

Pliocene (4.2 - 5 m.y. ago) when there was a major increase in upwelling and biological productivity (Keany and Kennett, 1975). This is contemporaneous with the decline in opal productivity in the equatorial Pacific that has continued to the Holocene. If the decline in opal productivity in the equatorial Pacific that has continued to the Holocene. If the decline in opal productivity in the equatorial Pacific during the last 4 - 5 m.y. is due to increased productivity of the Antarctic convergence zone it is analogous to changes in equatorial Pacific carbonate accumulation which have also been attributed to changes in rates of deposition in other parts of the ocean (van Andel, 1975; van Andel and others, 1975; Luz and Shackleton, 1975).

The final important tectonic event for Pacific circulation was the closing of the seaway across the Isthmus of Panama during the middle or late Pliocene (Kaneps, 1970; Malfait and Dinkelman, 1972). There is little available information about the effect of this closure on Pacific circulation. Since the seaway was north of the equator, flow from the Atlantic to Pacific (Luyendyk and others, 1972) probably influenced the North Equatorial Current rather than the South Equatorial Current with which present upwelling is associated.

In summary, the history of biogenic silica productivity and accumulation during the last 50 m.y. in the equatorial Pacific may be separated into three phases:

Phase I: Middle Eocene - late Oligocene (50 - 25 m.y.)

During this time the influence of the low latitude circum-global Tethys seaway on the equatorial Pacific was waning, apparently producing a decrease in the intensity of equatorial circulation, reduced meridional divergence and lowered fertility of equatorial Pacific waters. The supply and accumulation of opaline sediments decreased gradually throughout this interval to reach its lowest Tertiary level about 25 m.y. ago. Global ocean temperatures declined, possible as a result of the transition from the long term residence of ocean waters in low latitudes (Tethys) to the long term residence in high latitudes (Antarctic Circumpolar current) but did not directly affect equatorial Pacific productivity.

Phase II: Late Oligocene - late Miocene (25 - 5 m.y.)

After the late Oligocene the fertility of equatorial Pacific waters increased. The onset of glaciation in Antarctica in the early Miocene was accompanied by intensified circulation in the equatorial Pacific. The blocking of the western Pacific allowed the development of an equatorial undercurrent. Upwelling related to this current probably supplemented meridional divergence beginning the Late Miocene and further increased the fertility of equatorial Pacific waters. Opal supply continued at high levels through the Miocene.

Phase III: Pliocene - present (5 - 0 m.y.)

After the full development of upwelling at the Antarctic convergence zone, opal supply in the equatorial Pacific declined. This may be due to the concentration of oceanic biogenic silica productivity at the Antarctic convergence at the expense of equatorial regions.

REFERENCES

Arrhenius, G., 1952, Sediment cores from the East Pacific: Rept. Swedish Deep-Sea Exped., 1947-1948, v. 5, pt. 3, p. 189-201.

Bennett, R. H., and Keller, G. H., 1973, Physical properties evaluation, in van Andel, Tj. H., and Heath, G. R., eds., Initial Reports of the Deep Sea Drilling Project: U.S. Government Printing Office, Washington, D. C., v. 16, p. 513-519.

Berger, W. H., 1970, Planktonic foraminifera; selective solution and the lysocline, Marine Geol., v. 8, p. 111-138.

__________, 1973, Cenozoic sedimentation in the eastern tropical Pacific, Geol. Soc. Amer. Bull., v. 84, p. 1941-1954.

Berggren, W. A., 1972, Cenozoic time scale: some implications for regional geology and paleo-biogeography, Lethaia, v. 5, p. 195-215.

Berggren, W. A., and van Couvering, J. A., 1974, The late Neogene, biostratigraphy, geochronology and paleoclimatology of the last 15 million years in marine and continental sequences, Paleogeog., Paleoclimat., Paleoecol., v. 16.

Bernas, B., 1968, A new method for decomposition and comprehensive analysis of silicates by atomic absorption spectrometry, Anal. Chem., v. 40, p. 1682-1686.

Bezrukov, P. L., 1955, Distribution and rate of deposition of silicate sediments in the Sea of Okhotsk, Doklady Acad. Nauk., v. 103, p. 473-476.

Biscaye, P. E., 1965, Mineralogy and sedimentation of recent deep-sea clay in the Atlantic Ocean and adjacent seas and oceans, Geol. Soc. Amer. Bull., v. 76, p. 803-832.

Boström, K., and Fisher, D. E., 1971, Volcanogenic uranium, vanadium, and iron in Indian Ocean sediments, Earth Planet. Sci. Lett., v. 11, p. 95-98.

Boström, K., Joensuu, O., Valdes, S., and Riera, M., 1972, Geochemical history of South Atlantic Ocean sediments since the last Cretaceous, Marine Geol., v. 12, p. 85-122.

Bramlette, M. N., 1961, Pelagic sediments, in Sears, M., ed., Oceanography, Amer. Assoc. Advancement Science, Washington, D. C., Publ. 67, p. 345-366.

Burckle, L. D., Ewing, J. I., Saito, T., and Leyden, R. R., 1967, Tertiary sediments from the East Pacific Rise, Science, v. 157, p. 537-540.

Calvert, S. E., 1966, Accumulation of diatomaceous silica sediments in the Gulf of California, Geol. Soc. Amer. Bull., v. 77, p. 569-596.

__________, 1968, Silica balance in the ocean and diagenesis, Nature, v. 219, no. 5157, p. 919-920.

Chayes, F., 1960, On correlation between variables of constant sum, Jour. Geophys. Research, v. 65, p. 4185-4193.

Chester, R., and Elderfield, H., 1968, The infrared determination of opal in siliceous deep-sea sediments, Geochim. Cosmochim. Acta, v. 32, p. 1128-1140.

Clague, D. A., and Jarrard, R. D., 1973, Tertiary plate motion derived from the Hawaiian - Emperor chain, Geol. Soc. Amer. Bull., v. 84, p. 1135-1154.

Cromwell, T., 1953, Circulation in a meridional plane in the central equatorial Pacific, Jour. Marine Research, v. 12, p. 196-213.

Dinkelman, M. G., 1974, Late Quaternary radiolarian paleo-oceanography of the Panama Basin, eastern equatorial Pacific, Ph. D. Thesis, Corvallis, Oregon State University. 123 numb. leaves.

Douglas, R. G., and Savin, S. M., 1973, Oxygen and carbon isotope analyses of Cretaceous and Tertiary foraminifera from the central north Pacific, in Winterer, E. L., Ewing, J. I., and others, Initial Reports of the Deep Sea Drilling Project, v. 17, U. S. Government Printing Office, Washington, D. C., p. 591-605.

Dymond, J., Corliss, J. B., and Stillinger, R., in press, Chemical composition and metal accumulation rates of metalliferous sediments from Site 319, 320B and 321, in Initial Reports of the Deep Sea Drilling Project, v. 34, U. S. Government Printing Office, Washington, D. C.

Edmond, J. M., 1974, On the dissolution of carbonate and silicate in the deep ocean, Deep Sea Research, v. 21, p. 455-480.

Ellis, D. B., 1972, Holocene sediment of the South Atlantic Ocean: the calcite compensation depth and concentration of calcite, opal and quartz. Master's Thesis, Corvallis, Oregon State University, 77 numb. leaves.

Ellis, D. B., and Moore, T. C., Jr., 1973, Calcium carbonate, opal and quartz in Holocene pelagic sediments and the calcite compensation level in the South Atlantic Ocean, Jour. Marine Research, v. 31, p. 210-227.

El Wakeel, S. K., and Riley, J. P., 1961, Chemical and mineralogical studies of deep-sea sediments, Geochim. Cosmochim. Acta, v. 25, p. 110-146.

Francheteau, J., Harrison, C. G. A., Sclater, J. G., and Richards, M. L., 1970, Magnetization of Pacific seamounts: a preliminary polar curve for the northeastern Pacific, Jour. Geophys. Research, v. 75, p. 2035-2061.

Gervasio, F. C., 1964, A study of the tectonics of the Philippine archipelago, abstr., Int. Geol. Congress, 22nd, India, Rept. v. Abstr. p. 41.

Goldberg, E. D., 1958, Determination of opal in marine sediments, Jour. Marine Research, v. 17, p. 178-182.

Hashimoto, I., and Jackson, M. L., 1960, Rapid dissolution of allophane and kaolinite-halloysite after dehydration, in Proc. of the 7th National Conf. on Clays and Clay Minerals, Washington, D. C., 1958, Pergamon Press, p. 102-113.

Hays, J. D., Saito, T., Opdyke, N. D., and Burckle, L. H., 1969, Pliocene-Pleistocene sediments of the equatorial Pacific: their paleomagnetic, biostratigraphic and climate record, Geol. Soc. Amer. Bull., v. 80, p. 1481-1514.

Hays, J. D., Cook, H., Jenkins, G., Orr, W., Goll, R., Cook, F., Milow, D., and Fuller, J., 1972, An interpretation of the eastern equatorial Pacific from the frilling results of the Glomar Challenger, Leg 9, in Hays, J. D., ed., Initial Reports of the Deep Sea Drilling Project, U. S. Government Printing Office, Washington, D. C., v. 9, p. 909-931.

Heath, G. R., 1969a, Carbonate sedimentation in the abyssal equatorial Pacific during the past 50 million years, Geol. Soc. Amer. Bull., v. 80, p. 689-694.

__________, 1969b, Mineralogy of Cenozoic deep-sea sediments from the equatorial Pacific Ocean, Geol. Soc. Amer. Bull., v. 80, p. 1997-2018.

__________, 1974, Dissolved silica in deep-sea sediments, in Hay, W. W., ed., Soc. Econ. Paleont. and Mineral. Spec. Publ., p. 77-93.

__________, 1975, Processes controlling siliceous biogenous deposits, in Seibold, E., and Riedel, W. R., eds., Marine plankton and sediments, Third Planktonic Conference, Kiel.

Heath, G. R., and Culberson, C., 1970, Calcite: degree of saturation, rate of dissolution and the compensation depth in the deep ocean, Geol. Soc. Amer. Bull., v. 81, p. 3157-3160.

Heath, G. R., Moore, T. C., Jr., Dauphin, J. P., and Opdyke, N. D., 1975, Quartz, organic carbon, opal and calcium carbonate in Holocene, 600,000 yr., and Brunhes-Matuyama age pelagic sediments of the North Pacific, Geol. Soc. Amer. Bull., in press.

Hurd, D. C., 1972, Interactions of biogenic opal, sediment and seawater in the central equatorial Pacific, Ph.D. Thesis, Honolulu, University of Hawaii, 81 numb. leaves.

__________, 1973, Interactions of biogenic opal, sediment and seawater in the central equatorial Pacific, Geochim. Cosmochim. Acta, v. 37, p. 2257-2282.

Imbrie, J., van Donk, J., and Kipp, N. G., 1973, Paleoclimatic investigation of a Late Pleistocene Caribbean deep-sea core: comparison of isotopic and faunal methods, Quat. Research, v. 3, p. 10-38.

Johnson, T. C., 1974, The dissolution of siliceous microfossils in surface sediments of the eastern tropical Pacific, Deep-Sea Research, v. 21, p. 851-864.

Jones, J. H., 1973, Vertical mixing in the equatorial undercurrent, Jour. Phys. Oceanog., v. 3, p. 286-296.

Jones, M. M., and Pytkowicz, R. M., 1973, Solubility of silica in seawater at high pressures, Bull. de la Soc. Sciences de Liege, v. 42, p. 125-127.

Kaneps, A., 1970, Late Neogene biostratigraphy (planktonic Foraminifera), biogeography and depositional history, Ph. D. Thesis, New York, Columbia University, 185 numb. leaves.

Katili, J. A., 1971, A review of the geotectonic theories and tectonic maps of Indonesia, Earth Sci. Reviews, v. 7, p. 143-163.

Keany, J., and Kennett, J. P., 1974, Pliocene-Pleistocene radiolarian stratigraphy and paleoclimatology at DSDP Site 278 on the Antarctic convergence, in Kennett, J. P., and Houtz, R. E., 1974, Initial Reports of the Deep Sea Drilling Project, v. 29, Washington (U. S. Government Printing Office), p. 757-768.

Kennett, J. P., Houtz, R. E., Andrews, P. B., Edwards, A. R., Gostin, V. A., Hajos, M., Hampton, M., Jenkins, D. G., Margolis, S. V., Ovenshine, A. T., and Perch-Nielsen, K., 1974, Cenozoic paleoceanography in the southwest Pacific Ocean, Antarctic glaciation, and the development of the Circum-Antarctic Current, in Kennett, J. P., and Houtz, R. E., and others, 1974, Initial Reports of the Deep Sea Drilling Project, v. 29, Washington (U. S. Government Printing Office), p. 1155-1169.

Koblentz-Mishke, O. J., Volkovinsky, V. V., and Kabanova, J. G., 1970, Plankton primary productivity of the world ocean, in Wooster, W. S., ed., Scientific exploration of the South Pacific, U. S. National Acad. Science, Washington, D. C., p. 183-193.

Krauskopf, K. B., 1956, Dissolution and precipitation of silica at low temperatures, Geochim. Cosmochim. Acta, v. 10, p. 1-26.

Lamb, H. H., and Woodroffe, A., 1970, Atmospheric circulation during the last Ice Age, Quat. Research, v. 1, p. 29-58.

Lisitzin, A. P., 1971a, Distribution of siliceous microfossils in suspension and in bottom sediments, in Funnel, M. N., and Riedel, W. R., ed., The Micropaleontology of Oceans, Cambridge, 1971, Cambridge Univ. Press, p. 173-195.

Lisitzin, A. P., 1971b, Geochemical, mineralogical, paleontologic studies, Leg 6, in Fisher, A. G. and others, Initial Reports of the Deep Sea Drilling Project, v. 6, Washington (U. S. Government Printing Office), p. 829-961.

__________, 1972, Sedimentation in the world ocean, Soc. Econ. Paleontologists and Mineralogists Spec. Publ. 17, 218 p.

Luyendyk, B. P., Forsyth, D., and Phillips, J. D., 1972, Experimental approach to the paleocirculation of oceanic surface waters, Geol. Soc. Amer. Bull., v. 83, p. 2649-2664.

Luz, B., 1973, Stratigraphic and paleoclimate analysis of Pleistocene tropical southeast Pacific cores, Quat. Research, v. 3, p. 56-72.

Luz, B., and Shackleton, N. J., 1975, $CaCO_3$ solution in the tropical east Pacific during the past 130,000 years, Cushman Foundation for Foram. Research, Spec. Publ. 13, p. 142-150.

Malfait, B. T., and Dinkelman, M. G., 1972, Circum-Caribbean tectonic igneous activity and the evolution of the Caribbean plate, Geol. Soc. America Bull., v. 83, p. 251-272.

McIntyre, A., Ruddiman, W. F., and Jantzen, R., 1972, Southward penetrations of the North Atlantic Polar Front: faunal and floral evidence of large-scale surface water mass movements over the last 225,000 years, Deep-Sea Research, v. 19, p. 61-77.

McKenzie, D. P., and Sclater, J. G., 1971, The evolution of the Indian Ocean since the late Cretaceous, Roy. Astron. Soc. Geophys. Jour., v. 29, p. 65-78.

Mehra, O. P., and Jackson, M. L., 1960, Iron oxide removal from soils and clays by a dithionite-citrate system buffered with sodium bicarbonate, in Swineford, A., ed., Clays and Clay Minerals, Proc 7th National Conf., Pergamon Press, London, p. 317-327.

Minster, J. B., Jordan, T. H., Molnar, P., and Haines, E., 1974, Numerical modeling of instantaneous plate tectonics, Roy. Astron. Soc. Geophys. Jour., v. 36, p. 541-576.

Moberly, R., 1972, Origin of lithosphere behind island arcs with reference to the western Pacific, in Shagam, R., ed., Studies in earth and space sciences, Geol. Soc. Amer. Memoir 132, p. 35-56.

Molina-Cruz, A., 1975, Paleoceanography of the subtropical southeastern Pacific during Late Quaternary: a study of radiolaria, opal and quartz contents of deep-sea sediments, Master's Thesis, Corvallis, Oregon State University, 179 numb. leaves.

Morgan, W. J., 1972, Plate motions and deep mantle convections, in Shagam, R., ed., Studies in earth and space sciences, Geol. Soc. America Memoir 132, p. 7-32.

Newell, R. E., 1974, Changes in the poleward energy flux by the atmosphere and ocean as a possible cause for ice ages, Quat. Research, v. 4, p. 117-127.

Pak, H., and Zaneveld, J. R. V., 1974, Equatorial front in the eastern Pacific Ocean, Jour. Phys. Oceanog., v. 4, p. 570-578.

Pisias, N., 1974, Model of late Pleistocene-Holocene variations in rate of sediment accumulation: Panama Basin, Eastern Equatorial Pacific. Master's Thesis, Corvallis, Oregon State University, 77 numb. leaves.

Pisias, N., Heath, G. R., and Moore, T. C., Jr., 1975, Lag time for oceanic responses to climatic change, Nature, v. 256, n. 5520, p. 716-717.

Revelle, R., 1944, Marine bottom samples collected in the Pacific Ocean by the Carnegie on its seventh cruise, Carnegie Inst., Washington, D. C., Pub. 556, 182 p.

Rex, R. W., and Goldberg, E. D., 1958, Quartz contents of pelagic sediments of the Pacific Ocean, Tellus, v. 1, p. 153-159.

Ryther, J. H., 1963, Geographic variations in productivity, in Hill, M. N., ed., The Sea, v. 2, Interscience, New York, p. 347-380.

Sclater, J. G., Anderson, R. N., and Bell, M. L., 1971, Elevation of ridges and evolution of the central eastern Pacific, Jour. Geophys. Research, v. 76, p. 7888-7915.

Shackleton, N. J., and Kennett, J. P., 1974, Paleotemperature history of the Cenozoic and the initiation of Antarctic glaciation: oxygen and carbon isotope analyses in DSDP Sites 277, 279, and 281, in Kennett, J. P., and Houtz, R. E., 1974, Initial Reports of the Deep Sea Drilling Project, v. 29, Washington (U. S. Government Printing Office), p. 743-756.

Strickland, J. D. H., and Parsons, T. R., 1968, A handbook of sea-water analysis, Bull. 167, Fisheries Research Board Canada (Ottawa), p. 65-70.

Till, R., and Spears, D. A., 1969, The determination of quartz in sedimentary rocks using an X-ray diffraction technique, Clays and Clay Min., v. 17, p. 323-327.

Tracey, J. I., Nesteroff, W. D., Galehouse, J. S., von der Borch, C. C., Moore, T. C., Jr., Bilal-ul-haq, U. Z., and Beckmann, L. P., 1971, Leg 8 summary, in Tracey, J. I. and Sutton, G. D., eds., Initial Reports of the Deep Sea Drilling Project, V. 8, Washington (U. S. Government Printing Office), p. 17-42.

Weaver, C. E., and Pollard, L. D., 1973, The chemistry of clay minerals, v. 15, Developments in Sedimentology, Amsterdam Elsevier, 213 p.

Weissel, J. K., and Hayes, D. E., 1972, Magnetic anomalies in the southeast Indian Ocean, in Antarctic Oceanology II: The Australian - New Zealand Sector, Antarctic Research Series, no. 19, p. 165-196.

Winterer, E. L., 1973, Sedimentary facies and plate tectonics of the equatorial Pacific, Amer. Assoc. Petroleum Geologists Bull., v. 57, p. 265-282.

Wyrtki, K., 1967, Circulation and water masses in the eastern equatorial Pacific Ocean, Internat. Jour. Oceanol. Limnol., v. 1, p. 117-147.

__________, 1974a, Equatorial currents in the Pacific from 1950 - 1970 and their relations to the trade winds, Jour. Phys. Oceanog., v. 4, p. 372-380.

Wyrtki, K., 1974b, Sea level and the seasonal fluctuations of the equatorial currents in the western Pacific Ocean, Jour. Phys. Oceanog., v. 4, p. 91-103.

van Andel, Tj. H., 1975, Mesozoic/Cenozoic calcite compensation depth and the global distribution of calcareous sediments, Earth Planet. Sci. Lett., v. 26, p. 187-194.

van Andel, Tj. H., and Buckry, D., 1973, Basement ages and basement depths in the eastern equatorial Pacific, Geol. Soc. Amer. Bull., v. 84, p. 2361-2370.

van Andel, Tj. H., and Heath, G. R., 1973, Initial Reports of the Deep Sea Drilling Project, Washington (U. S. Government Printing Office), v. 16, 949 p.

van Andel, Tj. H., and Moore, T. C., Jr., 1974, Cenozoic calcium carbonate distribution and calcite compensation depth in the central equatorial Pacific Ocean, Geology, v. 2, p. 87-92.

van Andel, Tj. H., Heath, G. R., and Moore, T. C., Jr., 1975, Cenozoic history and paleoceanography of the central equatorial Pacific, Geol. Soc. America Memoir 143, in press.

Veevers, J. J., 1969, Paleogeography of the Timor Sea region, Paleogeog., Paleoclimat., Paleoecol., v. 6, p. 125-140.

Veronis, G., 1960, An approximate theoretical analysis of the equatorial undercurrent, Deep Sea Research, v. 6, p. 318-327.

APPENDICES

APPENDIX I. Locations and Depths of Deep Sea Drilling Project Sites

Site	Leg	Latitude	Longitude	Depth
42	5	13°50.6'N	140°11.3'W	4844
69	8	6°00.0'N	152°51.9'W	4978
70	8	6°20.1'N	140°21.7'W	5059
71	8	4°28.3'N	140°18.9'W	4419
72	8	0°26.5'N	138°52.0'W	4326
73	8	1°54.6'S	137°28.1'W	4387
74	8	6°14.2'S	136°05.8'W	4431
75	8	12°31.0'S	134°16.0'W	4181
77	9	0°28.9'N	133°13.7'W	4291
78	9	7°57.0'N	127°21.3'W	4363
79	9	2°33.0'N	121°34.0'W	4566
80	9	0°57.7'N	121°33.2'W	4399
81	9	1°26.5'N	113°48.5'W	3854
82	9	2°35.5'N	106°56.5'W	3689
83	9	4°02.8'N	95°44.3'W	3632
159	16	12°19.9'N	122°17.3'W	4484
160	16	11°42.3'N	130°52.8'W	4940
161	16	10°14.3'N	139°57.2'W	4939
162	16	14°52.2'N	140°02.6'W	4854
163	16	11°14.7'N	150°17.5'W	5230

APPENDIX II. Composite Samples and Their Included DSDP Samples

Site	Age Interval	Carbonate Access. #	Atomic Abs. Access. #	Depth Interval at Site	DSDP Samples: Core	DSDP Samples: Section	DSDP Samples: Depth in Section
42	(24-25 m. y.)	JD06818	EP0958	35 - 195	1	1	35-36
					1	1	115-116
					1	2	44-45
42	(30-31 m. y.)	JD06819	EP0959	1569 - 1650	2	5	69-70
					2	5	100-150
42	(37-38 m. y.)	JD06820	EP0960	3175 - 3324	4	4	25-26
					4	5	23-24
42	(44-45 m. y.)	JD06821	EP0961	6621 - 7247	8	3	21-22
					8	5	24-25
					9	1	46-47
42	(46-47 m. y.)	JD06822	EP0962	9617 - 10576	11	5	17-18
					1A	1	28-29
					1A	3	15-16
					1A	5	75-76
69	(9-12 m. y.)	JD08124	EP0963	29 - 838	1	1	29-30
					1	3	47-48
					1	6	87-88

APPENDIX II. Continued.

Site	Age Interval	Carbonate Access. #	Atomic Abs. Access. #	Depth Interval at Site	DSDP Samples Core	DSDP Samples Section	DSDP Samples Depth in Section
69	(15-16 m.y.)	JD08125	EP0964	2870 - 2941	3	4	120-121
					3	4	30-31
					3	5	40-41
69	(24-25 m.y.)	JD08126	EP0986	6150 - 6748	1A	1	50-51
					1A	3	60-61
					1A	5	47-48
69	(28-29 m.y.)	JD08128	EP0987	9530 - 10161	4A	5	30-31
					5A	1	75-76
					5A	3	60-61
69	(38-39 m.y.)	JD07140	EP0988	14750 - 15056	9A	3	50-51
					9A	4	90-91
					9A	5	55-56
69	(43-44 m.y.)	JD07139	EP1472	18770 - 19316	6	1	70-71
					6	3	60-61
					6	5	15-16
69	(45-46 m.y.)	JD08127	EP0990	21586 - 22207	11A	2	36-37
					11A	4	40-41
					11A	6	56-57

APPENDIX II. Continued.

					DSDP Samples		
Site	Age Interval	Carbonate Access. #	Atomic Abs. Access. #	Depth Interval at Site	Core	Section	Depth in Section
70	(0-2 m.y.)	JD06830	EP0991	65 - 176	1	1	65-66
					1	1	125-126
					1	2	25-26
70	(9-10 m.y.)	JD06831	EP0992	1555 - 1766	2	1	55-56
					2	2	65-66
					2	2	115-116
70	(14-15 m.y.)	JD08129	EP0993	3260 - 3432	4	4	60-61
					4	5	81-82
70	(16-17 m.y.)	JD06832	EP0994	4005 - 4306	5	4	55-56
					5	5	55-56
					5	6	55-56
70	(20-21 m.y.)	JD06833	EP0995	6577 - 8156	8	3	77-78
					8	5	71-72
					9	1	50-51
					9	3	50-51
					9	5	60-61
					10	1	55-56
70	(28-29 m.y.)	JD06834	EP0996	18220 - 19881	8A	4	70-71
cont.					8A	6	85-86

APPENDIX II. Continued.

Site	Age Interval	Carbonate Access. #	Atomic Abs. Access. #	Depth Interval at Site	DSDP Samples Core	DSDP Samples Section	DSDP Samples Depth in Section
70	(28-29 m.y.)	JD06834	EP0996	18220 - 19881	9A	2	73-74
					9A	4	50-51
					10A	2	84-85
					10A	4	80-81
70	(32-33 m.y.)	JD08130	EP0997	29655 - 29801	23A	1	55-56
					23A	2	50-51
70	(36-37.5 m.y.)	JD06836	EP0998	32325 - 32521	27A	2	25-26
					27A	2	110-111
					27A	3	70-71
71	(0-1 m.y.)	JD07153	EP0999	71 - 276	1	1	71-72
					1	2	55-56
					1	2	115-116
71	(6-7 m.y.)	JD07154	EP1000	2445 - 2769	3	5	45-46
					3	6	80-81
					4	1	68-69
71	(8-9 m.y.)	JD07155	EP1001	4240 - 4690	5	6	90-91
					6	1	65-66
					6	3	90-91

APPENDIX II. Continued.

Site	Age Interval	Carbonate Access. #	Atomic Abs. Access. #	Depth Interval at Site	DSDP Samples		
					Core	Section	Depth in Section
71	(13-14 m.y.)	JD07156	EP1002	8555 - 14056	10	5	55-56
					10	6	55-56
					11	2	50-51
					11	4	50-51
					11	6	50-51
					12	2	50-51
					12	4	100-101
					12	6	50-51
					13	1	50-51
					13	3	60-61
					13	5	55-56
					14	1	55-56
					14	3	55-56
					14	5	50-51
					15	2	55-56
					15	4	55-56
					15	5	60-61
					16	1	56-57
71	(20-21 m.y.)	JD08131	EP1021	27910 - 29810	31	6	60-61
					32	2	50-51
					32	4	50-51
					32	6	50-51
cont.					33	2	50-51

APPENDIX II. Continued.

Site	Age Interval	Carbonate Access. #	Atomic Abs. Access. #	Depth Interval at Site	DSDP Samples Core	Section	Depth in Section
71	(20-21 m.y.)	JD08131	EP1021	27910 - 29810	33	4	50-51
					33	6	60-61
71	(26-27 m.y.)	JD08132	EP1022	41020 - 42045	46	2	70-71
					46	4	41-42
					47	2	94-95
71	(31-33 m.y.)	JD08133	EP1023	52855 - 52896	1A	1	55-56
					1A	1	95-96
71	(39-40 m.y.)	JD09841	EP1471	55591 - 55720	3A	1	91-92
					3A	2	69-70
72	(0-1 m.y.)	JD06823	EP1024	260 - 820	1	2	110-111
					1	4	60-61
					1	6	70-71
72	(3-4 m.y.)	JD06824	EP1025	3550 - 4741	3A	6	100-101
					4A	2	65-66
					4A	4	71-72
					4A	6	66-67
					5A	2	90-91

APPENDIX II. Continued.

Site	Age Interval	Carbonate Access. #	Atomic Abs. Access. #	Depth Interval at Site	DSDP Samples Core	Section	Depth in Section
72	(9-10 m.y.)	JD06825	EP1026	11110 - 11421	3	4	60-61
					3	5	30-31
					3	6	70-71
72	(14-15 m.y.)	JD06826	EP1027	21320 - 21921	5	2	70-71
					5	4	90-91
					5	6	70-71
72	(27-28 m.y.)	JD06654	EP1028	31448 - 32041	7	2	98-99
					7	4	117-118
					7	6	90-91
72	(36-37 m.y.)	JD06827	EP1029	33500 - 33721	9	4	50-51
					9	6	40-41
					9	5	120-121
72	(37-38 m.y.)	JD06828	EP1030	33909 - 34159	10	3	9-10
					10	3	110-111
					10	4	109-110
72	(39-40 m.y.)	JD06829	EP1031	34395 - 34471	11	1	24-25
					11	1	120-121

APPENDIX II. Continued.

Site	Age Interval	Carbonate Access. #	Atomic Abs. Access. #	Depth Interval at Site	DSDP Samples		
					Core	Section	Depth in Section
73	(0-1 m.y.)	JD07148	EP1032	240 - 856	1	2	90-91
					2	1	125-126
					2	3	105-106
73	(4-5 m.y.)	JD07149	EP1033	5103 - 5251	7	2	53-54
					7	3	42-43
					7	6	100-101
73	(8-9 m.y.)	JD07150	EP1034	6795 - 6971	9	1	95-96
					9	2	61-62
					9	2	120-121
73	(14-15 m.y.)	JD07151	EP1035	8436 - 8976	10	6	86-87
					11	2	45-46
					11	4	25-26
73	(20-22 m.y.)	JD06659	EP1036	20800 - 21391	13	2	50-51
					13	4	60-61
					13	6	40-41
73	(32-33 m.y.)	JD07152	EP1037	26320 - 27071	16	2	70-71
					16	4	70-71
					16	6	80-81
					17	1	70-71

APPENDIX II. Continued.

Site	Age Interval	Carbonate Access. #	Atomic Abs. Access. #	Depth Interval at Site	DSDP Samples		
					Core	Section	Depth in Section
73	(39-40 m. y.)	JD08134	EP1038	29310 - 29311	19	4	60-61
73	(43-44 m. y.)	JD08135	EP1039	30000 - 30191	21	2	10-11
					21	3	70-71
					21	3	140-141
74	(0-1 m. y.)	JD06655	EP1040	70-191	1	1	70-71
					1	1	115-116
					1	2	40-41
74	(7-8 m. y.)	JD06814	EP1041	1440 - 1721	2	1	90-91
					2	2	70-71
					2	3	70-71
74	(17-18 m. y.)	JD06815	EP1042	2470 - 2616	3	4	70-71
					3	4	120-121
					3	5	65-66
74	(25-26 m. y.)	JD06816	EP1043	5120 - 5720	6	4	70-71
					6	6	90-91
					7	2	70-71

APPENDIX II. Continued.

Site	Age Interval	Carbonate Access. #	Atomic Abs. Access. #	Depth Interval at Site	DSDP Samples		
					Core	Section	Depth in Section
74	(29-30 m.y.)	JD06817	EP1044	7395 - 7671	9	1	95-96
					9	2	30-31
					9	3	70-71
74	(44-45 m.y.)	JD07138	EP1045	10023 - 10200	12	1	23-24
					12	1	60-61
					12	2	60-61
					12	3	35-36
75	(0-1 m.y.)	JD06381	EP1046	40 - 81	1	1	130-131
					1	2	20-21
75	(16-18 m.y.)	JD06661	EP1047	280 - 411	1	3	70-71
					1	3	125-126
					1	4	50-51
75	(21-22 m.y.)	JD06382	EP1048	1420 - 2170	2	4	70-71
					2	6	70-71
					3	1	100-101
					3	3	70-71
75	(24-25 m.y.)	JD06383	EP1049	3500 - 3791	4	6	50-51
					5	1	70-71
					5	2	40-41

APPENDIX II. Continued.

Site	Age Interval	Carbonate Access. #	Atomic Abs. Access. #	Depth Interval at Site	DSDP Samples Core	Section	Depth in Section
75	(29-30 m. y.)	JD06384	EP1050	6020 - 6791	7	4	70-71
					8	1	30-31
					8	3	90-91
75	(31-32 m. y.)	JD06385	EP1051	7802 - 8181	9	4	52-53
					9	5	40-41
					9	5	140-141
					9	6	40-41
					9	6	70-71
					9	6	130-131
77	(0-1 m. y.)	JD06652	EP1052	50-1120	1	1	50-51
					1A	2	132-133
					1A	4	50-51
					1A	6	138-139
					1B	2	60-61
75	(3-4 m. y.)	JD06657	EP1053	4656 - 5903	5B	1	96-97
					5B	3	63-64
					5B	5	75-76
					6B	1	70-71
					6B	3	122-123

APPENDIX II. Continued.

Site	Age Interval	Carbonate Access. #	Atomic Abs. Access. #	Depth Interval at Site	DSDP Samples		
					Core	Section	Depth in Section
77	(7-8 m.y.)	JD06651	EP1054	13642 - 15093	14B	6	92-93
					15B	2	70-71
					15B	4	80-81
					15B	6	65-66
					16B	2	90-91
					16B	4	22-23
77	(15-16 m.y.)	JD06662	EP1055	23990 - 25211	26B	4	80-81
					26B	6	70-71
					27B	2	75-76
					27B	4	75-76
					27B	6	80-81
77	(22-23 m.y.)	JD06658	EP1056	30098 - 31287	33B	2	88-89
					33B	4	45-46
					33B	6	53-54
					34B	2	72-73
					34B	4	56-57
77	(26-27 m.y.)	JD06656	EP1057	35580 - 36776	39B	2	70-71
					39B	4	75-76
					39B	6	60-61
					40B	2	65-66

APPENDIX II. Continued.

Site	Age Interval	Carbonate Access. #	Atomic Abs. Access. #	Depth Interval at Site	DSDP Samples Core	DSDP Samples Section	DSDP Samples Depth in Section
77	(30-31 m.y.)	JD06660	EP1058	43699 - 44219	48B	1	119-120
					48B	3	18-20
					48B	5	38-39
77	(37-38 m.y.)	JD06653	EP1059	47190 - 47339	52B	1	110-111
					52B	2	28-29
					52B	2	108-109
78	(12-13 m.y.)	JD08136	EP1060	50 - 573	1	1	50-51
					1	2	90-91
					1	4	122-123
78	(15-16 m.y.)	JD08137	EP1061	2160 - 2611	3	3	40-41
					3	4	7-8
					3	5	34-35
					3	6	40-41
78	(18-19 m.y.)	JD08138	EP1062	4451 - 5131	5	6	41-42
					6	2	30-31
					6	4	110-111
78	(25-26 m.y.)	JD08139	EP1063	17581 - 18764	20	2	61-62
					20	4	27-28
cont.					20	6	80-81

APPENDIX II. Continued.

Site	Age Interval	Carbonate Access. #	Atomic Abs. Access. #	Depth Interval at Site	DSDP Samples		
					Core	Section	Depth in Section
78	(25-26 m.y.)	JD08139	EP1063	17581 - 18764	21	2	123-124
					21	4	23-24
78	(31-32 m.y.)	JD08140	EP1064	27312 - 28832	30	6	53-54
					31	2	47-48
					31	4	30-31
					31	6	23-24
					32	2	83-84
					32	4	31-32
78	(34-35 m.y.)	JD08141	EP1065	31660 - 31966	35	4	120-121
					35	6	125-126
79	(0-1 m.y.)	JD07141	EP1066	277 - 478	1	2	127-128
					1	4	27-28
79	(5-6 m.y.)	JD08142	EP1067	6818 - 7721	2	6	38-39
					2A	2	75-76
					2A	4	24-26
					2A	6	20-21
79	(9-10 m.y.)	JD08143	EP1068	14517 - 15124	3A	1	7-8
					3A	3	90-91
					3A	5	13-14

APPENDIX II. Continued.

Site	Age Interval	Carbonate Access. #	Atomic Abs. Access. #	Depth Interval at Site	DSDP Samples		
					Core	Section	Depth in Section
79	(15-16 m.y.)	JD08144	EP1069	19470 - 20025	4A	1	120-121
					4A	3	10-11
					4A	5	74-75
79	(19-20 m.y.)	JD07377	EP1070	36873 - 37227	11	4	2-3
					11	6	56-57
79	(22-23 m.y.)	JD08145	EP1071	40735 - 40993	16	1	135-136
					16	2	100-101
					16	3	92-93
80	(0-1 m.y.)	JD08146	EP1072	275 - 781	1	2	125-126
					1	4	40-41
					1	6	30-31
80	(6-7 m.y.)	JD08147	EP1073	6600 - 6872	2	4	50-51
					2	5	80-81
					2	6	21-22
80	(13-14 m.y.)	JD08148	EP1074	8765 - 9171	3A	1	105-106
					3A	2	29-30
					3A	4	60-61

APPENDIX II. Continued.

Site	Age Interval	Carbonate Access. #	Atomic Abs. Access. #	Depth Interval at Site	DSDP Samples		
					Core	Section	Depth in Section
80	(16-17 m.y.)	JD08149	EP1075	13390 - 15566	3	5	40-41
					3	6	60-61
					5A	1	65-66
80	(21-22 m.y.)	JD06386	EP1076	19390 - 19651	5	1	60-61
					5	2	55-56
					5	3	20-21
81	(0-1 m.y.)	JD07143	EP1077	29 - 621	1	1	29-30
					1	2	27-28
					1	3	50-51
					1	5	20-21
81	(14-15 m.y.)	JD07142	EP1078	31998 - 32601	2	1	28-29
					2	3	30-31
					2	5	30-31
82	(0-1 m.y.	JD07144	EP1080	30 - 656	1	1	30-31
					1	3	90-91
					1	5	55-56
82	(5-6 m.y.)	JD07145	EP1081	20185 - 21740	5	1	135-136
					5	2	25-26
					5	2	71-72

cont.

APPENDIX II. Continued.

Site	Age Interval	Carbonate Access. #	Atomic Abs. Access. #	Depth Interval at Site	DSDP Samples		
					Core	Section	Depth in Section
82	(5-6 m.y.)	JD07145	EP1081	20185 - 21740	6	2	55-56
					6	4	25-26
					6	6	29-30
83	(0-1 m.y.)	JD07146	EP1082	90 - 1772	1	2	60-61
					1	4	79-80
					2	1	19-20
					2	3	105-106
					2	5	8-9
					1A	2	60-61
					1A	4	17-18
					3	1	130-131
					3	3	41-42
83	(8-9 m.y.)	JD07147	EP1083	22660 - 22981	7	4	30-31
					7	6	50-51
159	(0-1 m.y.	JD06388	EP1084	12 - 382	1	1	12-13
					1	3	80-82
159	(6-7 m.y.)	JD06389	EP1085	1120 - 1216	2	2	70-72
					2	3	70-72
					2	3	15-16

APPENDIX II. Continued.

Site	Age Interval	Carbonate Access. #	Atomic Abs. Access. #	Depth Interval at Site	DSDP Samples Core	DSDP Samples Section	DSDP Samples Depth in Section
159	(13-14 m. y.)	JD06390	EP1086	2170 - 2472	3	3	70-72
					3	4	70-72
					3	5	70-72
159	(15-16 m. y.)	JD06391	EP1087	3070 - 3372	4	3	70-72
					4	4	60-62
					4	5	70-72
159	(17-18 m. y.)	JD06392	EP1088	4110 - 4412	5	4	60-62
					5	5	60-62
					5	6	60-62
159	(20-21 m. y.)	JD06393	EP1089	6077 - 6962	7	5	77-79
					7	6	60-62
					8	1	60-62
					8	2	60-62
					8	3	130-132
					8	4	60-62
					8	5	60-62
159	(23-24 m. y.)	JD06394	EP1090	10410 - 10712	12	4	60-62
					12	5	60-62
					12	6	60-62

APPENDIX II. Continued.

Site	Age Interval	Carbonate Access. #	Atomic Abs. Access. #	Depth Interval at Site	DSDP Samples		
					Core	Section	Depth in Section
160	(0-1 m.y.)	JD06395	EP1091	70 - 390	1	1	70-72
					1	2	60-62
					1	3	88-90
160	(15-16 m.y.)	JD06396	EP1092	540 - 692	2	4	90-92
					2	5	15-16
					2	5	90-92
160	(21-22 m.y.)	JD06397	EP1093	3690 - 3936	5	1	90-92
					5	2	90-92
					5	3	35-36
160	(26-27 m.y.)	JD06398	EP1094	6090 - 6960	7	5	90-92
					7	6	90-92
					8	1	90-92
					8	2	80-82
					8	3	90-92
					8	4	90-92
					8	5	58-60
160	(29-30 m.y.)	JD06399	EP1095	8790 - 9242	10	5	90-92
					10	6	90-92
					11	1	90-92
					11	2	90-92

APPENDIX II. Continued.

Site	Age Interval	Carbonate Access. #	Atomic Abs. Access. #	Depth Interval at Site	DSDP Samples		
					Core	Section	Depth in Section
160	(34-35 m. y.)	JD06400	EP1097	10675 - 10761	12	6	25-26
					12	6	90-92
					12	6	110-111
161	(18-19 m. y.)	JD08150	EP1098	55 - 232	1	1	55-57
					1	1	80-82
					1	2	80-82
161	(22-23 m. y.)	JD08151	EP1099	1730 - 2242	2	6	80-82
					3	1	80-82
					3	2	80-82
					3	3	80-82
					3	3	140-142
161	(29-30 m. y.)	JD08152	EP1100	9830 - 10882	11	6	80-82
					12	1	40-42
					12	2	80-82
					12	3	38-40
					12	4	80-82
					12	5	124-126
					12	6	70-72
					13	1	80-82

APPENDIX II. Continued.

Site	Age Interval	Carbonate Access. #	Atomic Abs. Access. #	Depth Interval at Site	DSDP Samples		
					Core	Section	Depth in Section
161	(34-35 m. y.)	JD08153	EP1101	17550 - 18282	7A	2	100-102
					7A	3	50-52
					7A	4	62-64
					7A	5	90-92
					7A	6	80-82
					8A	1	80-82
161	(40-41 m. y.)	JD08154	EP1102	21153 - 21522	11A	2	103-105
					11A	3	90-92
					11A	4	80-82
					11A	5	20-22
161	(43-44 m. y.)	JD08155	EP1103	23598 - 23723	14A	1	98-100
					14A	2	71-73
162	(30-31 m. y.)	JD08156	EP1104	90 - 382	1	1	90-92
					1	2	60-62
					1	3	80-82
162	(35-36 m. y.)	JD08157	EP1105	1030 - 1472	3	2	80-82
					3	3	80-82
					3	4	80-82
					3	5	70-72

APPENDIX II. Continued.

Site	Age Interval	Carbonate Access. #	Atomic Abs. Access. #	Depth Interval at Site	DSDP Samples Core	DSDP Samples Section	DSDP Samples Depth in Section
162	(37-38 m.y.)	JD08158	EP1106	2930 - 3472	4	2	80-82
					4	3	80-82
					4	4	80-82
					4	5	76-78
					4	6	20-22
162	(43-44 m.y.)	JD08159	EP1107	6380 - 7882	8	1	80-82
					8	2	80-82
					8	3	80-82
					8	4	80-82
					8	5	80-82
					8	6	80-82
					9	1	80-82
					9	2	80-82
					9	3	80-82
					9	4	80-82
					9	5	80-82
162	(46-47 m.y.)	JD08160	EP1119	11030 - 12232	13	2	80-82
					13	3	80-82
					13	4	80-82
					13	5	80-82
					13	6	80-82
					14	1	80-82

cont.

APPENDIX II. Continued.

Site	Age Interval	Carbonate Access. #	Atomic Abs. Access. #	Depth Interval at Site	DSDP Samples		
					Core	Section	Depth in Section
162	(46-47 m.y.)	JD08160	EP1119	11030 - 12232	14	2	80-82
					14	3	80-82
					14	4	80-82
162	(48-49 m.y.)	JD08161	EP1120	13590 - 14742	16	1	90-92
					16	2	90-92
					16	3	90-92
					17	1	39-41
					17	2	80-82
					17	3	40-42
162	(49-50 m.y.)	JD08162	EP1121	14974 - 14976	17	4	124-126
163	(25-26 m.y.)	JD08115	EP1122	210 - 482	2	1	110-112
					2	2	80-82
					2	3	80-82
163	(35-36 m.y.)	JD08116	EP1123	2515 - 2636	4	5	15-16
					4	5	80-82
					4	5	135-136
163	(42-43 m.y.)	JD08117	EP1124	4680 - 5226	7	1	80-82
					7	2	80-82
cont.					7	3	80-82

APPENDIX II. Continued.

Site	Age Interval	Carbonate Access. #	Atomic Abs. Access. #	Depth Interval at Site	DSDP Samples: Core	DSDP Samples: Section	DSDP Samples: Depth in Section
163	(42-43 m.y.)	JD08117	EP1124	4680 - 5226	7	4	80-82
					7	5	24-26
163	(49-51 m.y.)	JD08118	EP1125	9180 - 9482	12	1	80-82
					12	2	116-118
					12	3	80-82
163	(63-64 m.y.)	JD08119	EP1126	14244 - 14532	1A	2	94-96
					1A	3	80-82
					1A	4	80-82
163	(71-72 m.y.)	JD08120	EP1127	17180 - 17782	16	1	80-82
					16	2	80-82
					16	3	80-82
					16	4	80-82
					16	5	80-82
163	(77-78 m.y.)	JD08121	EP1128	27033 - 27126	27	1	33-34
					27	1	78-80
					27	1	125-126

APPENDIX III. Accumulation Rates and Percent of Biogenic Components

Accumulation Rates are in $g/cm^2/m.y.$
Two values are given for all accumulation rates:
1 Accumulation rate calculated using Berggren (1972) time scale
2 Accumulation rate calculated using alternate time scale of van Andeal and others (1975)

Bulk Sediment Accumulation Rates from van Andel and others (1975)

Site	Age Interval	Bulk Sed. Accum. Rate 1	Bulk Sed. Accum. Rate 2	% Biog. Silica Bulk	% Biog. Silica Carb-free	Biog. Silica Accum. Rate 1	Biog. Silica Accum. Rate 2	% $CaCO_3$	Carbonate Accum. Rate 1	Carbonate Accum. Rate 2	Non-biog. Accum. Rate 1	Non-biog. Accum. Rate 2
42	(24-25)	200		18.64	42.09	37		53.45	107		56	
42	(30-31)	210		10.01	61.90	21		81.79	172		17	
42	(37-38)	150		40.61	42.14	61		3.42	5		84	
42	(44-45)	810		35.23	62.07	285		41.00	332		193	
42	(46-47)	550		44.82	57.58	247		20.83	115		188	
69	(9-12)	130	325	48.44	48.83	63	157	.99	1	3	69	165
69	(15-16)	230	150	33.44	33.71	77	50	.75	2	1	151	99
69	(24-25)	590		11.50	26.50	68		55.26	326		196	
69	(28-29)	900		5.74	26.19	52		76.15	685		163	
69	(38-39)	220		66.24	66.65	146		.59	1		73	
69	(43-44)	710		82.77	83.07	588		.33	2		120	
69	(45-46)	1340		76.62	76.76	1027		.28	4		309	
70	(0- 2)	40		20.39	20.65	8		1.16	0		32	
70	(9-10)	100		56.81	57.27	57		.73	1		42	
70	(14-15)	300	120	19.80	25.98	59	24	23.05	69	28	172	68
70	(16-17)	280		39.48	40.93	110		3.38	9		161	
70	(20-21)	2160		5.31	26.05	115		78.03	1685		360	

APPENDIX III. Continued.

Site	Age Interval	Bulk Sed. Accum. Rate 1	Bulk Sed. Accum. Rate 2	% Biog. Silica Bulk	% Biog. Silica Carb-free	Biog. Silica Accum. Rate 1	Biog. Silica Accum. Rate 2	% $CaCO_3$	Carbonate Accum. Rate 1	Carbonate Accum. Rate 2	Non-biog. Accum. Rate 1	Non-biog. Accum. Rate 2
70	(28-29)	2610		3.70	28.90	97		86.05	2246		267	
70	(32-33)	980		9.32	28.93	91		66.81	655		234	
70	(36-37.5)	275		45.45	59.00	125		21.97	60		90	
71	(0- 1)	240		7.09	35.46	17		80.45	193		30	
71	(6- 7)	500		19.81	84.84	99		76.65	383		18	
71	(8- 9)	700		7.27	45.65	51		82.39	577		72	
71	(13-14)	5970	5970	4.61	32.82	275	275	84.32	5034	5034	661	248
71	(20-21)	2820		2.35	16.92	66		84.93	2395		359	
71	(26-27)	2190		1.39	12.06	30		87.48	1916		244	
71	(31-32)	1740		10.52	14.69	183		28.10	489		1068	
71	(39-40)	390		49.86	74.23	194		32.63	127		69	
72	(0- 1)	820		7.65	47.16	63		85.01	697		60	
72	(3- 4)	1120		11.79	26.64	132		53.31	597		391	
72	(9-10)	1020		9.95	53.11	102		79.41	810		108	
72	(15-16)	3420	1800	4.70	45.16	161	85	87.88	3005	1582	254	133
72	(27-28)	1260		1.03	20.77	13		93.89	1180		67	
72	(36-37)	340		3.95	29.88	13		85.54	291		36	
72	(37-38)	280		27.03	60.72	76		53.88	51		53	
72	(39-40)	90		13.54	49.15	12		70.29	63		15	
73	(0- 1)	720		7.07	47.16	51		85.01	612		57	
73	(4- 5)	480		23.79	42.19	114		41.39	199		167	
73	(8- 9)	110		40.73	50.06	45		17.23	19		46	
73	(14-15)	1260	500	3.52	21.18	44	18	82.15	1035	411	181	71
73	(20-22)	1165		.96	18.95	11		94.05	1096		58	
73	(32-33)	1370		4.14	40.06	57		88.68	1215		98	

APPENDIX III. Continued.

Site	Age Interval	Bulk Sed. Accum. Rate 1	Bulk Sed. Accum. Rate 2	% Biog. Silica Bulk	% Biog. Silica Carb-free	Biog. Silica Accum. Rate 1	Biog. Silica Accum. Rate 2	% $CaCO_3$	Carbonate Accum. Rate 1	Carbonate Accum. Rate 2	Non-biog. Accum. Rate 1	Non-biog. Accum. Rate 2
73	(39-40)	610		13.83	40.46	84		64.98	396		130	
73	(43-44)	270		5.50	21.50	15		73.32	198		57	
74	(0- 1)	90		33.21	33.56	30		1.17	1		6	
74	(7- 8)	220		33.02	33.32	73		.79	2		145	
74	(17-18)	210		5.15	19.64	11		70.74	149		50	
74	(25-26)	660		2.22	15.26	15		83.28	550		95	
74	(29-30)	460		.49	15.68	2		94.85	436		22	
74	(44-45)	340		1.66	4.21	6		58.69	200		134	
75	(1- 2)	60		1.85	1.87	1		.87	1		58	
75	(16-18)	100		.38	3.24	0		86.40	86		14	
75	(21-22)	1220		0	0	0		86.64	1057		163	
75	(24-25)	510		0	0	0		85.60	437		73	
75	(29-30)	990		0	0	0		83.73	829		161	
75	(31-32)	750		.08	.45	1		79.67	598		151	
77	(0- 1)	820		12.77	60.08	105		79.00	648		67	
77	(3- 4)	880		11.96	30.07	105		56.64	498		277	
77	(7- 8)	1590		9.42	47.12	150		77.23	1228		212	
77	(15-16)	1410	1105	7.61	39.39	107	84	78.93	1113	872	190	149
77	(22-23)	1540		2.21	28.86	34		90.93	1400		106	
77	(26-27)	2030		1.12	26.30	23		93.83	1905		102	
77	(30-31)	1030		17.06	63.82	176		71.67	738		116	
77	(37-38)	490		16.54	29.93	81		43.67	214		195	
78	(12-13)	570	570	2.40	13.38	14	14	79.35	452	452	104	104
78	(15-16)	520	310	4.45	23.29	23	14	77.83	405	241	92	55
78	(18-19)	620		3.90	19.36	24		77.14	478		118	

APPENDIX III. Continued.

Site	Age Interval	Bulk Sed. Accum. Rate 1	Bulk Sed. Accum. Rate 2	% Biog. Silica Bulk	% Biog. Silica Carb-free	Biog. Silica Accum. Rate 1	Biog. Silica Accum. Rate 2	% $CaCO_3$	Carbonate Accum. Rate 1	Carbonate Accum. Rate 2	Non-biog. Accum. Rate 1	Non-biog. Accum. Rate 2
78	(25-26)	1480		2.35	14.45	35		81.88	1212		233	
78	(31-32)	2470		3.63	29.55	90		85.99	2124		256	
78	(34-35)	690		7.14	32.67	49		76.48	528		113	
79	(0- 1)	320		12.09	75.88	39		62.38	200		81	
79	(5- 6)	1250		0	0	0		44.66	558		692	
79	(9-10)	420		25.57	47.38	107		43.35	182		131	
79	(15-16)	2870	1910	17.51	43.55	502	334	57.76	1658	1103	710	473
79	(22-23)	1440		3.17	19.89	46		82.47	1188		206	
80	(0- 1)	640		5.29	32.31	34		80.65	516		90	
80	(6- 7)	460		18.81	46.71	87		56.42	260		113	
80	(13-14)	390	390	37.77	74.83	147	147	45.89	179	179	64	64
80	(16-17)	1690		10.66	42.68	180		72.41	1223		286	
80	(21-22)	650		4.92	17.52	82		70.30	457		111	
81	(0- 1)			6.13	65.75			73.67				
81	(14-15)			18.32	66.15			65.51				
82	(0- 1)	1080		17.23	71.88	186		76.03	821		73	
82	(5- 6)	9190		18.14	58.14	1668		66.31	6094		1428	
83	(0- 1)	1060		15.03	24.61	159		56.69	601		300	
83	(8- 9)	3060		31.83	49.85	974		33.74	1032		1054	
159	(0- 1)	190		1.33	1.34	3		.26	0		187	
159	(6- 7)	90		0	0	0		.23	0		90	
159	(13-14)	240	240	0	0	0	0	2.05	5	5	235	235
159	(15-16)	230	140	7.34	8.97	17	10	16.92	39	24	174	106
159	(17-18)	260		5.42	5.78	14		5.85	15		231	
159	(20-21)	800		7.61	16.04	61		50.19	402		337	

APPENDIX III. Continued.

Site	Age Interval	Bulk Sed. Accum. Rate 1	Bulk Sed. Accum. Rate 2	% Biog. Silica Bulk	% Biog. Silica Carb-free	Biog. Silica Accum. Rate 1	Biog. Silica Accum. Rate 2	% $CaCO_3$	Carbonate Accum. Rate 1	Carbonate Accum. Rate 2	Non-biog. Accum. Rate 1	Non-biog. Accum. Rate 2
159	(23-24)	1040		6.08	14.24	63		55.61	578		399	
160	(0- 1)	320		8.34	8.37	27		.37	1		292	
160	(15-16)	140		0	0	0		.27	0		140	
160	(21-22)	270		11.60	26.33	31		53.13	143		96	
160	(26-27)	1150		1.82	12.27	21		82.96	954		175	
160	(29-30)	690		1.59	15.94	11		88.26	609		70	
160	(34-35)	170		9.68	50.99	16		79.42	135		19	
161	(18-19)	180		16.04	19.56	29		17.40	31		120	
161	(22-23)	600		10.39	29.87	62		62.57	375		163	
161	(29-30)	1890		2.41	19.06	46		85.82	1620		222	
161	(34-35)	1010		5.27	29.95	53		79.91	807		150	
161	(40-41)											
161	(43-44)	910		27.79	52.65	253		46.26	421		236	
162	(30-31)	360		10.81	18.24	39		72.00	259		62	
162	(35-36)	420		6.68	23.80	28		69.96	294		98	
162	(37-38)	200		50.65	52.51	101		3.30	7		92	
162	(43-44)	1080		27.63	48.36	298		40.77	440		342	
162	(46-47)	680		47.44	62.14	323		22.16	151		206	
162	(48-49)	500		32.08	39.30	160		17.93	90		250	
162	(49-50)	1360		3.08	9.78	42		68.04	925		393	
163	(25-26)	120		3.75	3.79	5		.80	1		114	
163	(35-36)	30		51.24	51.66	15		.74	0		15	
163	(42-43)	290		74.11	74.63	215		.63	2		73	
163	(49-51)	180		89.17	89.65	161		.48	1		18	

APPENDIX IV. Salt-Free Analytical Concentrations of Elements Analyzed by Atomic Absorption (AAS), Error (1 σ) and Percent Error.

Sample	AAS Access. No.	Element	Concentration	Error (1 σ)	% Error
EP 42(24-25)	EP 958				
		MG	7059.8969	152.4938	2.16
		AL	20481.1178	137.2235	.67
		AL	16286.0442	296.4060	1.82
		AL	14401.5159	488.2114	3.39
		AL	19959.0039	2299.2777	11.52
		SI	144020.2892	6264.8826	4.35
		MN	2117.8139	36.6393	1.73
		MN	2240.5540	33.1602	1.48
		MN	2386.2657	18.8515	.79
		FE	12049.3541	437.3916	3.63
		FE	12636.1092	120.0430	.95
		FE	11551.0269	124.7511	1.08
EP42(30-31)	EP 959				
		MG	4822.8651	56.9098	1.18
		AL	3548.7367	85.5246	2.41
		AL	5990.1590	189.8880	3.17
		SI	63046.0397	2200.3068	3.49
		MN	575.8665	6.2194	1.08
		MN	606.7239	5.2785	.87
		FE	2738.1735	249.4476	9.11
		FE	3213.3819	37.5966	1.17
EP42(37-38)	EP 960				
		AL	26103.4356	15.6621	.06
		AL	26313.4834	7.8940	.03
		SI	279904.3080	13043.5408	4.66
		MN	4510.2611	50.9660	1.13
		FE	29658.7884	658.4251	2.22
EP 42(44-45)	EP 961				
		MG	7252.5013	147.9510	2.04
		AL	7533.1284	204.9011	2.72
		AL	7249.5460	177.5894	2.45
		SI	193469.7929	10041.0823	5.19
		MN	3277.8816	79.9803	2.44
		MN	3382.8193	53.1103	1.57
		FE	15373.1660	453.5084	2.95
		FE	15473.7671	204.2537	1.32
EP 42(46-47)	EP 962				
		MG	7012.5044	113.6026	1.62
		AL	6605.7347	150.6108	2.28
		AL	5939.4172	102.1539	1.72
		SI	235394.4555	9557.0153	4.06
		MN	3812.1438	86.5358	2.27
		FE	17112.7179	628.0366	3.67
		FE	17047.2940	240.3668	1.41
EP69(9-12)	EP 963				
		AL	26768.9601	16.0614	.06
		AL	27508.5756	22.0069	.08
		AL	26709.6725	21.3677	.08
		SI	320689.6710	12987.9317	4.05
		MN	5403.4333	58.3571	1.08
		FE	32297.7590	842.9715	2.61
EP63(15-16)	EP 964				
		AL	42337.3679	5220.1975	12.33
		SI	299842.1900	10310.0556	3.45
		MN	5113.8209	49.6041	.97
		FE	24034.3949	297.6545	1.24

Sample	AAS Access. No.	Element	Concentration	Error (1σ)	% Error
EP69(24-25)	EP 986				
		AL	10058.7183	529.0886	5.26
		SI	89908.9216	4909.0271	5.46
		CA	300520.6718	5485.9033	1.83
		CA	303084.2969	38398.8730	12.67
		MN	1896.3837	29.2043	1.54
		FE	10181.8297	377.7459	3.71
EP69(28-29)	EP 987				
		AL	4333.4382	249.1727	5.75
		AL	4138.0803	244.1467	5.90
		SI	44095.1362	1710.8913	3.88
		SI	40902.9609	1807.9109	4.42
		CA	495354.3281	17334.3560	3.50
		CA	433141.5468	13886.7209	3.21
		MN	595.7049	10.8418	1.82
		MN	598.5807	13.8971	2.32
		FE	4244.4640	149.8296	3.53
		FE	4639.0774	187.4197	4.04
EP69(38-39)	EP 988				
		AL	13139.2882	6.5696	.05
		SI	361918.6118	11436.6281	3.16
		MN	3741.4294	92.0392	2.46
		FE	20372.8938	240.4001	1.18
EP69(45-46)	EP 990				
		AL	7316.7311	128.7745	1.76
		SI	385459.2986	9713.5743	2.52
		FE	11529.8510	189.0896	1.64
EP 70(0-2)	EP 991				
		MG	18247.7880	463.4938	2.54
		AL	67086.9285	1851.5992	2.76
		AL	62697.8303	106.5863	.17
		AL	83936.6119	5447.4861	6.49
		SI	515005.9686	22248.2578	4.32
		SI	307256.2728	12566.7816	4.09
		CA	42739.4171	0	47.93
		CA	25363.3900	0	6.39
		CA	25925.3866	0	4.63
		MN	9375.0407	102.1879	1.09
		MN	7350.0302	147.7356	2.01
		MN	9451.3987	114.3619	1.21
		FE	31333.4604	485.6686	1.55
		FE	40590.1357	621.0291	1.53
EP 70(9-10)	EP 992				
		MG	10731.2215	267.2074	2.49
		AL	28503.6459	433.2554	1.52
		AL	25207.3488	5.0415	.02
		SI	360254.4817	13617.6194	3.78
		MN	5178.5171	84.9277	1.64
		MN	5264.1041	52.6410	1.00
		FE	27320.8556	732.1989	2.68
EP70(14-15)	EP 993				
		AL	20777.4178	1018.0935	4.90
		SI	173202.2272	18047.6717	10.42
		SI	158302.6370	8215.9069	5.19
		CA	281659.3672	17184.2192	6.10
		MN	3762.1628	74.1146	1.97
		FE	18136.5871	467.9239	2.58
EP 70(16-17)	EP 994				
		MG	9472.5979	242.4985	2.56
		AL	30055.5006	577.0656	1.92
		AL	26980.9468	8.0943	.03
		SI	284043.8949	10651.6460	3.75
		MN	4081.9787	77.5576	1.90
		MN	4085.0479	79.6584	1.95

Sample	AAS Access. No.	Element	Concentration	Error (1σ)	% Error
EP70(20-21)	EP 995				
		MG	2828.1131	57.6935	2.04
		AL	4400.9846	74.8167	1.70
		AL	3875.3514	265.0740	6.84
		SI	41301.3431	1420.7662	3.44
		SI	38754.8939	7103.7721	18.33
		MN	825.2864	8.5005	1.03
		MN	744.4752	0	0
		FE	5948.5557	224.2605	3.77
		FE	4478.8212	220.8059	4.93
EP70(28-29)	EP 996				
		MG	3424.8791	33.9063	.99
		AL	2765.8829	103.9972	3.76
		AL	2773.5257	229.0932	8.26
		SI	27360.1027	891.9393	3.26
		MN	595.0255	12.6145	2.12
		MN	529.4626	7.3595	1.39
		FE	3288.4904	192.7055	5.86
EP70(32-33)	EP 997				
		AL	4982.2981	241.1432	4.84
		SI	66143.8780	5007.0916	7.57
		SI	59376.0888	3699.1303	6.23
		MN	1443.1631	22.2247	1.54
		FE	5620.1302	109.0305	1.94
EP70(36-37.5)	EP 998				
		MG	411.7134	21.9855	5.34
		AL	20615.5956	138.1245	.67
		AL	14731.2723	85.4414	.58
		SI	276117.9372	9498.4570	3.44
		MN	2987.1007	106.0421	3.55
		MN	3088.5369	46.6369	1.51
		FE	25369.6310	484.5600	1.91
EP 71(6-7)	EP1000				
		MG	7338.8922	148.9795	2.03
		AL	14599.7203	195.6363	1.34
		AL	12902.8374	2.5806	.02
		SI	136500.8515	2716.3669	1.99
		SI	130309.6305	5798.7786	4.45
		SI	136500.8515	2716.3669	1.99
		MN	34550.5434	321.3291	.93
		MN	1641.1328	40.8642	2.49
		FE	10608.9627	528.3263	4.98
		FE	10800.8394	165.2528	1.53
		FE	10514.9854	394.3120	3.75
EP71(8-9)J07155	EP1001				
		MG	2059.9920	35.2259	1.71
		AL	2003.8525	75.7456	3.78
		AL	1645.6238	.8228	.05
		SI	42048.7921	1610.4687	3.83
		MN	519.9852	6.0839	1.17
		MN	480.4074	5.2845	1.10
		FE	1518.6795	38.5745	2.54
EP 71(13-14)	EP1002				
		MG	1584.5948	25.9874	1.64
		AL	1229.4577	60.7352	4.94
		AL	1674.4192	145.5070	8.69
		SI	28704.2975	668.8101	2.33
		MN	168.2661	3.8196	2.27
		MN	182.4278	2.9553	1.62
		FE	1013.3478	25.4350	2.51
		FE	1057.9618	10.1564	.96
EP71(20-21)	EP1021				
		AL	1384.4923	115.1898	8.32
		SI	17880.3882	879.7151	4.92
		MN	212.4064	1.3806	.65
		FE	3605.4474	90.1362	2.50

Sample	AAS Access. No.	Element	Concentration	Error (1σ)	%Error
EP71(26-27)	EP1022				
		AL	748.1897	115.4457	15.43
		AL	961.7653	56.9365	5.92
		SI	11460.8117	420.6118	3.67
		MN	234.3991	1.5002	.64
		FE	1157.5066	14.7003	1.27
		FE	1111.6955	137.8502	12.40
EP71(31-33)	EP1023				
		AL	2518.3108	193.9099	7.70
		SI	72598.2889	152.4564	.21
		FE	1895.9620	10.2382	.54
EP 72(0-1)	EP1024				
		MG	1223.3460	34.6207	2.83
		AL	4161.6144	121.9353	2.93
		AL	4217.6951	296.9257	7.04
		AL	5138.5951	154.6717	3.01
		AL	3788.4749	161.3890	4.26
		SI	51758.9040	807.4389	1.56
		MN	631.0575	6.1844	.98
		MN	637.5567	4.1441	.65
		MN	661.1143	4.3634	.66
		FE	2851.6711	209.8830	7.36
		FE	2869.4854	0	0
		FE	2882.6056	0	0
		FE	2781.5907	68.9834	2.48
EP 72(3-4)	EP1025				
		MG	4679.1129	76.7375	1.64
		AL	8978.8908	169.7010	1.89
		AL	8011.2575	1.6023	.02
		SI	82817.7940	2004.1906	2.42
		MN	2145.8451	7.2959	.34
		MN	1931.4579	47.9002	2.48
		FE	6809.9262	537.3032	7.89
EP 72(9-10)	EP1026				
		MG	1510.0358	30.6537	2.03
		AL	951.0243	62.8627	6.61
		SI	51671.1574	976.5849	1.89
		MN	262.0378	4.6905	1.79
		MN	259.2056	2.6439	1.02
		FE	759.1415	29.1510	3.84
EP 72(14-15)	EP1027				
		MG	1452.4624	30.7922	2.12
		MG	1574.7222	37.7933	2.40
		AL	1089.9519	75.6427	6.94
		AL	940.1857	57.5394	6.12
		AL	925.6809	125.8926	13.60
		SI	26226.7730	1258.8851	4.80
		MN	355.3557	5.2948	1.49
		MN	359.9373	3.9233	1.09
		MN	362.2254	4.2018	1.16
		FE	742.5216	22.2014	2.99
		FE	777.2856	30.4696	3.92
		FE	894.7942	14.1377	1.58
EP72(27-28)	EP1028				
		MG	2744.9978	23.3325	.85
		AL	657.1776	48.1054	7.32
		AL	692.6118	124.0469	17.91
		SI	7494.1519	415.9254	5.55
		MN	190.4631	6.3043	3.31
		MN	166.9629	3.6899	2.21
		FE	592.6362	7.6450	1.29

Sample	AAS Access. No.	Element	Concentration	Error (1σ)	% Error
EP 72(36-37)	EP1029				
		MG	3561.7929	122.1695	3.43
		AL	2589.6213	57.2306	2.21
		AL	2411.0955	167.3300	6.94
		AL	2395.8545	72.8340	3.04
		SI	27463.7756	472.3769	1.72
		SI	27802.8416	636.6851	2.29
		MN	231.3229	3.9788	1.72
		MN	237.3700	2.8247	1.19
		FE	2476.0960	151.2895	6.11
		FE	2082.6938	34.9893	1.68
		FE	2165.1205	186.6334	8.62
EP72(37-38)	EP1030				
		AL	6325.5486	241.6360	3.82
		SI	151128.8898	4004.9156	2.65
		MN	1392.7556	21.4484	1.54
		FE	9476.4081	306.0880	3.23
EP 72(39-40)	EP1031				
		MG	7525.4471	225.0109	2.99
		AL	4925.1543	97.5181	1.98
		AL	4844.8582	240.7895	4.97
		SI	81617.1983	1518.0799	1.86
		MN	2228.8562	10.9214	.49
		MN	2302.6959	46.9751	2.04
		FE	11415.1186	429.2085	3.76
		FE	11930.1535	139.5828	1.17
EP 73(0-1)	EP1032				
		MG	2280.4249	38.3111	1.68
		AL	4053.8816	52.2951	1.29
		AL	3529.4736	194.4740	5.51
		AL	3640.3268	194.3934	5.34
		SI	47700.5520	3348.5788	7.02
		MN	509.1187	7.1786	1.41
		MN	546.6099	8.6364	1.58
		MN	545.0060	5.6681	1.04
		MN	469.1004	6.2859	1.34
		FE	2557.7803	27.8798	1.09
		FE	3028.6404	68.7501	2.27
EP 73(4-5)	EP1033				
		MG	4734.4805	84.2738	1.78
		AL	7124.1860	91.1896	1.28
		AL	6802.7974	248.3021	3.65
		SI	138012.1082	3146.6761	2.28
		SI	140621.7839	7452.9545	5.30
		MN	663.8751	8.3648	1.26
		MN	631.5564	11.1785	1.77
		FE	5601.1329	277.8162	4.96
		FE	6330.4955	184.2174	2.91
EP 73(8-9)	EP1034				
		MG	7480.1706	115.1946	1.54
		AL	7393.0309	164.1253	2.22
		SI	222796.1260	7218.5945	3.24
		MN	4925.5860	98.5117	2.00
		MN	4873.1189	45.3200	.93
		FE	14397.0184	348.4078	2.42
		FE	14567.7922	225.8008	1.55
EP 73(14-15)	EP1035				
		MG	1915.3555	38.8817	2.03
		AL	2707.0660	207.0905	7.65
		AL	2883.2145	89.6680	3.11
		SI	27065.4340	395.1553	1.46
		MN	803.4366	5.9454	.74
		MN	794.7733	0	0
		FE	2021.0990	39.6135	1.96
		FE	2186.9009	48.1118	2.20

Sample	AAS Access. No.	Element	Concentration	Error (1σ)	% Error
EP 73(20-22)	EP1036				
		MG	1231.5175	26.8471	2.18
		AL	971.0484	89.6278	9.23
		AL	927.7998	79.8836	8.61
		SI	8001.9627	321.6789	4.02
		MN	147.8184	4.5972	3.11
		MN	151.1092	2.3271	1.54
		FE	511.1844	17.8915	3.50
		FE	662.5532	11.3297	1.71
EP 73(32-33)	EP1037				
		MG	1228.2813	29.9701	2.44
		AL	868.8414	72.8089	8.38
		AL	875.3867	104.2586	11.91
		SI	23235.8811	592.5150	2.55
		MN	169.6029	3.5786	2.11
		MN	134.2332	2.1746	1.62
		FE	958.3223	10.0624	1.05
EP73(39-40)	EP1038				
		MG	3477.3276	81.7172	2.35
		AL	6497.2717	113.7023	1.75
		AL	6255.4023	143.2487	2.29
		SI	88363.4658	2111.8868	2.39
		MN	1419.8294	64.0343	4.51
		FE	9184.3327	308.5936	3.36
		FE	4291.2098	411.0979	9.58
EP73(43-44)	EP1039				
		AL	2443.5070	218.4495	8.94
		SI	35787.3324	2014.8268	5.63
		MN	2982.3147	52.7870	1.77
		FE	15375.1679	278.2905	1.81
EP74(0-1)	EP1040				
		AL	40142.4842	959.4054	2.39
		AL	35520.2199	738.8206	2.03
		AL	34806.9096	1736.8648	4.99
		AL	46575.5276	3535.0825	7.59
		SI	291883.1851	13893.6396	4.76
		SI	266113.6870	12188.0069	4.58
		CA	45630.8740	4302.6531	9.43
		MN	9747.5044	110.1468	1.13
		MN	9687.7334	83.3145	.86
		MN	9029.0520	289.8326	3.21
		FE	43552.3861	766.5220	1.76
		FE	47435.6477	1152.6862	2.43
		FE	47141.6647	28.2850	.06
		FE	45130.3716	699.5208	1.55
EP74(7-8)	EP1041				
		AL	33129.5489	1202.6026	3.63
		SI	268411.9692	10817.0024	4.03
		MN	20766.6103	166.1329	.80
		FE	51829.6557	932.9338	1.80
		FE	54705.6353	1280.1119	2.34
EP 74(17-18)	EP1042				
		MG	5358.1845	134.4904	2.51
		AL	7307.8985	127.8882	1.75
		AL	5940.2110	122.9624	2.07
		SI	47632.5265	3158.0365	6.63
		MN	3075.8152	161.4803	5.25
		FE	11913.1307	279.9586	2.35
		FE	12034.8231	196.1676	1.63

Sample	AAS Access. No.	Element	Concentration	Error (1σ)	% Error
EP 74(25-26)	EP1043				
		MG	3695.2973	89.7957	2.43
		AL	5444.0940	117.5924	2.16
		AL	4901.2341	168.1123	3.43
		SI	28100.2736	615.3960	2.19
		MN	1686.6361	12.3124	.73
		FE	8171.0697	257.3887	3.15
		FE	7467.6324	188.9311	2.53
EP74(29-30)	EP1044				
		MG	2986.8673	24.7910	.83
		AL	1080.4251	77.5745	7.18
		AL	1183.1425	103.6433	8.76
		SI	6143.9181	377.2366	6.14
		MN	431.3365	7.0308	1.63
		MN	382.9149	4.6333	1.21
		FE	2824.4119	173.7013	6.15
		FE	1463.3511	0	0
EP 74(44-45)	EP1045				
		MG	7332.5221	136.3849	1.86
		AL	9501.5489	134.9220	1.42
		AL	7940.5678	832.9656	10.49
		SI	40409.0139	2032.5734	5.03
		MN	20052.4916	511.3385	2.55
		MN	21563.2145	256.6023	1.19
		FE	64397.2665	637.5329	.99
		FE	69636.2888	3816.0686	5.48
EP75(1-2)	EP1046				
		AL	46367.3859	1590.4013	3.43
		AL	53716.8335	3008.1427	5.60
		SI	152572.9512	35000.2350	22.94
		SI	153229.2409	9530.8588	6.22
		CA	60025.2441	6832.0509	11.38
		MN	40056.1596	584.8199	1.46
		MN	40828.3563	1363.6671	3.34
		MN	43112.0770	405.2535	.94
		MN	45951.3067	280.3030	.61
		FE	165814.2357	9965.4356	6.01
		FE	168794.2959	1485.3898	.88
		FE	187138.3763	5951.0004	3.18
EP75(16-18)	EP1047				
		AL	2752.2289	117.7954	4.28
		AL	3021.5373	171.0190	5.66
		SI	12050.4604	483.2235	4.01
		SI	10804.9125	517.5553	4.79
		MN	3056.7076	51.3527	1.68
		MN	3283.7494	63.7047	1.94
		FE	17564.8159	289.8195	1.65
		FE	17833.5639	219.3528	1.23
EP75(21-22)	EP1048				
		AL	711.4787	124.2953	17.47
		SI	3169.6854	594.6330	18.75
		MN	708.0353	9.6293	1.36
EP75(24-25)	EP1049				
		AL	1108.9934	190.3033	17.16
		AL	1090.3473	127.2435	11.67
		SI	4269.7688	317.2438	7.43
		MN	609.3205	.9749	.16
		MN	783.4902	0	0
		FE	8031.7318	301.9931	3.76
		FE	7860.3758	192.5792	2.45

Sample	AAS Access. No.	Element	Concentration	Error (1σ)	% Error
EP 75(29-30)	EP1050				
		MG	2969.6696	21.6786	.73
		AL	1143.3429	109.0749	9.54
		AL	1171.1236	.1171	.01
		SI	4260.8390	278.6589	6.54
		MN	2788.6882	105.1335	3.77
		MN	2511.5514	42.4452	1.69
		FE	16076.9580	191.3158	1.19
		FE	9201.0909	524.4622	5.70
EP75(31-32)	EP1051				
		AL	833.9914	130.0193	15.59
		AL	839.7213	184.3188	21.95
		SI	3597.4191	646.8160	17.98
		MN	19258.8968	304.2906	1.58
		FE	40489.5170	558.7553	1.38
EP 77(0-1)	EP1052				
		MG	3036.3305	61.0302	2.01
		AL	4009.0945	67.3528	1.69
		AL	4936.5831	269.0438	5.45
		AL	4678.7560	222.2409	4.75
		SI	78839.3952	1852.7258	2.35
		SI	68085.4050	10260.4705	15.07
		SI	66480.3886	1150.1107	1.73
		MN	1729.5007	12.1065	.70
		MN	1521.5199	27.8438	1.83
		MN	1569.5550	53.6788	3.42
		FE	4037.6960	125.1686	3.10
		FE	3259.7018	0	0
		FE	3245.0685	0	0
EP77(3-4)	EP1053				
		AL	5870.9579	212.5287	3.62
		SI	78743.5174	1244.1476	1.58
		MN	2520.4963	60.7449	2.41
EP77(7-8)	EP1054				
		AL	1189.9030	165.3965	13.90
		SI	50055.9625	1877.0986	3.75
		MN	351.0549	4.4233	1.26
EP77(15-16)	EP1055				
		AL	1351.8615	150.1918	11.11
		SI	42021.7313	600.9108	1.43
		MN	529.3968	10.1115	1.91
EP77(23-24)	EP1056				
		AL	686.2853	177.4734	25.86
		SI	13371.6712	383.7670	2.87
		MN	396.5406	4.8774	1.23
EP77(26-27)	EP1057				
		AL	768.3211	207.6004	27.02
		SI	8092.6893	331.8003	4.10
		MN	150.5868	2.1383	1.42
EP77(30-31)	EP1058				
		MG	2923.7069	33.9150	1.16
		AL	870.7729	203.6738	23.39
		SI	85559.6982	1565.7425	1.83
		MN	183.6669	6.1528	3.35
		MN	126.8833	1.8398	1.45
		FE	2492.9662	435.5212	17.47

Sample	AAS Access. No.	Element	Concentration	Error (1σ)	% Error
EP77(37:38)	EP1059				
		AL	10278.9462	496.4731	4.83
		SI	120114.0752	1321.2548	1.10
		MN	18028.9069	1.8029	.01
EP78(12-13)	EP1060				
		AL	4197.2599	285.4137	6.80
		SI	26285.8944	528.3465	2.01
		MN	1433.6044	112.1079	7.82
EP78(15-16)	EP1061				
		AL	4372.8248	271.1151	6.20
		SI	36567.7844	490.0083	1.34
		MN	1229.4984	16.9671	1.38
EP78(18-19)	EP1062				
		AL	3332.5243	181.6226	5.45
		SI	30902.2113	336.8341	1.09
		MN	1368.5752	89.2311	6.52
		MN	1567.5423	60.1936	3.84
		FE	9597.7402	309.0472	3.22
EP78(25-26)	EP1063				
		AL	4912.5895	478.9775	9.75
		SI	28092.8128	369.0158	1.31
		MN	662.7306	.0663	.01
EP78(31-32)	EP1064				
		AL	1563.9261	159.3641	10.19
		AL	1625.7581	103.8859	6.39
		SI	21483.6414	296.4743	1.38
		FE	3564.8274	345.0753	9.68
EP78(34-35)	EP1065				
		AL	3267.5671	269.5743	8.25
		SI	47494.9820	3690.3601	7.77
		CA	368342.0156	20286.6294	5.51
		MN	1599.1222	83.9539	5.25
		FE	9366.8873	314.7274	3.36
EP 79(0-1)	EP1066				
		MG	4032.6475	68.9533	1.71
		AL	7586.6976	106.9724	1.41
		AL	8006.3072	309.8441	3.87
		AL	6770.4771	329.7222	4.87
		SI	83051.0023	2001.5292	2.41
		SI	87021.9636	9502.7984	10.92
		CA	357238.8125	7519.3058	2.10
		CA	322368.2343	35292.8389	10.95
		CA	334542.6250	19997.8394	5.98
		MN	4171.6024	110.1303	2.64
		MN	3948.7519	69.4980	1.76
		MN	4196.3305	61.2664	1.46
		MN	4332.2440	77.1139	1.78
		FE	8008.2918	199.4065	2.49
		FE	7635.3902	172.5598	2.26
		FE	8256.7678	277.4274	3.36
EP79(5-6)	EP1067				
		AL	4895.4086	168.4021	3.44
		SI	19125.1105	2448.0141	12.80
		FE	6549.0636	184.0287	2.81

Sample	AAS Access. No.	Element	Concentration	Error (1 σ)	% Error
EP79(9-10)A JD08	EP1068				
		AL	4030.1704	154.7585	3.84
		SI	138332.2974	22077.8347	15.96
		FE	15622.3133	476.4806	3.05
EP79(15-16)AJD81	EP1069				
		AL	2559.9033	98.3003	3.84
		SI	94531.1723	330.8591	.35
		MN	684.1980	13.0682	1.91
		FE	5183.2249	107.8111	2.08
EP79(22-23)A JD0	EP1071				
		AL	1349.5360	59.9194	4.44
		SI	21448.6434	394.6550	1.84
		FE	11221.8301	461.2172	4.11
EP80(0-1)A JD814	EP1072				
		AL	2099.6680	143.4073	6.83
		SI	34136.4173	102.4093	.30
		MN	493.1263	9.2708	1.88
		FE	1213.7551	31.4363	2.59
EP80(6-7)A JD081	EP1073				
		AL	3854.5773	104.8445	2.72
		AL	3444.8243	110.5789	3.21
		SI	102049.2364	602.0905	.59
		SI	105861.9733	296.4135	.28
		FE	2982.8914	202.8366	6.80
		FE	3044.8978	110.2253	3.62
EP80(13-14)AJD81	EP1074				
		AL	2131.8672	79.5186	3.73
		SI	189037.6472	16068.2000	8.50
		FE	2232.0399	135.9312	6.09
EP80(16-17)A JD0	EP1075				
		AL	4313.8708	111.7293	2.59
		AL	2611.7982	60.0714	2.30
		SI	65488.2943	2567.1411	3.92
		SI	65134.6668	7229.9480	11.10
		SI	58051.9305	1526.7658	2.63
		FE	27138.0149	1753.1158	6.46
		FE	5204.6936	159.2636	3.06
EP80(21-22)AJD63	EP1076				
		AL	1848.9518	155.4968	8.41
		SI	31337.7565	360.3842	1.15
		MN	8849.5033	49.5572	.56
		FE	27983.3938	607.2396	2.17
EP81(0-1)A JD071	EP1077				
		AL	2907.2247	124.7199	4.29
		AL	2619.3456	155.8511	5.95
		SI	41341.7565	2294.4675	5.55
		SI	41555.0140	2954.5615	7.11
		CA	356955.9375	32566.6338	9.12
		MN	541.6326	5.9580	1.10
		MN	510.5419	4.6970	.92
		MN	477.9922	9.9900	2.09
		FE	3216.2764	.3216	.01
		FE	3113.4547	30.2005	.97
		FE	3314.8366	74.9153	2.26
EP81(14-15)A JD0	EP1078				
		AL	1221.1885	178.7820	14.64
		SI	96416.1100	1301.6175	1.35
		MN	2093.8511	49.8337	2.38

Sample	AAS Access. No.	Element	Concentration	Error (1σ)	% Error
EP82(0-1)	EP1080				
		AL	5080.9292	170.2111	3.35
		AL	3231.3326	108.2496	3.35
		SI	100355.5505	4475.8576	4.46
		SI	82771.0701	13814.4916	16.69
		SI	41119.5347	2940.0467	7.15
		SI	36581.2897	4605.5844	12.59
		CA	353430.7187	39773.8594	11.25
		MN	1291.2872	8.9099	.69
		MN	1235.6178	50.1661	4.06
		FE	6655.1290	202.9814	3.05
		FE	6025.4606	126.5347	2.10
		FE	6259.2592	93.8889	1.50
EP82(5-6)	EP1081				
		AL	1618.1762	103.8869	6.42
		SI	93482.6518	243.0549	.26
		MN	960.4609	15.3674	1.60
		FE	6924.7870	144.7280	2.09
EP83(0-1)	EP1082				
		AL	20512.1711	0	0
		AL	18355.1306	614.8969	3.35
		AL	18880.2161	373.8283	1.98
		AL	17891.0062	982.2162	5.49
		SI	131965.5877	3022.0120	2.29
		SI	137346.9592	5727.3682	4.17
		SI	107018.0739	7694.5995	7.19
		SI	104347.6329	8953.0269	8.58
		CA	230474.8476	6509.8855	2.82
		MN	7703.5676	118.6349	1.54
		MN	7902.0291	120.1108	1.52
		MN	7879.8250	115.8334	1.47
		FE	31921.9145	1117.2670	3.50
		FE	34244.5580	308.2010	.90
		FE	36458.6022	473.9618	1.30
EP83889)	EP1083				
		AL	3540.5939	118.2558	3.34
		SI	168799.5591	3527.9109	2.09
		FE	25135.2872	755.8586	3.00
EP159(0-1)	EP1084				
		AL	86418.0284	4260.4084	4.93
		AL	86126.2190	5245.0857	6.09
		SI	220661.8799	10988.9616	4.98
		SI	242324.9035	15799.5837	6.52
		SI	269195.2181	18143.7577	6.74
		SI	254239.2143	18712.0062	7.36
		CA	10471.9790	388.8856	3.71
		CA	10603.5264	512.4302	4.83
		MN	19694.1685	577.0391	2.93
		MN	20964.7644	635.2324	3.03
		FE	52078.3959	15.6235	.03
		FE	53127.0084	31.8762	.05
		FE	52338.9716	2438.9961	4.65
EP159(6-7)	EP1085				
		AL	82437.0715	3033.6842	3.68
		SI	254565.1918	2087.4346	.82
		MN	12756.0947	457.9439	3.59
		FE	55937.6888	352.4074	.63
EP159(13-14)	EP1086				
		AL	97690.8337	4376.5493	4.48
		SI	271051.1646	3984.4521	1.47
		SI	259665.4456	17631.2838	6.79
		MN	11437.0698	122.3766	1.07
		FE	79474.5471	1286.8397	1.62

Sample	AAS Access. No.	Element	Concentration	Error (1σ)	% Error
EP159(15-16)B J0	EP1087				
		AL	34957.7448	1789.8365	5.12
		SI	152011.2247	5502.8063	3.62
		FE	47942.1927	6841.3509	14.27
EP159(17-18)B J0	EP1088				
		AL	44302.3439	3313.8153	7.48
		SI	173299.8680	12217.6407	7.05
		MN	10067.0710	269.7975	2.68
		FE	76507.5219	1117.0098	1.46
159(20-21)A J063	EP1089				
		AL	10116.8489	146.6943	1.45
		SI	76984.2193	1068.6906	1.39
		FE	40771.0630	615.6431	1.51
159(23-24)A J063	EP1090				
		AL	4911.0778	152.7345	3.11
		SI	50790.6795	1036.1299	2.04
		MN	15455.6835	123.6455	.80
		FE	53129.4289	361.2801	.68
8 EP160(0-1)J063	EP1091				
		AL	88369.6751	459.5223	.52
		AL	88994.2828	4245.0273	4.77
		SI	294895.7217	11559.9123	3.92
		SI	260869.7812	12991.3151	4.98
		CA	20952.0054	3818.3136	18.22
		CA	19916.1919	1990.3159	9.99
		MN	10284.8065	115.1898	1.12
		MN	9996.8618	290.9087	2.91
		FE	63141.3635	2374.1153	3.76
EP160(15-16)B J0	EP1092				
		AL	85043.4393	3665.3722	4.31
		SI	239322.4342	5145.4323	2.15
		MN	10440.6158	110.6705	1.06
		FE	66030.7868	759.3540	1.15
EP160(21-22)A J0	EP1093				
		AL	12054.4614	191.6659	1.59
		SI	96645.7050	2454.8009	2.54
		MN	2156.4753	47.0112	2.18
		FE	3755.8350	94.6470	2.52
EP160(26-27)A J0	EP1094				
		AL	3315.6265	168.1022	5.07
		SI	20515.8427	332.3567	1.62
		MN	438.7110	5.0013	1.14
		FE	7289.4617	145.0603	1.99
EP160(29-30)J063	EP1095				
		MG	3675.1904	54.3928	1.43
		AL	2267.4233	70.9703	3.13
		AL	2262.4360	94.1173	4.16
		AL	1845.6238	94.8651	5.14
		SI	14966.0843	239.4573	1.60
		MN	295.8332	3.4612	1.17
		FE	3410.9905	160.3166	4.70
		FE	3331.0775	221.5167	6.65
		FE	3274.5808	69.7486	2.13
EP160(34-35)AJ06	EP1097				
		AL	3913.0271	102.9126	2.63
		SI	61299.8068	1134.0464	1.85
		FE	4437.2209	170.8330	3.85

Sample	AAS Access. No.	Element	Concentration	Error (1σ)	% Error
P161(18-19)	EP1098				
		AL	30249.5184	12.0998	.04
		AL	40206.1089	2637.5207	6.56
		SI	186524.9412	1268.3696	.68
		SI	195874.5343	7737.0441	3.95
		SI	180160.7757	13854.3637	7.69
		SI	211534.4263	9984.4249	4.72
		FE	30055.4508	1490.7504	4.96
		FE	31586.8737	754.9263	2.39
EP161(22-23)	EP1099				
		AL	7839.1658	135.6937	1.72
		SI	75218.0002	3587.8986	4.77
		SI	78893.1926	4993.9391	6.33
		MN	1588.2200	22.5527	1.42
		FE	8479.2828	226.3969	2.67
EP161(29-30)	EP1100				
		MG	2630.9521	34.4655	1.31
		AL	1790.4831	88.2708	4.93
		AL	1608.7698	48.1022	2.99
		SI	18121.8036	527.3445	2.91
		SI	17910.9483	549.8661	3.07
		MN	472.9468	12.1547	2.57
		MN	428.9297	4.3751	1.02
		FE	1192.0395	141.0183	11.83
		FE	1530.8746	26.7903	1.75
EP161(34-35)	EP1101				
		AL	2257.8242	51.9300	2.30
		SI	34404.0792	1348.6399	3.92
		SI	32934.9785	365.5783	1.11
		FE	2074.7459	70.1264	3.38
EP161(40-41)	EP1102				
		AL	10183.9770	193.4956	1.90
EP161(43-44)	EP1103				
		AL	4274.0320	111.1248	2.60
		SI	136599.9880	4712.6996	3.45
		SI	158284.7917	7850.9257	4.96
		MN	3334.0222	46.3429	1.39
		FE	16030.9232	307.7937	1.92
EP162(30-31)	EP1104				
		AL	22044.9286	4.4090	.02
		SI	109419.6436	831.5893	.76
		SI	125297.6990	864.5541	.69
		SI	125925.3644	8424.4069	6.69
		FE	22437.7926	170.5272	.76
EP162(35-36)	EP1105				
		AL	6573.4238	114.3776	1.74
		AL	6698.3355	122.5795	1.83
		SI	55030.6476	3065.2071	5.57
		MN	1990.6430	33.6419	1.69
		FE	10575.3530	143.8248	1.36
EP162(37-38)	EP1106				
		AL	22968.2695	179.1525	.78
		SI	319097.0916	9126.1768	2.86
		FE	37566.0157	3200.6245	8.52

Sample	AAS Access. No.	Element	Concentration	Error (1σ)	% Error
EP162(43-44)	EP1107				
		AL	7245.2534	163.7427	2.26
		AL	7212.6027	191.8552	2.66
		SI	157380.4045	1101.6628	.70
		FE	17596.5045	415.2775	2.36
EP162(46-47)	EP1119				
		AL	14608.6021	105.1819	.72
		SI	277003.4271	8614.8066	3.11
		FE	23764.8319	254.2837	1.07
EP162(48-49)	EP1120				
		AL	6986.8156	139.0376	1.99
		AL	6978.7316	282.6386	4.05
		SI	178462.3823	1195.6980	.67
		SI	254530.6191	8934.0247	3.51
		MN	13415.8121	191.8461	1.43
		FE	47968.6067	983.3564	2.05
EP162(49-50)	EP1121				
		AL	4207.2189	63.9497	1.52
		SI	30735.6403	771.4646	2.51
		FE	43557.3536	4965.5383	11.40
EP163(25-26)	EP1122				
		AL	70799.9749	1812.4794	2.56
		SI	248096.4893	13397.2104	5.40
		FE	44388.3408	2290.4384	5.16
EP163(35-36)	EP1123				
		AL	36846.0645	1333.8275	3.62
		AL	27139.2168	1354.2469	4.99
		SI	351779.1596	11116.2214	3.16
		FE	25534.5201	495.3697	1.94
EP163(42-43)	EP1124				
		AL	11846.6299	133.8569	1.13
		SI	387727.2631	8568.7725	2.21
		FE	14534.0470	302.3082	2.08
EP163(49-51)	EP1125				
		AL	2822.4993	102.7390	3.64
		SI	431202.3795	15609.5261	3.62
		FE	7280.5800	126.6821	1.74
EP163(63-64)	EP1126				
		AL	74155.1685	2283.9792	3.08
		SI	259753.1411	5896.3967	2.27
		MN	9276.1961	237.4706	2.56
		FE	53219.7364	633.3149	1.19
EP163(71-72)	EP1127				
		AL	10100.6087	675.7307	6.69
		SI	66838.0459	3194.8586	4.78
		MN	2898.4538	33.0424	1.14
		FE	17578.0351	221.4832	1.25
EP163(77-78)	EP1128				
		AL	6327.3655	110.7289	1.75
		SI	40142.3180	895.1737	2.23
		MN	1118.4011	13.9800	1.25
		FE	8161.9069	154.2600	1.89

Sample	AAS Access. No.	Element	Concentration	Error (1σ)	% Error
EP71(39-40)	EP1471				
		AL	6402.3644	339.9655	5.31
		SI	265780.1244	11083.0312	4.17
		CA	145283.2930	6000.4376	4.13
		MN	779.6321	23.2330	2.98
		FE	15746.8632	283.4435	1.80
EP69(43-44)	EP1472				
		AL	5963.8205	294.0164	4.93
		SI	410360.9836	10661.5830	2.60
		MN	461.0064	3.9647	.86
		FE	6485.0546	1448.7612	22.34
EP160(1-2)	EP1481				
		AL	94192.3720	2431.0055	2.58
		SI	233315.3949	5366.2679	2.30
		MN	10808.0746	323.1614	2.99
		FE	67944.6755	2541.1309	3.74

APPENDIX V. Salt-Free and Carbonate-Free Analytical Concentration of Elements Analyzed by Atomic Absorption (AAS), Error (1 σ) and Percent Error.

Sample	AAS Access. No.	Element	Concentration	Error (1 σ)	% Error
EP 42(24-25)	EP 958				
		MG	15942.4924	344.3578	2.16
		AL	46249.9763	309.8748	.67
		AL	36776.7603	669.3370	1.82
		AL	32521.1629	1102.4674	3.39
		AL	45070.9511	5192.1736	11.52
		SI	325223.2145	14147.2098	4.35
		MN	4782.4085	82.7357	1.73
		MN	5059.5660	74.8816	1.48
		MN	5388.6088	42.5700	.79
		FE	27209.5668	987.7073	3.63
		FE	28534.5429	271.0782	.95
		FE	26084.2560	281.7100	1.08
EP42(30-31)	EP 959				
		MG	29830.5087	352.0000	1.18
		AL	21949.7369	528.9887	2.41
		AL	37050.4844	1174.5004	3.17
		SI	389953.9770	13609.3938	3.49
		MN	3561.8644	38.4681	1.08
		MN	3752.7242	32.6487	.87
		FE	16936.2209	1542.8897	9.11
		FE	19875.4920	232.5433	1.17
EP42(37-38)	EP 960				
		AL	27089.6249	16.2538	.06
		AL	27307.6083	9.1923	.03
		SI	290479.1036	13536.3265	4.66
		MN	4681.6591	52.8914	1.13
		FE	30779.2981	683.3004	2.22
EP 42(44-45)	EP 961				
		MG	12777.9149	260.6695	2.04
		AL	13272.3414	361.0077	2.72
		AL	12770.9462	312.8882	2.45
		SI	340867.3027	17591.0130	5.16
		MN	5775.1789	140.9144	2.44
		MN	5960.0647	93.5730	1.57
		FE	27085.4150	799.0197	2.95
		FE	27262.6614	359.8671	1.32
EP 42(46-47)	EP 962				
		MG	9006.6002	145.9069	1.62
		AL	8484.1603	193.4389	2.28
		AL	7628.3668	131.2079	1.72
		SI	302331.9078	12274.6755	4.06
		MN	4896.1823	111.1433	2.27
		FE	21978.9341	806.6269	3.67
		FE	21894.9112	308.7182	1.41
EP69(9-12)	EP 963				
		AL	27056.9941	16.2342	.06
		AL	27804.5678	22.2437	.08
		AL	26937.0685	21.5977	.08
		SI	324140.2908	13127.6818	4.05
		MN	5461.5793	58.9851	1.08
		FE	32645.2818	852.0419	2.61
EP69(15-16)	EP 964				
		AL	42680.9144	5262.5567	12.33
		SI	301267.1447	10393.7155	3.45
		MN	5155.3170	50.0060	.97
		FE	24199.1786	300.0698	1.24

Sample	AAS Access. No.	Element	Concentration	Error (1σ)	% Error
EP69(24-25)	EP 986				
		AL	23195.7609	1220.0970	5.26
		SI	207333.1594	11320.3905	5.46
		CA	300520.6718	5485.9033	1.33
		CA	303084.2969	38398.8730	12.67
		MN	4373.1281	67.3462	1.54
		FE	23479.6601	871.0954	3.71
EP69(28-29)	EP 987				
		AL	19767.8469	1136.6512	5.75
		AL	18876.6828	1113.7243	5.90
		SI	201148.8038	7804.5736	3.88
		SI	186587.0561	8247.1479	4.42
		CA	495354.3281	17334.3560	3.50
		CA	433141.5468	13886.7209	3.21
		MN	2717.4271	49.4572	1.82
		MN	2730.5460	63.3487	2.32
		FE	19361.9736	683.4777	3.53
		FE	21162.0817	854.9481	4.04
EP69(38-39)	EP 988				
		AL	13220.9201	6.6105	.05
		SI	364167.1451	11507.6818	3.16
		MN	3764.6742	92.6110	2.46
		FE	20499.4669	241.8957	1.18
EP69(45-46)	EP 990				
		AL	7331.0102	129.0258	1.76
		SI	386211.5492	9730.5310	2.52
		FE	11592.3523	189.4586	1.64
EP 70(0-2)	EP 991				
		MG	18480.3348	469.4005	2.54
		AL	67941.8732	1875.1957	2.76
		AL	63496.8411	107.9446	.17
		AL	85006.2962	5515.9081	6.49
		SI	521569.1193	22531.7860	4.32
		SI	311171.8958	12725.9305	4.09
		CA	42739.4171	[illegible]	47.93
		CA	25363.3900	[illegible]	6.39
		CA	25925.3866		4.63
		MN	9494.5147	103.4902	1.09
		MN	7443.6978	149.6183	2.01
		MN	9571.8457	115.8193	1.21
		FE	31732.7688	491.8579	1.55
		FE	41137.4096	628.9434	1.53
EP 70(9-10)	EP 992				
		MG	10817.6874	269.3604	2.49
		AL	28733.3117	436.7463	1.52
		AL	25410.4550	5.0821	.02
		SI	363157.2027	13727.3423	3.78
		MN	5220.2425	85.6120	1.64
		MN	5306.5192	53.0652	1.00
		FE	27540.9912	738.0986	2.68
EP70(14-15)	EP 993				
		AL	27254.4779	1335.4694	4.90
		SI	227195.5165	23673.7729	10.42
		SI	207651.1994	10777.0972	5.19
		CA	281659.3672	17184.2192	6.10
		MN	4934.9628	97.2188	1.97
		FE	23790.4064	613.7925	2.58
EP 70(16-17)	EP 994				
		MG	9819.5056	251.3793	2.56
		AL	31156.2000	598.1990	1.92
		AL	27969.0492	8.3907	.03
		SI	294446.2145	11041.7330	3.75
		MN	4231.4699	80.3979	1.90
		MN	4234.6515	82.5757	1.95

Sample	AAS Access. No.	Element	Concentration	Error (1σ)	% Error
EP70(20-21)	EP 995				
		MG	13864.4695	282.8352	2.04
		AL	21575.2748	366.7797	1.70
		AL	18998.4237	1299.4922	6.84
		SI	202474.6512	6965.1280	3.44
		SI	189991.0036	34825.3510	18.33
		MN	4045.8631	41.6724	1.03
		MN	3649.6964	[illegible]	[illegible]
		FE	29162.0475	1099.4092	3.77
		FE	21956.8589	1082.4731	4.93
EP70(28-29)	EP 996				
		MG	26747.3173	264.7984	.99
		AL	21600.7470	812.1881	3.76
		AL	21660.4355	1789.1520	8.26
		SI	213674.5082	6965.7890	3.26
		MN	4646.9778	98.5159	2.12
		MN	4134.9501	57.4758	1.39
		FE	25682.1613	1504.9747	5.86
EP70(32-33)	EP 997				
		AL	15460.7522	748.3004	4.84
		SI	205253.4972	15537.6897	7.57
		SI	184252.1218	11478.9072	6.23
		MN	4478.3325	68.9663	1.54
		FE	17440.0323	338.3368	1.94
EP70(36-37.5)	EP 998				
		MG	534.4691	28.5407	5.34
		AL	26762.3050	179.3074	.67
		AL	19123.5223	110.9164	.58
		SI	358444.7718	12330.5001	3.44
		MN	3877.7293	137.6594	3.55
		MN	4009.4096	60.5421	1.51
		FE	32933.7952	629.0355	1.91
EP 71(6-7)	EP1000				
		MG	39560.8520	803.0853	2.03
		AL	78700.8935	1054.5920	1.34
		AL	69553.7179	13.9107	.02
		SI	735818.1349	14642.7809	1.99
		SI	702443.8907	31258.7531	4.45
		MN	186247.3102	1732.1000	.93
		MN	8846.6504	220.2815	2.49
		FE	57188.4187	2847.9830	4.98
		FE	58222.7395	890.8379	1.53
		FE	56681.8216	2125.5683	3.75
EP71(8-9)	EP1001				
		AL	10339.1563	5.1696	.05
		MG	12942.5565	221.3177	1.71
		AL	12589.8424	475.8960	3.78
		SI	264184.9457	10118.2834	3.83
		MN	3018.3128	33.2014	1.10
		MN	3266.9727	38.2236	1.17
		FE	9541.5833	242.3563	2.54
EP 71(13-14)	EP1002				
		MG	11273.0475	184.8780	1.64
		AL	8746.5489	432.0795	4.94
		AL	11912.0721	1035.1591	8.69
		SI	204206.7260	4758.0167	2.33
		MN	1197.0706	27.1735	2.27
		MN	1297.8189	21.0247	1.62
		FE	7209.1101	180.9487	2.51
		FE	7526.5008	72.2544	.96

Sample	AAS Access. No.	Element	Concentration	Error (1σ)	% Error
EP71(20-21)	EP1021				
		AL	9983.0623	830.5908	8.32
		SI	128928.8675	6343.3003	4.92
		MN	1531.5843	9.9553	.65
		FE	25997.5479	649.9387	2.50
EP71(26-27)	EP1022				
		AL	6491.7780	1001.6813	15.43
		AL	8344.8986	494.0180	5.92
		SI	99441.4252	3649.5003	3.67
		MN	2033.7982	13.0163	.64
		FE	10043.2769	127.5496	1.27
		FE	9645.7903	1196.0780	12.40
EP71(31-33)	EP1023				
		AL	3518.1969	270.9012	7.70
		SI	101423.1720	212.9887	.21
		FE	2648.7467	14.3032	.54
EP 72(0-1)	EP1024				
		MG	6339.6972	179.4134	2.83
		AL	21566.5685	631.9005	2.93
		AL	21857.1936	1538.7464	7.04
		AL	26629.5368	801.5491	3.01
		AL	19632.8625	835.3599	4.25
		SI	268228.1087	4184.3585	1.56
		MN	3270.3042	32.0430	.98
		MN	3303.9850	21.4759	.65
		MN	3426.0665	22.6120	.66
		FE	14778.1017	1087.6686	7.36
		FE	14870.4203	0	0
		FE	14938.4126	0	0
		FE	14414.9266	357.4302	2.48
EP 72(3-4)	EP1025				
		MG	10570.6714	173.3590	1.64
		AL	20284.3798	383.3748	1.89
		AL	18098.3814	5.6197	.02
		SI	187395.2257	4527.7045	2.42
		MN	4847.7188	16.4822	.34
		MN	4363.3925	108.2121	2.48
		FE	15384.4316	1213.8317	7.89
EP 72(9-10)	EP1026				
		MG	8056.1540	163.5399	2.03
		AL	5073.7855	335.3772	6.61
		SI	275669.4845	5210.1533	1.89
		MN	1397.9911	25.0240	1.79
		MN	1382.8811	14.1054	1.02
		FE	4050.0767	155.5229	3.84
EP 72(14-15)	EP1027				
		MG	13960.4026	295.9605	2.12
		MG	15135.5081	363.2522	2.40
		AL	10476.1179	727.0426	6.94
		AL	9036.6341	553.0420	6.12
		AL	8897.2209	1210.0220	13.60
		SI	252079.7231	12099.8267	4.80
		MN	3415.5164	50.8912	1.49
		MN	3459.5520	37.7091	1.09
		MN	3481.5448	40.3859	1.16
		FE	7136.7772	213.3896	2.99
		FE	7470.9134	292.8599	3.92
		FE	8600.3518	135.8856	1.58

Sample	AAS Access. No.	Element	Concentration	Error (1σ)	% Error
EP72(27-28)	EP1028				
		MG	55229.3711	469.4497	.85
		AL	13222.4168	967.8809	7.32
		AL	13935.3541	2495.8219	17.91
		SI	150782.3789	8368.4220	5.55
		MN	3832.1183	126.8431	3.31
		MN	3359.2942	74.2404	2.21
		FE	32237.4028	1579.6327	4.90
		FE	11923.8443	153.8176	1.29
EP 72(36-37)	EP1029				
		MG	26950.5712	924.4046	3.43
		AL	19594.5624	433.0398	2.21
		AL	18243.7341	1266.1151	6.94
		AL	18128.4116	551.1037	3.04
		SI	207806.7550	3574.2753	1.72
		SI	210372.2731	4817.5251	2.29
		MN	1750.3217	30.1055	1.72
		MN	1796.0778	21.3735	1.19
		FE	18735.5650	1144.7430	6.11
		FE	15758.8577	264.7488	1.68
		FE	16382.5457	1412.1754	8.62
EP72(37-38)	EP1030				
		AL	14209.6636	542.8092	3.82
		SI	339494.7746	8996.6115	2.65
		MN	3128.6754	48.1816	1.54
		FE	21287.7301	687.5937	3.23
EP 72(39-40)	EP1031				
		MG	27321.8847	816.9244	2.99
		AL	17881.2629	354.0490	1.98
		AL	17589.7401	874.2101	4.97
		SI	296319.3628	5511.5401	1.86
		MN	8092.0842	39.6512	.49
		MN	8360.1811	170.5477	2.04
		FE	41443.7244	1558.2840	3.76
		FE	43313.6099	506.7692	1.17
EP 73(0-1)	EP1032				
		MG	11251.1400	189.0192	1.68
		AL	20001.0048	258.0130	1.29
		AL	17413.6851	959.4941	5.51
		AL	17960.6116	959.0967	5.34
		SI	235344.5561	16521.1878	7.02
		MN	2511.8854	35.4176	1.41
		MN	2696.8590	42.6104	1.58
		MN	2688.9456	27.9650	1.04
		MN	2314.4431	31.0135	1.34
		FE	12619.5536	137.5531	1.09
		FE	14942.6789	339.1988	2.27
EP 73(4-5)	EP1033				
		MG	8398.6029	149.4951	1.78
		AL	12637.7561	161.7633	1.28
		AL	12067.6375	440.4688	3.65
		SI	244822.8276	5581.9605	2.28
		SI	249452.1910	13220.9661	5.30
		MN	1177.6632	14.8385	1.26
		MN	1120.3323	19.8299	1.77
		FE	9935.9775	492.8245	4.95
		FE	11229.8103	326.7875	2.91
EP 73(8-9)	EP1034				
		MG	9193.1810	141.5750	1.54
		AL	9086.0857	201.7111	2.22
		SI	273817.9678	8871.7022	3.24
		MN	6053.5790	121.0716	2.00
		MN	5989.0966	55.6986	.93
		FE	17694.0344	428.1956	2.42
		FE	17903.9166	277.5107	1.55

Sample	AAS Access. No.	Element	Concentration	Error (1σ)	% Error
EP 73(14-15)	EP1035				
		MG	11512.9751	233.7134	2.03
		AL	16271.8534	1244.7968	7.65
		AL	17330.6615	538.9836	3.11
		SI	162687.1219	2375.2320	1.46
		MN	4829.3623	35.7373	.74
		MN	4777.2891	0	0
		FE	12148.5870	238.1123	1.96
		FE	13145.2024	289.1945	2.20
EP 73(20-22)	EP1036				
		MG	24375.2123	531.3796	2.18
		AL	19219.7922	1773.9868	9.23
		AL	18363.7806	1581.1215	8.61
		SI	158381.4586	6366.9346	4.02
		MN	2925.7448	90.9907	3.11
		MN	2990.8782	46.0595	1.54
		FE	10117.7840	354.1224	3.50
		FE	13113.7996	224.2460	1.71
EP 73(32-33)	EP1037				
		MG	11897.9215	290.3093	2.44
		AL	8416.1562	705.2739	8.38
		AL	8479.5575	1009.9153	11.91
		SI	225077.6689	5739.4806	2.55
		MN	1642.8823	34.6648	2.11
		MN	1300.2694	21.0644	1.62
		FE	9282.9250	97.4707	1.05
EP73(39-40)	EP1038				
		MG	10175.2906	239.1193	2.35
		AL	19012.1941	332.7134	1.75
		AL	18304.4405	419.1717	2.29
		SI	258567.5106	6179.7635	2.39
		MN	4154.6780	187.3760	4.51
		FE	26875.0214	903.0007	3.36
		FE	12556.8574	1202.9469	9.58
EP73(43-44)	EP1039				
		AL	9468.5556	846.4889	8.94
		SI	138675.4133	7807.4258	5.63
		MN	11556.4279	204.5488	1.77
		FE	59578.5610	1078.3720	1.81
EP74(0-1)	EP1040				
		AL	40569.7540	969.6171	2.39
		AL	35898.2911	746.6845	2.08
		AL	35177.3884	1755.3517	4.99
		AL	47071.2697	3572.7094	7.59
		SI	294989.9404	14041.5212	4.76
		SI	268946.1561	12317.7339	4.58
		CA	45630.8740	4302.6531	9.43
		MN	9851.2552	111.3192	1.13
		MN	9790.8480	84.2013	.86
		MN	9125.1557	292.9175	3.21
		FE	44015.9504	774.6807	1.76
		FE	47940.5447	1164.9552	2.43
		FE	47643.4326	28.5861	.06
		FE	45610.7316	706.9663	1.55
EP74(7-8)	EP1041				
		AL	33427.2694	1213.4099	3.63
		SI	270824.0679	10914.2099	4.03
		MN	20953.2306	167.6258	.80
		FE	52295.4257	941.3177	1.80
		FE	55197.2504	1291.6157	2.34

Sample	AAS Access. No.	Element	Concentration	Error (1σ)	% Error
EP 74(17-18)	EP1042				
		MG	20427.9240	512.7409	2.51
		AL	27861.1523	487.5702	1.75
		AL	22646.8832	468.7905	2.07
		SI	181597.6343	12039.9232	6.63
		MN	11726.4568	615.6390	5.25
		FE	45418.4674	1067.3340	2.35
		FE	45882.4161	747.8834	1.63
EP 74(25-26)	EP1043				
		MG	25346.4685	615.9192	2.43
		AL	37341.6654	806.5800	2.16
		AL	33618.1276	1153.1018	3.43
		SI	192743.0022	4221.0717	2.19
		MN	11568.8308	84.4525	.73
		FE	56046.3053	1765.4586	3.15
		FE	51221.3477	1295.9001	2.53
EP74(29-30)	EP1044				
		MG	96015.9365	796.9323	.83
		AL	34731.3875	2493.7131	7.18
		AL	38033.3377	3331.7204	8.76
		SI	197502.5941	12126.6593	6.14
		MN	13865.7559	226.0118	1.63
		MN	12309.1948	148.9413	1.21
		FE	90793.6391	5583.8088	6.15
		FE	47040.9332	0	0
EP 74(44-45)	EP1045				
		MG	18648.4603	346.8614	1.86
		AL	24164.8447	343.1408	1.42
		AL	20194.8747	2118.4424	10.49
		SI	102770.3545	5169.3488	5.03
		MN	50998.5638	1300.4634	2.55
		MN	54840.7145	652.6045	1.19
		FE	163778.5550	1621.4077	.99
		FE	177102.7152	9705.2288	5.48
EP75(1-2)	EP1046				
		AL	46774.9285	1604.38[illegible]	3.43
		AL	54188.9734	3034.5825	5.60
		SI	153913.9793	35307.8669	22.94
		SI	154576.0374	9614.6295	6.22
		CA	60025.2441	6832.0509	11.38
		MN	40408.2301	589.9602	1.46
		MN	41187.2139	1375.6529	3.34
		MN	43491.0072	408.8155	.94
		MN	46355.1922	282.7667	.61
		FE	167271.6470	10053.0260	6.01
		FE	170277.9003	1498.4455	.88
		FE	188783.2145	6003.3362	3.18
EP75(16-18)	EP1047				
		AL	23659.1653	1012.6123	4.28
		AL	25974.2386	1470.1419	5.66
		SI	103590.1612	4153.9655	4.01
		SI	92882.9767	4449.0946	4.79
		MN	26276.5755	441.4465	1.68
		MN	28228.3101	547.6292	1.94
		FE	150993.5759	2491.3940	1.65
		FE	153303.8323	1885.6371	1.23
EP75(21-22)	EP1048				
		AL	6062.2019	1059.0667	17.47
		SI	27007.5178	5066.6103	18.76
		MN	6032.8626	82.0469	1.36

Sample	AAS Access. No.	Element	Concentration	Error (1σ)	% Error
EP75(24-25)	EP1049				
		AL	8542.8982	1465.9613	17.16
		AL	8399.2616	980.1938	11.67
		SI	32891.2680	2443.8212	7.43
		MN	4693.7728	7.5100	.16
		MN	6035.4527	0	0
		FE	61870.7604	2326.3406	3.76
		FE	60550.7556	1483.4935	2.45
EP 75(29-30)	EP1050				
		MG	20214.2984	147.5644	.73
		AL	7782.6419	742.4640	9.54
		AL	7971.7423	.7972	.01
		SI	29003.1831	1896.8082	6.54
		MN	18982.3728	715.6355	3.77
		MN	17095.9250	288.9211	1.69
		FE	109434.5393	1302.2710	1.19
		FE	62631.0739	3569.9712	5.70
EP75(31-32)	EP1051				
		AL	4601.4635	717.3682	15.59
		AL	4633.0778	1016.9606	21.95
		SI	19848.3979	3568.7419	17.98
		MN	106259.0252	1678.8926	1.58
		FE	223396.8354	3082.8763	1.38
EP 77(0-1)	EP1052				
		MG	10011.7839	201.2369	2.01
		AL	13219.3077	222.0844	1.68
		AL	16277.5439	887.1261	5.45
		AL	15427.4026	732.8016	4.75
		SI	259959.5066	6109.0484	2.35
		SI	224500.0517	33832.1578	15.07
		SI	219207.7828	3792.2946	1.73
		MN	5702.7345	39.9191	.70
		MN	5016.9533	91.8102	1.83
		MN	5175.3409	176.9967	3.42
		FE	13313.6164	412.7221	3.10
		FE	10748.3126	0	0
		FE	10700.0618	0	0
EP77(3-4)	EP1053				
		AL	14756.9843	534.2028	3.62
		SI	197926.2790	3127.2352	1.58
		MN	6335.4099	152.6834	2.41
EP77(7-8)	EP1054				
		AL	5951.7100	827.2877	13.90
		SI	250372.1516	9388.9557	3.75
		MN	1755.9223	22.1246	1.26
EP77(15-16)	EP1055				
		AL	6996.1992	777.2777	11.11
		SI	217472.2793	3109.8536	1.43
		MN	2739.7521	52.3293	1.91
EP77(23-24)	EP1056				
		AL	8945.2975	2313.2539	25.86
		SI	174291.3349	5002.1613	2.87
		MN	5168.6577	63.5745	1.23
EP77(26-27)	EP1057				
		AL	18095.4263	4889.3841	27.02
		SI	190598.2478	7814.5282	4.10
		MN	3546.6050	50.3618	1.42

Sample	AAS Access. No.	Element	Concentration	Error (1σ)	% Error
EP77(30-31)	EP1058				
		MG	10990.7419	127.4926	1.16
		AL	3273.3927	765.6465	23.39
		SI	321634.3479	5885.9086	1.83
		MN	690.4371	23.1296	3.35
		MN	476.9771	6.9162	1.45
		FE	9371.5098	1637.2028	17.47
EP77(37:38)	EP1059				
		AL	18690.9807	898.4274	4.83
		SI	217360.7623	2390.9684	1.10
		MN	32625.4598	3.2625	.01
EP78(12-13)	EP1060				
		AL	23422.4270	1592.7250	6.80
		SI	146686.0431	2948.3895	2.01
		MN	8000.0987	625.6077	7.82
EP78(15-16)	EP1061				
		AL	22884.6053	1418.8455	6.20
		SI	191372.7048	2564.3942	1.34
		MN	6434.4187	88.7950	1.38
EP78(18-19)	EP1062				
		AL	16535.9299	901.2082	5.45
		SI	153336.2571	1671.3652	1.09
		MN	6790.8471	442.7632	6.52
		MN	7778.1186	293.6798	3.84
		FE	47623.8269	1533.4872	3.22
EP78(25-26)	EP1063				
		AL	30181.1344	2942.6509	9.75
		SI	172591.2876	2260.9459	1.31
		MN	4071.5582	.4072	.01
EP78(31-32)	EP1064				
		AL	12721.7939	1296.3508	10.19
		AL	13224.7675	845.0626	6.39
		SI	174759.1890	2411.6768	1.38
		FE	28998.1730	2807.0232	9.68
EP78(34-35)	EP1065				
		AL	14948.0051	1233.2104	8.25
		SI	217273.3479	16882.1391	7.77
		CA	368342.0156	20286.6294	5.51
		MN	7315.4389	384.0605	5.25
		FE	42850.3155	1439.7706	3.36
EP 79(0-1)	EP1066				
		MG	11981.7232	204.8375	1.71
		AL	22541.4469	317.8344	1.41
		AL	23788.1827	920.6027	3.87
		AL	20116.3087	979.6642	4.87
		SI	246759.5078	5946.9041	2.41
		SI	258557.9502	28234.5282	10.92
		CA	357238.8125	7519.3058	2.10
		CA	322368.2343	35292.8389	10.95
		CA	334542.6250	19997.8394	5.98
		MN	12394.5830	327.2170	2.64
		MN	11732.4540	206.4912	1.76
		MN	12468.0548	182.0336	1.46
		MN	12871.8784	229.1194	1.78
		FE	23794.0793	592.4726	2.49
		FE	22686.1214	512.7063	2.26
		FE	24532.3466	824.2868	3.36

Sample	AAS Access. No.	Element	Concentration	Error (1σ)	% Error
EP79(5-6)	EP1067				
		AL	9290.3700	319.5887	3.44
		SI	36295.1014	4645.7731	12.80
		FE	12428.6302	349.2445	2.81
EP79(9-10)	EP1068				
		AL	7466.5934	286.7172	3.84
		SI	256284.7002	40903.0381	5.96
		FE	28943.0592	882.7633	3.05
EP79(15-16)	EP1069				
		AL	6368.0604	244.5335	3.84
		SI	235157.4028	823.0509	.35
		MN	1702.0229	32.5086	1.91
		FE	12893.8813	268.1927	2.08
EP79(22-23)	EP1071				
		AL	8468.6368	376.0075	4.44
		SI	134594.9845	2476.5477	1.84
		FE	70419.4677	2894.2401	4.11
EP80(0-1)	EP1072				
		AL	12820.4424	875.6352	6.83
		SI	208434.8450	625.3045	.30
		MN	3010.9983	56.6068	1.88
		FE	7411.1136	191.9478	2.59
EP80(6-7)	EP1073				
		AL	9568.8752	260.2734	2.72
		AL	8551.6754	274.5088	3.21
		SI	253334.2375	1494.6720	.59
		SI	262799.2451	735.8379	.28
		FE	7404.9405	503.5360	6.80
		FE	7558.8695	273.6311	3.62
EP80(13-14)	EP1074				
		AL	4224.3136	157.5659	3.73
		SI	374579.7639	31839.2799	8.50
		FE	4422.8067	269.3489	6.09
EP80(16-17)	EP1075				
		AL	17267.2724	447.2224	2.59
		AL	10454.3308	240.4496	2.30
		SI	262132.1499	10275.5803	3.92
		SI	260716.6736	28939.5508	11.10
		SI	232366.3721	6111.2356	2.63
		FE	108626.2250	7017.2541	6.46
		FE	20832.9984	637.4898	3.06
EP80(21-22)	EP1076				
		AL	6586.8330	553.9527	8.41
		SI	111639.7795	1283.8575	1.15
		MN	31526.0792	176.5460	.56
		FE	99689.9671	2163.2723	2.17

Sample	AAS Access. No.	Element	Concentration	Error (1σ)	% Error
EP81(0-1)	EP1077				
		AL	12475.5502	535.2011	4.29
		AL	11240.1967	668.7917	5.95
		SI	177406.7078	9846.0723	5.55
		SI	178321.8431	12678.6830	7.11
		CA	356955.9375	32566.6338	9.12
		MN	2324.2662	25.5669	1.10
		MN	2190.8493	20.1558	.92
		MN	2051.1714	42.8695	2.09
		FE	13801.7602	1.3802	.01
		FE	13360.5293	129.5971	.97
		FE	14224.7040	321.4783	2.26
EP81(14-15)	EP1078				
		AL	4410.6140	645.7139	14.64
		SI	348229.8251	4701.1026	1.35
		MN	7562.4436	179.9362	2.38
EP82(0-1)	EP1080				
		AL	19585.0127	656.0979	3.35
		AL	12455.5346	417.2604	3.35
		SI	386831.7495	17252.6960	4.46
		SI	319050.3933	53249.5106	16.69
		SI	158499.8686	11332.7406	7.15
		SI	141006.6931	17752.7427	12.59
		CA	353430.7187	39773.8594	11.25
		MN	4977.4116	34.3441	.69
		MN	4762.8279	193.3708	4.06
		FE	25652.9429	782.4148	3.05
		FE	23225.8151	487.7421	2.10
		FE	24127.0183	361.9053	1.50
EP82(5-6)	EP1081				
		AL	5185.2435	332.8926	6.42
		SI	299553.4858	778.8391	.26
		MN	3077.6771	49.2428	1.60
		FE	22189.6153	463.7630	2.09
EP83(0-1)	EP1082				
		AL	33596.1544	0	0
		AL	30063.2146	1007.1177	3.35
		AL	30923.2334	612.2800	1.98
		AL	29303.0418	1608.7370	5.49
		SI	216141.7354	4949.6457	2.29
		SI	224955.6921	9380.6524	4.17
		SI	175281.0912	12602.7105	7.19
		SI	170907.2710	14663.8439	8.58
		CA	230474.8476	6509.8855	2.82
		MN	12617.3989	194.3079	1.54
		MN	12942.4520	196.7253	1.52
		MN	12906.0846	189.7194	1.47
		FE	52283.7666	1829.9318	3.50
		FE	56087.9418	504.7915	.90
		FE	59714.2458	776.2852	1.30
EP83889)	EP1083				
		AL	5544.1363	185.1742	3.34
		SI	264319.4331	5524.2762	2.09
		FE	39452.7335	1183.5820	3.00
EP159(0-1)	EP1084				
		AL	86657.8385	4272.2314	4.93
		AL	86365.2273	5259.6423	6.09
		SI	221274.2372	11019.4570	4.98
		SI	242997.3777	15843.4290	6.52
		SI	269942.2601	18194.1083	6.74
		SI	254944.7519	18763.9337	7.36
		CA	10471.9790	388.8856	3.71
		CA	10603.5264	512.4302	4.83
		MN	19748.8216	578.6405	2.93
		MN	21022.9436	636.9952	3.03
		FE	52222.9183	15.6669	.03
		FE	53274.4408	31.9647	.06
		FE	52484.2171	2445.7645	4.66

Sample	AAS Access. No.	Element	Concentration	Error (1σ)	% Error
EP159(6-7)	EP1085				
		AL	82639.9207	3041.1491	3.68
		SI	255191.5885	2092.5710	.82
		MN	12787.4830	459.0706	3.59
		FE	56075.3321	353.2746	.63
EP159(13-14)	EP1086				
		AL	78592.0225	3520.9226	4.48
		SI	218059.9596	3205.4814	1.47
		SI	208900.1781	14184.3221	6.79
		MN	9201.0930	98.4517	1.07
		FE	63904.8873	1035.2592	1.62
EP159(15-16)	EP1087				
		AL	42708.0609	2186.6527	5.12
		SI	185712.9137	6722.8075	3.62
		FE	58571.2293	8358.1144	14.27
EP159(17-18)	EP1088				
		AL	47268.4225	3535.6780	7.48
		SI	184902.4376	13035.6219	7.05
		MN	10741.0698	287.8607	2.68
		FE	81629.7638	1191.7946	1.46
159(20-21)	EP1089				
		AL	21325.1429	309.2146	1.45
		SI	162063.0073	2252.6758	1.39
		FE	85940.6669	1297.7041	1.51
159(23-24)	EP1090				
		AL	11497.8587	357.5834	3.11
		SI	118911.5880	2425.7964	2.04
		MN	36184.9829	289.4799	.80
		FE	124387.0887	845.8322	.68
8 EP160(0-1)	EP1091				
		AL	88696.5008	461.2218	.52
		AL	89323.4186	4260.7271	4.77
		SI	295986.3619	11602.6654	3.92
		SI	261834.5801	13039.3621	4.98
		CA	20952.0054	3818.3136	18.22
		CA	19916.1919	1990.3159	9.99
		MN	10322.8438	115.6159	1.12
		MN	10033.8341	291.9846	2.91
		FE	63374.8851	2382.8957	3.76
EP160(15-16)	EP1092				
		AL	85289.8357	3675.9919	4.31
		SI	240015.8231	5160.3402	2.15
		MN	10470.8654	110.9912	1.06
		FE	66222.0978	761.5541	1.15
EP160(21-22)	EP1093				
		AL	27366.8050	435.1322	1.59
		SI	219411.2277	5573.0452	2.54
		MN	4895.7675	106.7277	2.18
		FE	8526.7356	214.8737	2.52
EP160(26-27)	EP1094				
		AL	22311.3712	1131.1865	5.07
		SI	138054.3479	2236.4804	1.62
		MN	2952.1553	33.6546	1.14
		FE	49051.9399	976.1336	1.99

Sample	AAS Access. No.	Ele- ment	Concentration	Error (1σ)	% Error
EP160(29-30)	EP1096				
		MG	36818.1053	544.9080	1.48
		AL	22715.0768	711.9819	3.13
		AL	22665.1136	942.8687	4.16
		AL	18489.4842	950.3595	5.14
		SI	149930.4316	2398.8869	1.60
		MN	2963.6607	34.6748	1.17
		FE	34171.3483	1606.0534	4.70
		FE	33370.7792	2219.1568	6.65
		FE	32804.7940	698.7421	2.13
EP160(34-35)	EP1097				
		AL	20613.2734	542.1291	2.63
		SI	322918.7133	5973.9962	1.85
		FE	23374.6522	899.9241	3.85
P161(18-19)	EP1098				
		AL	36887.2926	14.7549	.04
		AL	49028.6981	3216.2826	6.56
		SI	227454.8641	1546.6931	.68
		SI	238856.0764	9434.8150	3.95
		SI	219694.1841	16894.4828	7.69
		SI	257952.2819	12175.3477	4.72
		FE	36650.6400	1817.8717	4.96
		FE	38518.1093	921.5828	2.39
EP161(22-23)	EP1099				
		AL	22674.6533	390.0040	1.72
		SI	216187.8851	10312.1621	4.77
		SI	226750.9430	14353.3347	6.33
		MN	4564.7839	64.8199	1.42
		FE	24370.7386	650.6987	2.67
EP161(29-30)	EP1100				
		MG	20780.4649	272.2241	1.31
		AL	14142.0556	697.2033	4.93
		AL	12706.8013	379.9334	2.99
		SI	143134.3089	4165.2084	2.91
		SI	141468.8767	4343.0945	3.07
		MN	3735.5509	96.0037	2.57
		MN	3387.8836	34.5564	1.02
		FE	9415.2739	1113.8269	11.83
		FE	12091.5492	211.6021	1.75
EP161(34-35)	EP1101				
		AL	12833.3297	295.1666	2.30
		SI	195550.6016	7665.5836	3.92
		SI	187200.3269	2077.9236	1.11
		FE	11792.7238	398.5941	3.38
EP161(40-41)	EP1102				
		AL	12998.8643	246.9784	1.90
EP161(43-44)	EP1103				
		AL	8097.0382	210.5230	2.60
		SI	258784.9886	8928.0821	3.45
		SI	299866.2636	14873.3667	4.96
		MN	6316.2149	87.7954	1.39
		FE	30370.1511	583.1069	1.92
EP162(30-31)	EP1104				
		AL	37221.8039	7.4444	.02
		SI	184749.8112	1404.0986	.76
		SI	211559.1508	1459.7581	.69
		SI	212618.9336	14224.2067	6.69
		FE	37885.1358	287.9270	.76

Sample	AAS Access. No.	Element	Concentration	Error (1σ)	% Error
EP162(35-36)	EP1105				
		AL	23419.6373	407.5017	1.74
		AL	23864.6697	436.7235	1.83
		SI	196061.8775	10920.6466	5.57
		MN	7092.2153	119.8584	1.69
		FE	37677.6151	512.4156	1.36
EP162(37-38)	EP1106				
		AL	23813.4649	185.7450	.78
		SI	330839.3504	9462.0054	2.86
		FE	38948.3846	3318.4024	8.52
EP162(43-44)	EP1107				
		AL	12683.1849	286.6400	2.26
		AL	12626.0281	335.8523	2.66
		SI	275502.4070	1928.5168	.70
		FE	30803.5767	726.9644	2.35
EP162(46-47)	EP1119				
		AL	19134.0677	137.7653	.72
		SI	362813.7910	11283.5089	3.11
		FE	31126.7224	333.0559	1.07
EP162(48-49)	EP1120				
		AL	8559.7863	170.3397	1.99
		AL	8549.8824	346.2702	4.05
		SI	218640.3567	1464.8904	.67
		SI	311834.1504	10945.3787	3.51
		MN	16436.1694	235.0372	1.43
		FE	58767.9776	1204.7435	2.05
EP162(49-50)	EP1121				
		AL	13364.0083	203.1329	1.52
		SI	97630.1356	2450.5164	2.51
		FE	138357.6295	15772.7698	11.40
EP163(25-26)	EP1122				
		AL	71434.5297	1828.7240	2.56
		SI	250320.0893	13517.2848	5.40
		FE	44786.1776	2310.9668	5.16
EP163(35-36)	EP1123				
		AL	37148.9974	1344.7937	3.62
		AL	27362.3441	1365.3810	4.99
		SI	354671.3403	11207.6144	3.16
		FE	25744.4542	499.4424	1.94
EP163(42-43)	EP1124				
		AL	11929.7561	134.8062	1.13
		SI	390447.8929	8628.8984	2.21
		FE	14636.0304	304.4294	2.08
EP163(49-51)	EP1125				
		AL	2837.4979	103.2849	3.64
		SI	433493.7640	15692.4743	3.62
		FE	7319.2686	127.3553	1.74
EP163(63-64)	EP1126				
		AL	74843.5354	2305.1809	3.08
		SI	262164.3751	5951.1313	2.27
		MN	9362.3051	239.6750	2.56
		FE	53713.7641	639.1938	1.19

Sample	AAS Access. No.	Element	Concentration	Error (1σ)	% Error
EP163(71-72)	EP1127				
		AL	25438.5989	1701.8423	6.69
		SI	168333.0465	8046.3196	4.78
		MN	7299.8179	83.2179	1.14
		FE	44270.6570	557.8103	1.25
EP163(77-78)	EP1128				
		AL	26339.8375	460.9472	1.75
		SI	167106.2199	3726.4687	2.23
		MN	4655.7297	58.1966	1.25
		FE	33976.7475	642.1605	1.89
EP71(39-40)	EP1471				
		AL	9531.5738	506.1266	5.31
		SI	395682.3945	16499.9559	4.17
		CA	145283.2930	6000.4376	4.13
		MN	1160.6838	34.5884	2.98
		FE	23443.2750	421.9789	1.80
EP69(43-44)	EP1472				
		AL	5985.0566	295.0633	4.93
		SI	411521.0361	10699.5469	2.60
		MN	462.6479	3.9788	.86
		FE	6508.1467	1453.9200	22.34
EP160(1-2)	EP1481				
		AL	95186.6655	2427.2600	2.55
		SI	235778.8757	5422.9141	2.30
		MN	10922.1645	326.5727	2.99
		FE	68661.8987	2567.9550	3.74